Study on the Effectiveness of Windbreak Trees for Reduction of Evaporation in an Agricultural Land in the Nile-Delta, Egypt

Tatsuki SHIMIZU
201121267

January 2013

A Dissertation Submitted to
The Graduate School of Life and Environmental Sciences,
The University of Tsukuba
in Partial Fulfillment of the Requirements
for the Degree of Master of Environmental Sciences

Abstract

The effect of windbreak trees which are expected to reduce evaporation in an agricultural land was validated by comparison between evaporation in an agricultural land and transpiration of windbreak trees. Annual transpiration of windbreak trees was estimated by measurement of sap flow, sap wood area at Tomida farm in El Brigat, Penman-Monteith equation and Jarvis model. Measured transpiration of *Casuarina* at Tomida Farm had obvious seasonal change in the summer period, from July to September, in 2011. The measured transpiration used to estimate surface conductance by Jarvis model. Estimated surface conductance from measured transpiration of *Casuarina* had correlations between five environmental factors, such as air temperature, photon flux density, specific humidity deficit, soil moisture deficit and CO_2 concentration), which were similar to the result of *Pine* trees. The photon flux density, air temperature and CO_2 concentration were the main factors to determine the seasonal variation of surface conductance, and estimated transpiration by Penman-Monteith equation with substitution of surface conductance estimated by Jarvis model could represent the seasonal variation of transpiration of *Casuarina* in summer period in 2011. As results of measurements at Al Krakat, it was found that there is a horizontal variation of wind velocity in leeward of windbreak trees against relative distance from windbreak trees. Wind velocity became smallest around relative distance of 4, and after that it gradually recovers to 100% as the relative distance gets longer. This horizontal variation of wind velocity was very similar to the wind profile from model estimation in Wang and Takle (1997). On the other hand, other environmental factors, such as air temperature, relative humidity and specific humidity did not have such kind of horizontal variation. From TOPLATS model analysis, in the no-crop period in 2011, the agricultural land without windbreak trees had 221 mm evaporation for 2 months, on the other hand, the agricultural land with windbreak trees had only 116 mm evaporation and 5.2 mm transpiration of the windbreak trees. By comparing the estimations between a field with and without windbreak trees, in the no-crop period, the amount of evapotranspiration of the field and windbreak trees in a field with windbreak trees were much smaller than the field without windbreak trees by 100 mm per 2 months equals to around 50% of the evaporation. In the estimations in the summer crop growing period for 3 months, the amount of evaporation of the soil, transpiration of the crops and transpiration of windbreak trees from the field with windbreak trees was also much smaller than the amount of evapotranspiration from the field without windbreak trees by 575 mm per 3 months equals to around 50% of the evapotranspiration.

According to this analysis, windbreak trees reduces total amount of evaporation from the soil by 348 mm per 5 months, on the other hand, the total amount of transpiration of windbreak trees occupies only 15.2 mm per 5 months, and the amount of transpiration of windbreak trees equals to 4.4% of the amount of reduced evaporation in the land. However, at the same time, transpiration of crops is reduced by 274 mm per 5 months by windbreak trees. Thus windbreak trees reduce evaporation from the soil by 348 mm and transpiration of crops by 274 mm for 5 months. These results mentioned that actually windbreak trees have the effectiveness to reduce evaporation in an agricultural land by large amount, however, at the same time, windbreak trees have also the possibility to prevent the growth of crops by reducing transpiration of crops. When windbreak trees are practically used in agricultural fields, the possibility which windbreak trees might prevent growth of crops must be considered with the assumed impact of the effect for each species of crops. In this case of *Maize*, if behalf of the amount of transpiration of *Maize* were reduced by windbreak trees, the amount of photosynthesis of *Maize* would be reduced by 50%. This reduction of the amount of photosynthesis can be thought that it might have certain negative effects on the growth of *Maize*.

Keywords: Reduction of evaporation, Windbreak trees, Jarvis model, Penman-Monteith equation, TOPLATS model

Table of Contents

Tables

Figures

1. Introduction

A problem of food and water shortage is getting more acute as it is one of the most serious international issues all over the world. Such kind of problem occurs by rapid increase of population. Especially, water shortage which is actually one of the causes of food shortage is getting more acute in arid and semi-arid areas in the world.

In Egypt, the population is rapidly growing these days. According to the Water Resources and Irrigation of Arab Republic of Egypt Ministry (2005), Egypt will not be able to feed all population with own agricultural production because of rapid increase of population. It is also mentioned in this paper that the government of Egypt elected a project called the National Water Resources Plan (NWRP) which would increase agricultural lands in the Nile-Delta by controlling loss of water in existent agricultural lands, for the purpose of increase in production of agriculture with limited water resources mainly from the Nile River. In the beginning of Arab Republic of Egypt Ministry of Water Resources and Irrigation (2005), there is a preface of this project planning report written by Dr. Mahmoud Abu-Zeid, the minister of Water Resources and Irrigation, cited here as follows.

"The National Water Resources Plan (NWRP) has been developed within the framework of the NWRP project, carried out by the Ministry of Water Resources and irrigation (MWRI) with support of the Government of the Netherlands. The main objective of NWRP is to describe how Egypt will safeguard its water resources in the future, both with respect to quantity and quality and how it will use these resources in the best way from a socio-economic point of view. The planning horizon for the NWRP is the year 2017."

"NWRP is based on an Integrated Water Resources Management (IWRM) approach and considers all components of Egypt's water resources system and all functions and water user sectors. This means that NWRP includes also the policy areas of other ministries and that this document is 'owned' by all stakeholders involved. To this end there has been an intensive interaction between the NWRP project and the stakeholders, in particular within the inter-ministerial Technical Committee for Water Resources Management. The resulting plan and policies have been discussed and agreed upon in the inter-ministerial Technical and High Committees for the National Water Resources Plan project." He also mentioned in this report that other important results are the Policy Document and the supporting Technical Reports, and actually, these are complementary in the senses as follows,

- ✓ "the Policy Document presents the broad policy guidelines for the development and the management of the water resources in Egypt",
- ✓ "the National Water Resources Plan describes the specific actions to be taken to

implement the policy and provides the necessary background information"

- ✓ "the supporting technical reports contain the detailed information and data underlying the plan and describe also the analysis process that has been followed to develop the policy and the plan."

Thus, the NWRP project needs not only technical studies, but also political guidelines which give broad management and development of water resources in Egypt. To support the decision making of policy sector, technical report must produce the situation and background information. Furthermore, technical report must contain detailed information and data.

According to Kitamura *et al*. (1994), water resource from the Nile River occupies 90% of all water resources of Egypt (Figure 1), and in the Arab Republic of Egypt Ministry of Water Resources and Irrigation (2005), the ratio of water use in agricultural sector occupies 95% of all purpose of water use of Egypt (Figure 2). In such situation of Egypt, it can be said that water saving in agricultural sector is very important to solve problems such as food shortage and water shortage. As one of the sources of loss of water in agriculture, evaporation which is from soil surface can be pointed out. In a surface water balance in an agricultural land, input of water is generally irrigation and precipitation, and output is infiltration, surface runoff, evaporation and transpiration. Infiltration, surface runoff and transpiration are for growth of crops and sustainable water use in agricultural irrigation systems. So it can be said that reduction of evaporation is very effective to increase available water resource in the Nile-Delta. In this study, one of the solutions which reduce evaporation in an agricultural land is focused on. It is introduction of windbreak trees.

Windbreak tree is generally and qualitatively known to block wind, and at the same time, it also reduces evapotranspiration from soil surface of an agricultural land. However, windbreak trees add own transpiration into the surface water balance of an agricultural land. Furthermore, it reduces not only evaporation but also transpiration of crops. To validate the effectiveness of windbreak trees which reduce evaporation, it is very important to estimate the reduction of evaporation and transpiration, and transpiration of windbreak trees. If transpiration of windbreak trees is less or equal than reduced evaporation, windbreak trees are effective to reduce evaporation, because windbreak trees can be used for other purposes such as building materials. However, at a same time, it must be considered if the effect of reduction of transpiration has no negative impact on growth of crops.

In this study, the objective is set as validation of the effectiveness of windbreak trees which reduce evaporation in an agricultural land. To achieve this goal, estimation of annual transpiration of windbreak trees, estimation of reduction of evaporation and transpiration in an agricultural land and comparison between transpiration of windbreak

trees and reduced evaporation must be clarified.

Actually, there a line of trees were along an agricultural land now in the Nile-Delta. However they are not thought as windbreak trees but were introduced to fix canal bank in Egypt. Thus, if the effectiveness of such line of trees as windbreak trees in the Nile-Delta is quantitatively clarified by this study, total reduction of evaporation in the Nile-Delta might be estimated.

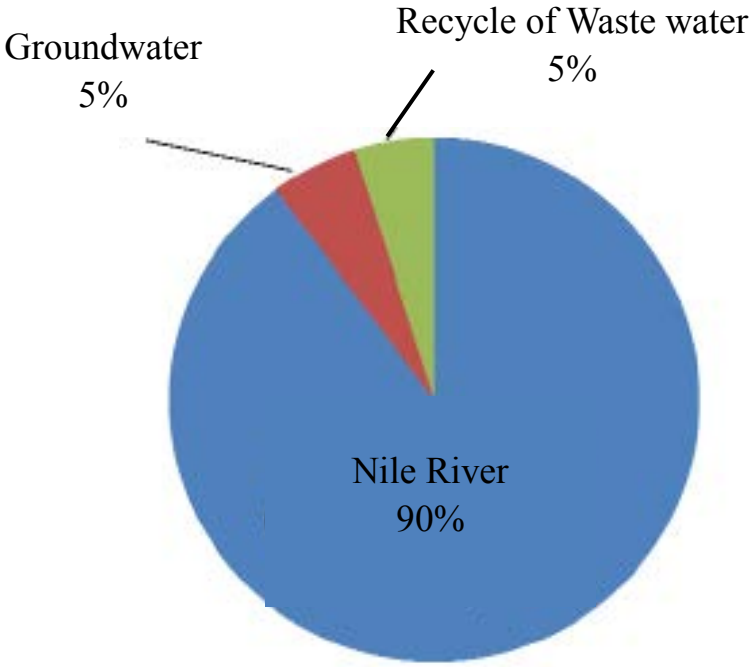

Figure 1 Available water resources in Egypt (from Kitamura *et al*. 1994)

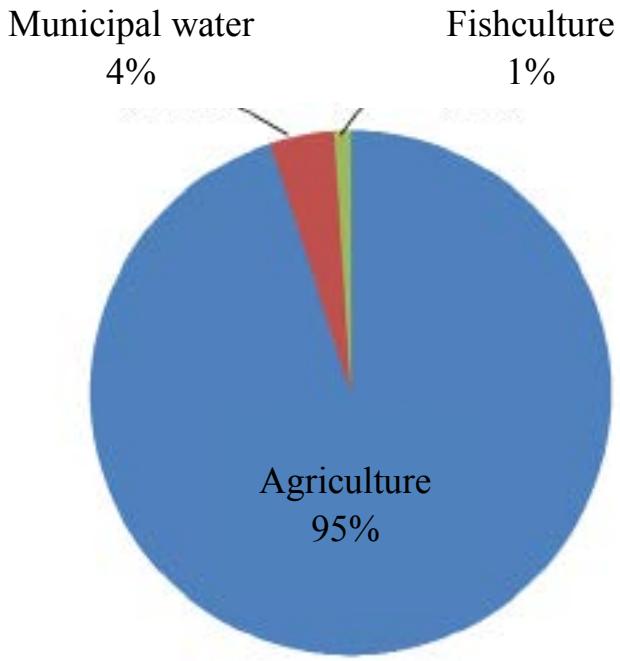

Figure 2　Water use in Egypt (Water Resources and Irrigation of Arab Republic of Egypt Ministry, 2005)

2. Methods

2-1. Study areas

This study has three main fields for measurements, Tomida farm (N 30’ 30’ 11.7, E 30’ 48’ 06.41, altitude: 16 m), Sakha (N 31’ 05’ 54.2, E 30’ 55’ 24.2, altitude: 13 m) and Al Krakat (N 31’ 18’ 02.2, E 31’ 12’ 26.67, altitude: 14 m) shown in Figure 3. At Tomida farm, measurements of sap flow, sap wood, general meteorological data, LAI and projected leaf area, stomatal conductance, leaf temperature and transpiration rate were measured. Measured data from Tomida farm is mainly for estimation of annual transpiration of windbreak trees. At Sakha, measurements of general meteorological data including surface flux of evaporation, soil physics data, seasonal change of crops were measured. Measured data from Sakha is mainly for estimation of evaporation and transpiration from an agricultural land, and it can be said that Sakha is a typical agricultural land in the Nile-Delta. At Al Krakat, measurements of general meteorological data, soil physics and crops data and characteristic of windbreak trees were measured. It can be said that the windbreak trees at Al Krakat are typical windbreak trees in the Nile-Delta. The detailed explanations of each measurement are shown in Tables 1 – 3 for each fields, and the detailed map of each fields are shown in Figures 3 – 6.

These three fields have different purposes for each, Tomida Farm is for estimation of windbreak trees’ transpiration, Sakha is for separate estimation of evaporation and transpiration of crops in an agricultural land, and Al Krakat is for the horizontal profile of meteorological factors and situation of the soil and crops. The study flow representing such purposes is shown in Figure 7. This study can be divided into three parts, and the purposes are set for one by one. Finally, the results from each part were combined and integrated in the conclusions and discussions.

2-2. Estimation of annual transpiration of windbreak trees

2-2-1. Measurements of sap flow and sap wood area

In Shimizu (2011), transpiration of windbreak trees was measured at Tomida farm for 10 days in summer. The target kind of tree was *Casuarina*. *Casuarina* can be seen in coastal areas and arid areas in the world. *Casuarina* has thin leaves look like *Pine*. In this study, transpiration of windbreak trees was continuously measured at Tomida farm. In general, transpiration of trees is given by following equation.

$$T_r = u \times A \tag{1.1}$$

T_r is Transpiration of a tree, u is sapflow rate and A is sapwood area. At Tomida farm, u was measured by sapflow sensor (UP GmbH, model of CUP-SPF-M), shown in Figure 8, and A was measured by dying experiment. The dying experiment aimed at estimating

sapwood areas of sample trees by dying their sap with bottles (shown in Figure 14) which were filled with stain liquid, and in 100 minutes after starting infusing the stain liquid, the core samples of sap wood areas were taken by an increment borer (shown in Figure 15). After starting infusing of stains, the stains were carried above by sap flow and dying sap wood area, in about 100 minutes, the dyed sap wood areas could be observed with the core samples of sap wood areas which were taken by an increment borer at upper points than an infusing point. This experiment was done in August 2010. The results of sap wood areas estimation by ding experiment were shown in Figure 16.

On the other hand, the sapflow sensor is based on Granier (1985). Granier method calculates sapflow from difference of temperature between two probes one with heater and another without heater. In daytime, the difference of temperature becomes larger because of heat transfer by sapflow, and in nighttime, the difference of temperature becomes smaller because of weakness of sapflow.

However, it is generally known that the velocity of sapflow is different between in the area near bark and in the area near the core. It means that sapflow has horizontal variation in sap wood area, and velocity of sap flow gets smaller as horizontal depth from bark gets deeper. Thus, if estimation of transpiration was calculated by only surface sap wood area sapflow measurement, estimated transpiration would be over-estimation.

To avoid this miss-estimation, the horizontal variation of the velocity of sapflow was measured against No.11, by setting two couples of sensors at two different horizontal depths against the sap wood area of No.11. As the result of dying experiment shows in Figure 16, the range of measured sap wood area of No.11 was 4 cm around 20 cm height from infusing point. Furthermore, the 2 couples of sapflow sensors whose length were 2 cm were set at the height of around 20 cm above from the infusing point. Thus, two measurements at two depths in the sap wood area of No.11 were suitable to estimate the horizontal variation of sapflow. The result of estimation of the horizontal variation of sapflow is shown in Figure 17. The horizontal variations of sapflow of other 4 samples were assumed that they have same horizontal variations of sapflow as No.11.

For estimation of transpiration of windbreak trees, it is important to measure sap flow and sap wood area, as seen in the Equation (1.1). At Tomida farm, five trees were chosen as samples, shown in Figures 9 - 13. The characteristics of these samples are listed in Table 4. After estimating transpiration, transpiration was divided by projected leaf area to get the unit mm/h. The period of measurement of sap flow is from August first to fifteenth in 2010 and from July fifteenth to December twentieth in 2011

2-2-2. Estimation of surface conductance with Jarvis model

In Jarvis (1976), stomatal conductance k_s is given in the following equation. It means k_s is given by five environmental factors (photon flux density, temperature, specific

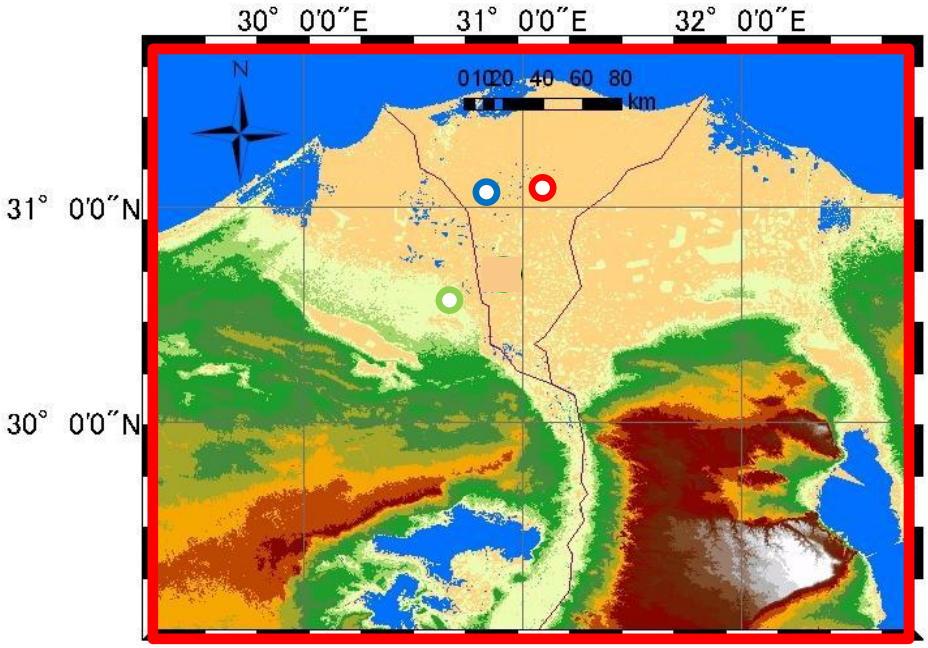

Figure 3 Map of the study areas in the Nile-Delta
(green circle: Tomida farm, red circle: Al Krakat and blue circle: Sakha)

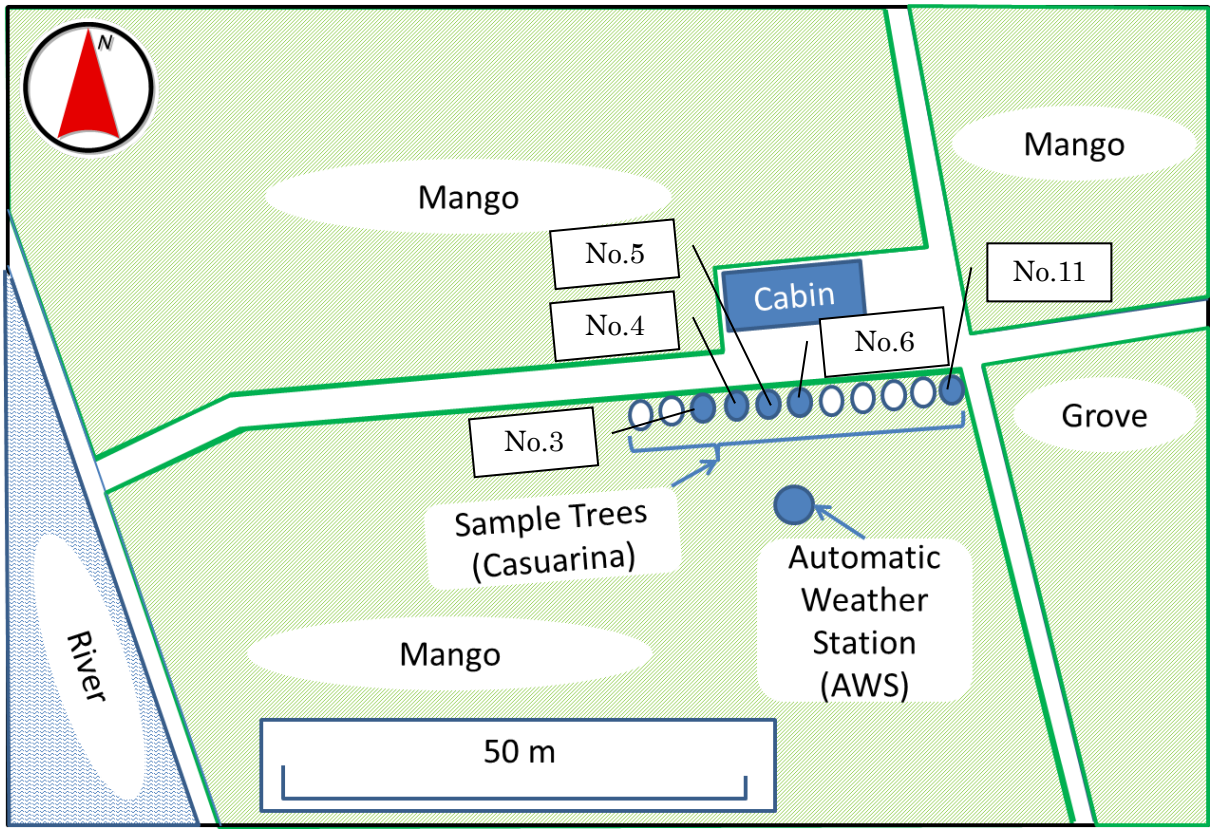

Figure 4 Detailed map of Tomida Farm (El Brigat).
The numbers, such as No.11, 6, 5, 4 and 3 means names for each tree sample and the characteristics of each sample are shown in Table 54.

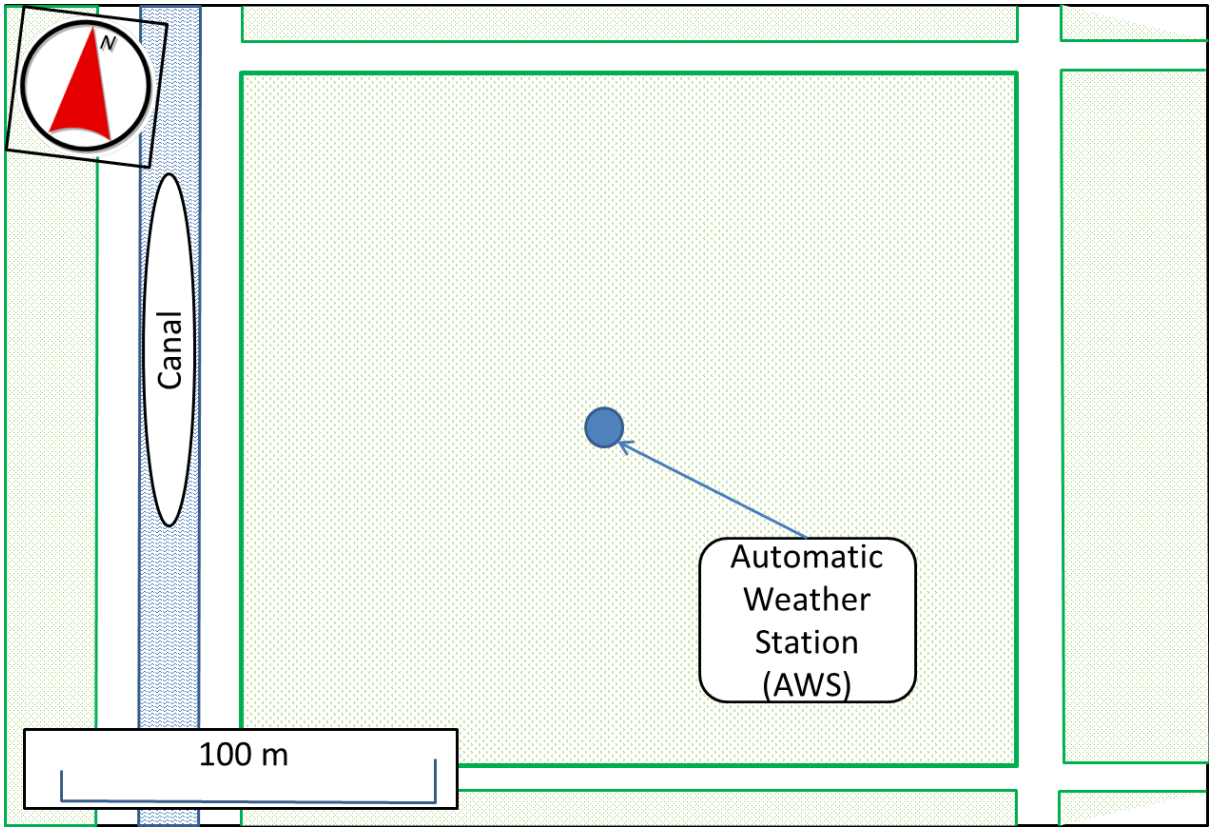

Figure 5 Detailed map of Sakha

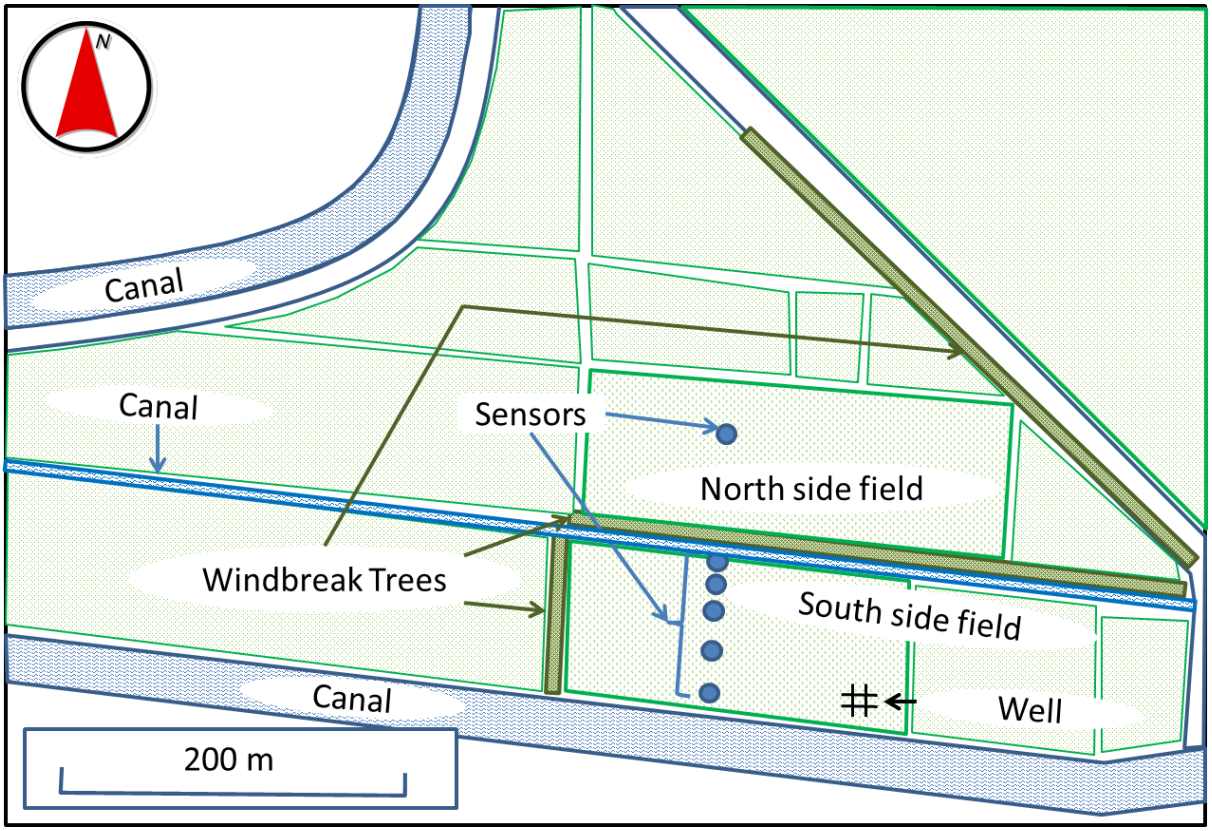

Figure 6 Detailed map of Al Krakat

Table 1　Measured variables at Tomida farm

Tomida farm					
Measured variables	Unit	Sensor / Experiment	Measurement height (m)	Sampling interval	Average period
Sapflow	cm/s	Sapflow sensor (UP GmbH, CUP-SPF-M)	1.3	30 seconds	10 minutes
Sapwood area	cm^2	Dying experiment	1.0	Instantaneous	N/A
Projected leaf area	m^2	GPS and tape measure	1.3	Instantaneous	N/A
Air temperature	℃	Hygrothermometer (Vaisala, MP155)	7.0	30 seconds	10 minutes
Relative humidity	%				
Wind verocity	m/s	Anemometer (Young, CYG-3002)	7.0		
Wind direction	Degree				
Soil moisture	%	TDR (Campbell, C-CS-616)	-0.2		

Table 2　Measured variables at Sakha

Sakha					
Measured variables	Unit	Sensor Experiment	Measurement height (m)	Sampling interval	Average period
Air temperature	℃	Hygrothermometer (Vaisala, MP155)	3.0 1.0 0.5	10 seconds	30 minutes
Relative humidity	%			10 seconds	
Air pressure	hPa	Barometer (Vaisala, PTB210)	0.8	0.1 seconds	
Three components wind velocity	m/s	Sonic anemometer (GILL Instruments, R3-50)	5.8	0.1 seconds	
CO_2 concentration	m mol/m^3	Open path gas analyzer (LI-COR, Inc., LI-7500)	5.8	0.1 seconds	
Downward short radiation	W/m^2	Four components radiometer (Hukseflux, NR01)	4.2	10 seconds	
Upward short radiation	W/m^2				
Downward long radiation	W/m^2				
Upward long radiation	W/m^2				
Soil heat flux	W/m^2	Soil heat plate (Hukseflux, HFP-01)	-0.03	10 seconds	
Latent heat flux	W/m^2	Calculated by eddy correlation method	-	10 seconds	
Sensible heat flux	W/m^2				
Net radiation	W/m^2				

Table 3　Measured variables at Al Krakat

Al Krakat					
Measured variables	Unit	Sensor	Measurement height (m)	Sampling interval	Average period
Wind velocity	m/s	Weather transmitter (Vaisala WXT520)	1.5	10 seconds	10 minutes
Wind direction	degree				
Max wind velocity	m/s				
Direction of max wind velocity	degree				
Temperature	℃				
Relative humidity	%				
Air pressure	hPa				
Precipitation	mm				
Soil & Leaf surface temperature	℃	IRT	0	10 - 30 times in a day	Instantaneous value
Soil thermal conductivity	μmol/m^2/s	KD2	-0.6	50 - 60 times in a day	Instantaneous value
Soil water content	%	HS Ⅱ	-0.6	50 - 60 times in a day	Instantaneous value
Temperature in canopy	℃	LI-1600	0.1 - 1.5	20 - 90 times in a day	Instantaneous value
Leaf temperature	℃				
Relative humidity in canopy	%				
Quantum	μmol/m^2/s				
Stomatal resistance	s/cm				
Transpiration rate	mg/m^2/s				
LAI	no unit	LAI-2000	0.1 - 2.0	1time in a day	Instantaneous value
Evaporation from Soil Surface	mm/h	Chamber	0 - 0.1	4 times in a day (2012/9/12)	Instantaneous value

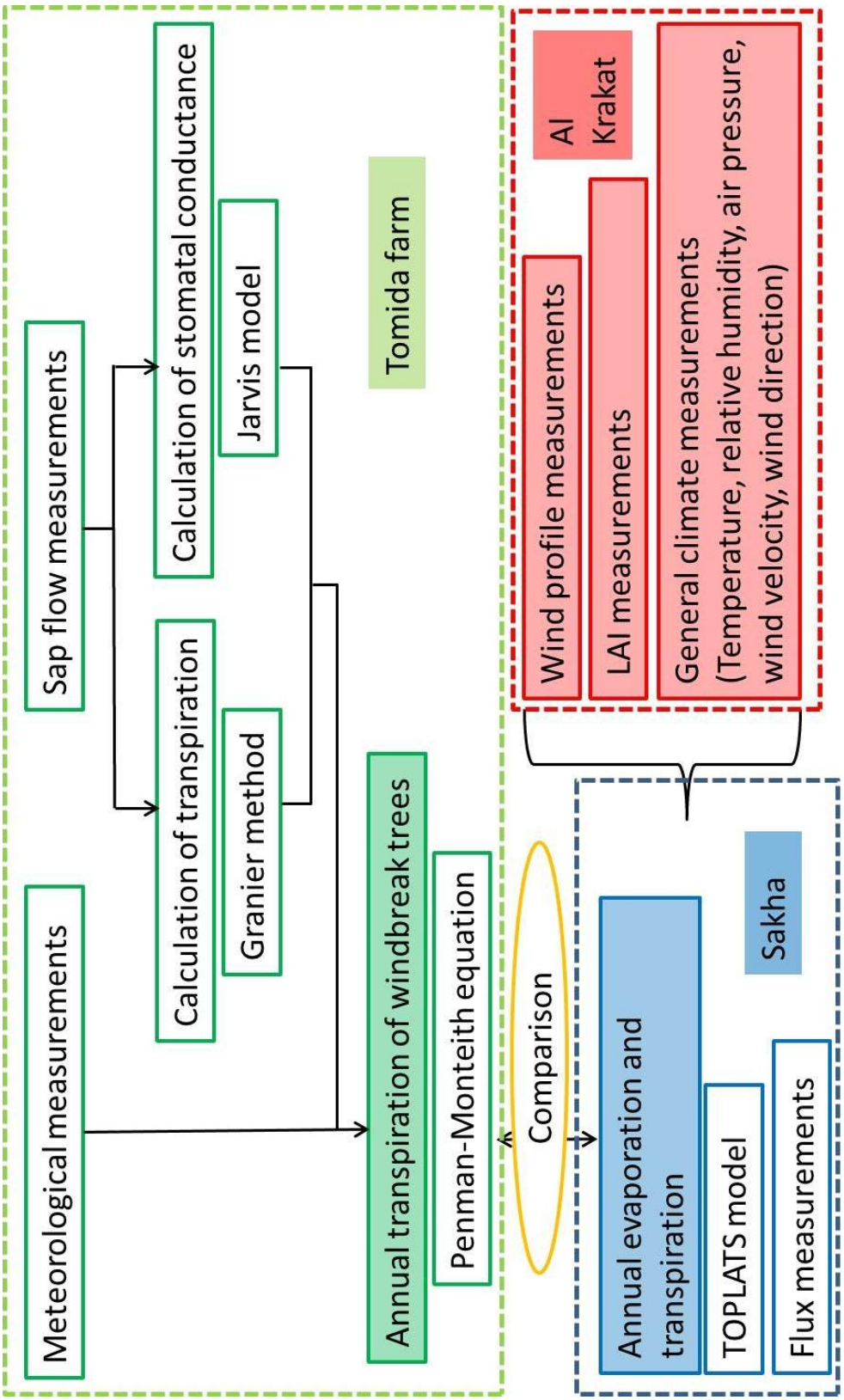

Figure 7 The Study flow of this study (Green part is to estimate transpiration of windbreak trees, Blue part is to estimate evaporation and transpiration from an agricultural land, and Red part is to measure environmental factors leeward of windbreak trees)

humidity deficit, leaf water potential and ambient CO_2 concentration) in a tree system as follows

$$k_s = k_s\left(Q_p\right)k_s\left(T\right)k_s\left(\delta e\right)k_s\left(\psi_l\right)k_s\left(C_a\right) \tag{1.2}$$

where Q_p is photon flux density, T is air temperature, δe is vapor pressure difference, ψ_l is leaf water potential and C_a is ambient CO_2 concentration. Jarvis (1976) regarded that k_s was given by these five environmental factors. These estimated values, such as $k_s(Q_p)$, $k_s(T)$, $k_s(\delta_e)$, $k_s(\Psi_l)$ and $k_s(C_a)$ mean relative surface conductance, and the ranges of each value were zero to one.

On the other hand, in Stewart (1988) who modified Jarvis (1976), surface conductance g_s is given in the following equation. Because of the littleness of impact of ambient CO_2 concentration, Stewart (1988) treated it as negligible, and instead of leaf water potential, soil moisture deficit was adopted.

$$g_s = LK_1g\left(S_t\right)g\left(\delta q\right)g\left(T\right)g\left(\delta\theta\right) \tag{1.3}$$

where L is LAI of tree, K_1 is a parameter which usually means the maximum value of surface conductance, S_t is solar radiation, δq is specific humidity deficit, T is temperature of the air and $\delta\theta$ is soil moisture deficit. These values, such as $g(S_t)$, $g(\delta q)$, $g(T)$ and $g(\delta\theta)$ mean relative surface conductance, and these ranges were zero to one. Actually at Tomida farm, because S_t was not measured, the regression equation between net radiation and solar radiation divided for Sakha AWS (Figure 21) data was applied for calculation of S_t at Tomida farm with the data of net radiation by the AWS at Tomida farm (Figures 18 - 20). Calder (1976) defined that $\delta\theta$ is difference between actual soil moisture and field capacity.To estimate surface conductance g_s as in a whole system of surface water balance, Stewart (1988) is more preferable for this study. Thus Stewart (1988) was adopted in this study, and g_s was estimated by measured three environmental factors (temperature, specific humidity deficit and soil moisture deficit) at Tomida farm and one estimated factor from the data at Sakha (solar radiation and CO_2 concentration).

In this study, the correlations between g_s and $g(Q_p)$, $g(T)$, $g(\delta q)$ and $g(C_a)$was estimated with Jarvis (1976) and $g(\delta\theta)$ was estimated with Stewart (1988). Finally surface conductance g_s was given from the following equation.

$$g_s = LK_1g\left(Q_p\right)g\left(T\right)g\left(\delta q\right)g\left(\delta\theta\right)g\left(C_a\right) \tag{1.4}$$

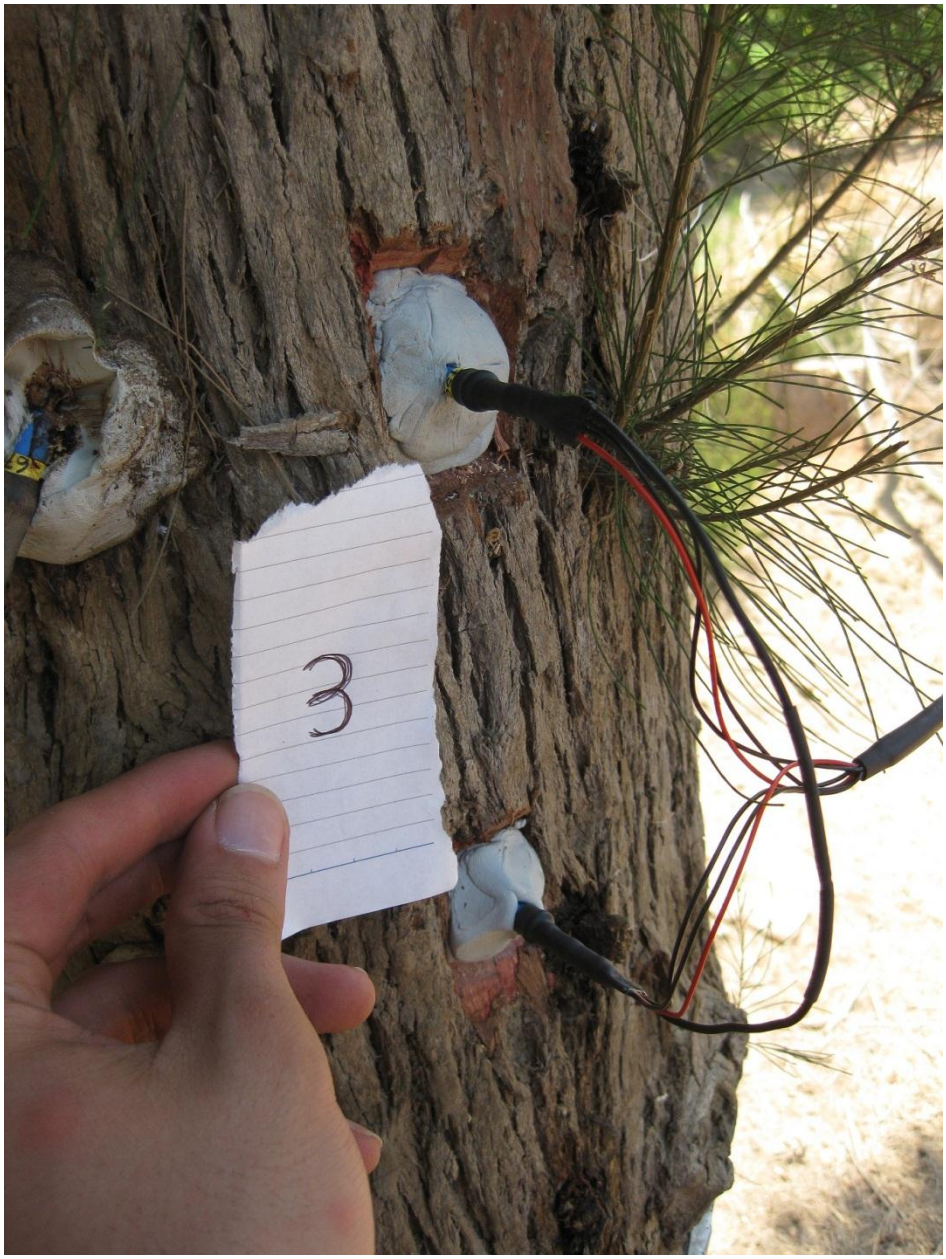

Figure 8　Photograph of a sapflow sensor which was attached on No. 3 (Tomida farm, July 2011)

Figure 9　One of the tree samples named No.11
(Tomida farm, August 2010)

Figure 10　One of the tree samples named No.6
(Tomida farm, August 2010)

Figure 11　One of the tree samples named No.5
(Tomida farm, August 2010)

Figure 12　One of the tree samples named No. 4
(Tomida farm, August 2010)

Figure 13　One of the tree samples named No. 3
(Tomida farm, August 2010)

Figure 14　The bottle which was filled with stain liquid was attached against tree stem to infuse stains into sap wood area to estimate sap wood area of the tree. This photograph was taken in preparatory experiment against *Japanese red pine* done in TERC, the University of Tsukuba in July 2010. (Shimizu, 2011)

Figure 15　The photograph of core samples of trees taken by an increment borer in August 2010. Left sides of core samples are bark and the red parts were dyed with stains. (Shimizu, 2011)

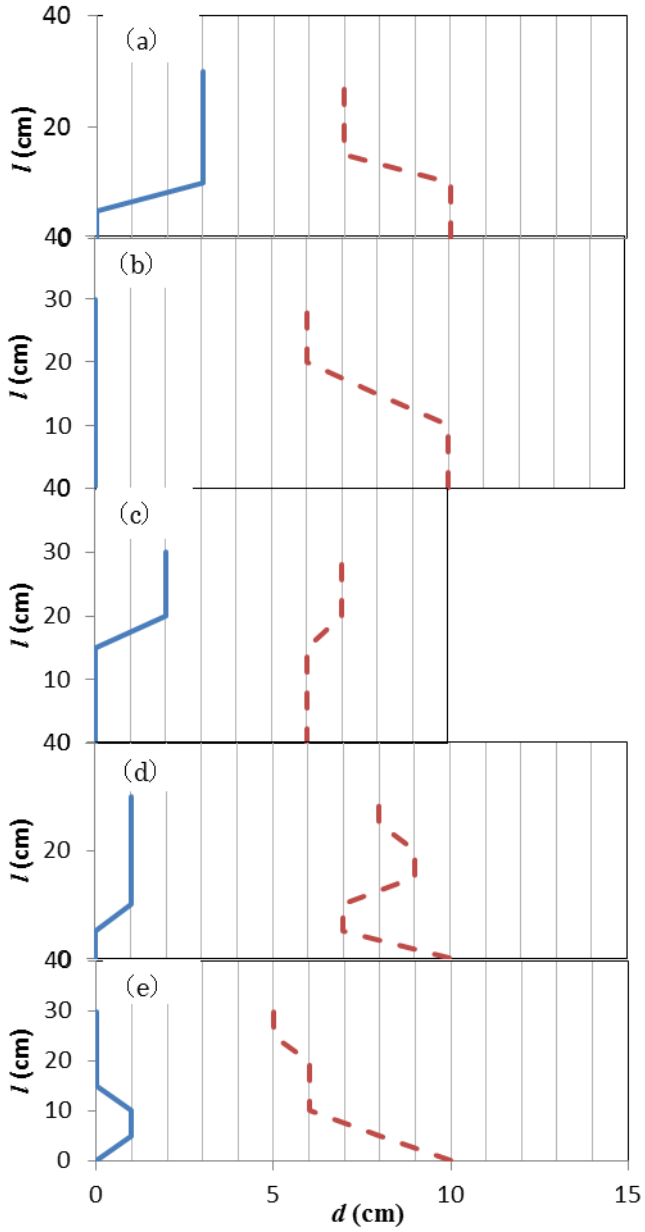

Figure 16　The results of estimation of sap wood areas of each tree sample, (a) No.11, (b)No.6, (c)No.5, (d)No.4 and (e)No.3. The x-axis means horizontal depth from the bark, and the y-axis means height from infusing point: *l* (cm). The areas between blue line and red line were estimated as sap wood areas. (Shimizu, 2011)

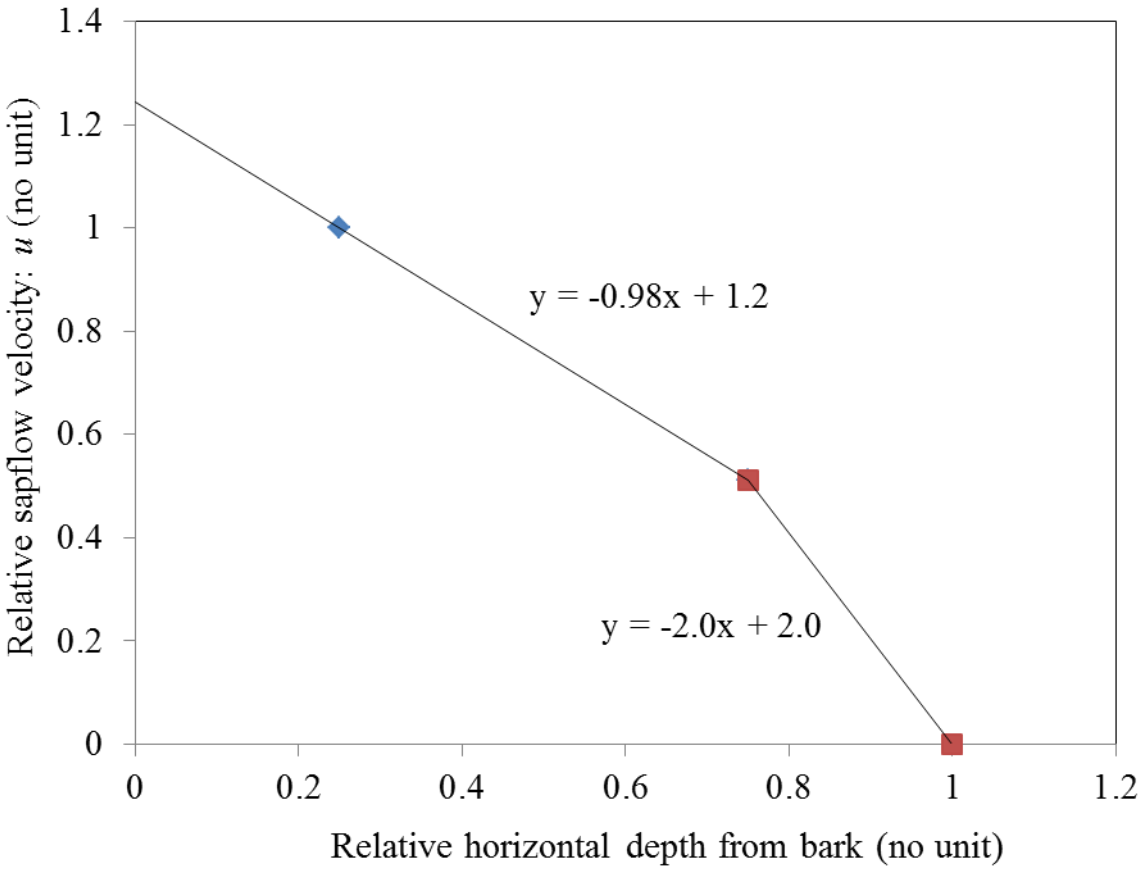

Figure 17　Horizontal variation of sapflow velocity in the sap wood area of No.11. The x-axis means relative horizontal depth from bark and the y-axis means relative sapflow velocity which based on the measured sapflow velocity near the bark. These three plots were determined by measurements. (Shimizu, 2011)

It was clarified in Stewart (1988) and Jarvis (1976) that each components $g(Q_p)$, $g(T)$, $g(\delta\theta)$, $g(\delta q)$, and $g(C_a)$ have correlations between g_s such as Figures 45 and 46, and each correlations were assumed to be given by the following equations.

$$g\left(Q_p\right)=\frac{b_1 b_2\left(Q_p-q\right)}{b_1+b_2\left(Q_p-q\right)} \tag{1.5}$$

where

$$b_1=\lim_{Q_p\to\infty} g\left(Q_p\right) \tag{1.6}$$

q and b_2 are parameters, and calibrated with measured g_s.

$$g\left(T\right)=b_3\left(T-T_l\right)\left(T_h-T\right)^{b_4}\ (0\le g\left(T\right)\le 1) \tag{1.7}$$

where

$$b_3=\frac{1}{\left(T_0-T_l\right)\left(T_h-T_0\right)^{b_4}} \tag{1.8}$$

$$b_4=\frac{T_h-T_0}{T_h-T_l} \tag{1.9}$$

$$g\left(\delta q\right)=1-K_3\delta q\left(0<\delta q<K_4\right) \tag{1.10}$$

$$=1-K_3K_4\left(K_4\le\delta q\right)$$

where K_3 is the slope of the relation.

$$g\left(\delta\theta\right)=1-\exp K_9 \tag{1.11}$$

where

$$K_9 = K_6\left(\delta\theta - \delta\theta_m\right) \tag{1.12}$$

$$g\left(C_a\right) = \begin{cases} 1 & (\text{Ca} < 250) \\ 1 - b_7 C_a & (250 < \text{Ca} < 800) \\ b_8 & (800 < \text{Ca}) \end{cases} \tag{1.13}$$

where

$$0 \le g\left(C_a\right) \le 1$$

where K_6 and $\delta\theta_m$ are parameters calibrated with measured g_s. In this study, the surface conductance was calculated by equations from (1.4) to (1.13) after calibrating each equation with measurements.

2-2-3. Penman-Monteith equation

In Penman-Monteith equation (Monteith, 1965), latent heat flux is given in the following equation.

$$L_e E_{pm} = \frac{\Delta\left(R_n - G\right) + \gamma L_e E_A}{\Delta + \gamma\left(1 + g_a / g_s\right)} \tag{1.13}$$

where

$$\Delta = \frac{abc}{\left(T+b\right)^2}\exp\left(\frac{aT}{T+b}\right) \tag{1.14}$$

$$\gamma = \frac{c_p p}{0.622 L_e} \tag{1.15}$$

$$g_a = \frac{1}{C_H \bar{u}} \tag{1.16}$$

$$C_H = \frac{k^2}{\ln\left(\frac{z}{z_0}\right)\ln\left(\frac{z}{z_{0h}}\right)} \tag{1.17}$$

$$L_e = a + bT \tag{1.18}$$

$$E_A = \rho \frac{0.622}{p} C_E \bar{u}\left(e^*\left(\bar{T}\right) - \bar{e}\right) \tag{1.19}$$

$$C_E = \frac{k^2}{\ln\left(\frac{z}{z_0}\right)\ln\left(\frac{z}{z_{0v}}\right)} \tag{1.20}$$

$$\rho = \rho_d \frac{T_0}{T + T_0} \frac{p}{p_s}\left(1 - 0.378\frac{e}{p}\right) \tag{1.21}$$

$$e^*\left(T\right) = c\exp\left(\frac{aT}{T+b}\right) \tag{1.22}$$

$$r = \frac{e}{e^*} \tag{1.23}$$

where E_{pm} is transpiration of tree in this study, L_e is evaporative latent heat, R_n is net radiation, Δ is saturated water vapor curve's gradient, E_A is aerodynamics term, G is soil heat flux, γ is psychrometric constant and g_a is aerodynamic conductance.

The input meteorological data were measured by the AWS at Tomida farm except for air pressure. The data of air pressure was from the AWS at Sakha, under the assumption that the air pressure at Tomida farm was similar to that of Sakha. A photograph of the AWS at Sakha is shown in Figure 21.

2-2-4. Estimation of annual transpiration of windbreak trees

For estimation of transpiration of windbreak trees, most of input data were from the AWS at Tomida farm and Sakha. The data of surface conductance which is one of the input data is calculated by Jarvis model. By substituting g_s calculated from Jarvis model into Penman-Monteith equation, the transpiration of windbreak trees was obtained as E_{pm} from Penman-Monteith equation. In estimating annual transpiration of windbreak trees,

Figure 18　Photograph of AWS at Tomida Farm
(Tomida farm, July 2011)

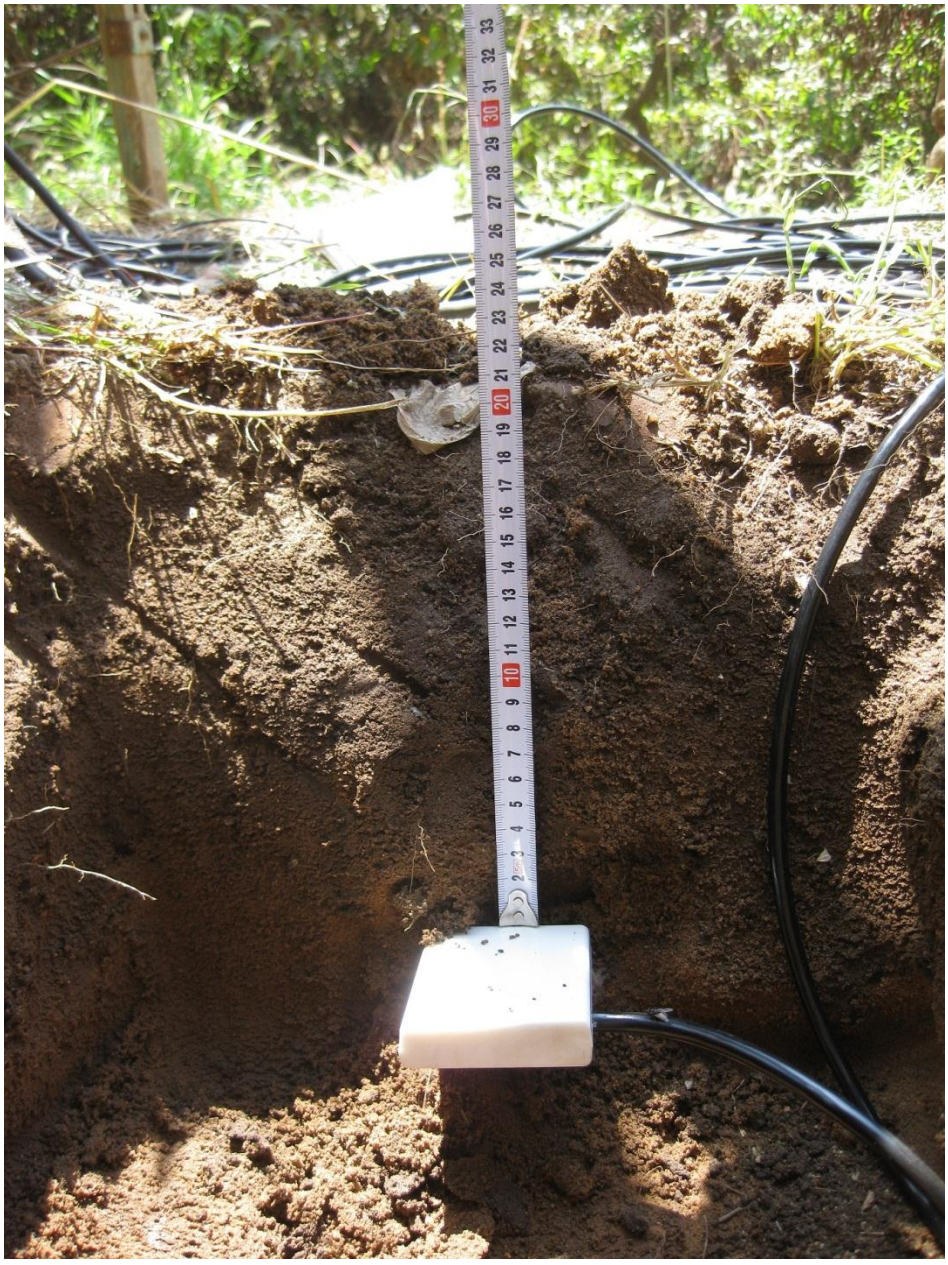

Figure 19　Photograph of TDR under the AWS at Tomida Farm
(Tomida farm, July 2011)

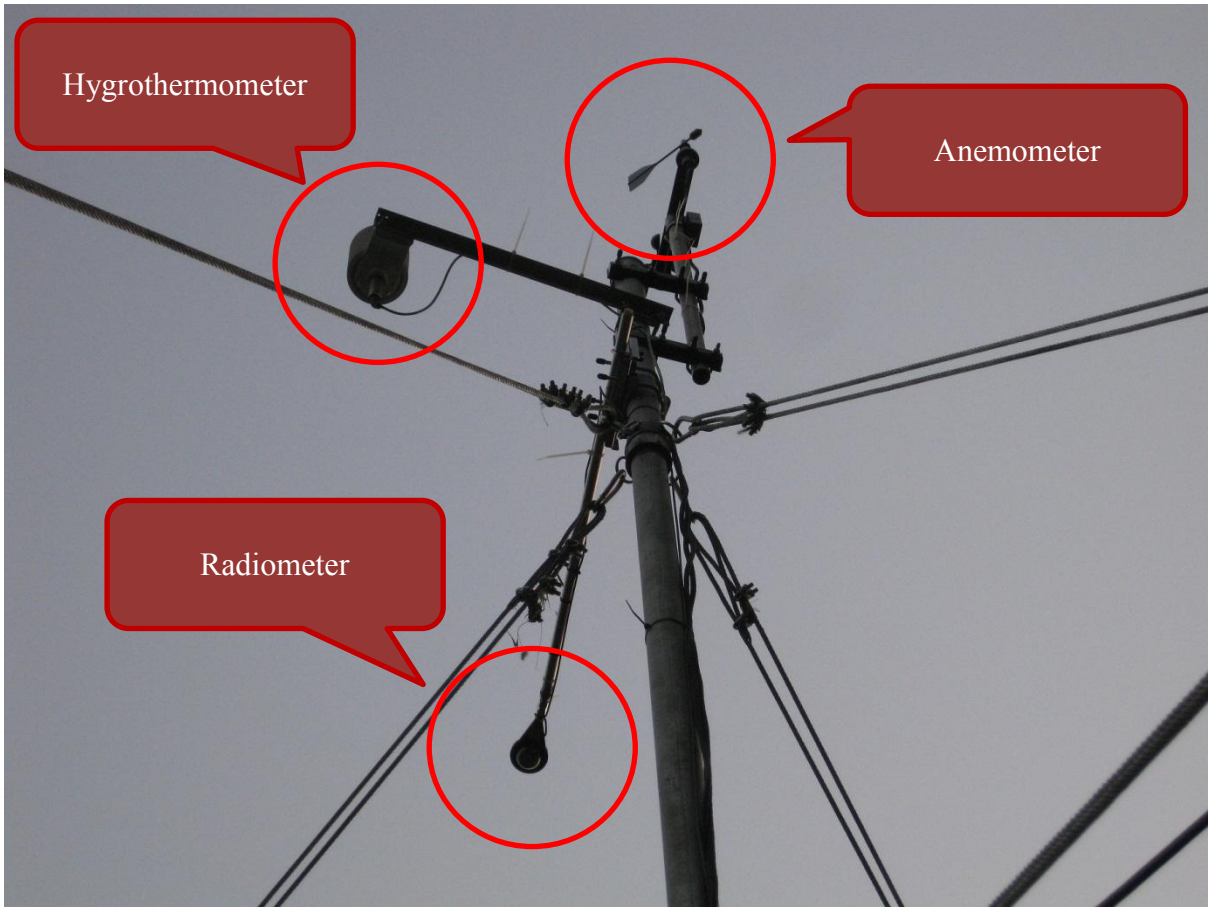

Figure 20　Photograph of the sensors at the top of the AWS at Tomida Farm (Tomida farm, July 2011)

g_s can be calculated by Jarvis model with four environmental factors, and transpiration of trees can be calculated by Penman-Monteith equation with meteorological data which were measured at a certain field and g_s from Jarvis model. In other words, transpiration of trees can be estimated by Penman-Monteith equation and Jarvis model with some meteorological data and LAI of the trees.

2-3. Measurements of meteorological data

2-3-1. Measurements of meteorological data for setting of the field in TOPLATS model

The agricultural land at Al Krakat can be divided by the windbreak trees into two fields, North side and South side, and the main wind direction was North in the measurement period, shown in Figures 69 and 72. At Al Krakat, some meteorological data were measured such as air temperature, wind velocity, maximum wind velocity, wind direction, air pressure and precipitation by Vaisala weather transmitter (WXT520). In this study, because there were no precipitation during measurement period, data of precipitation were not used. The meteorological data were measured six points, one sensor named No.1 for the North field of Al Krakat and five sensors named Nos.2-6 for south field. The No.1 sensor was set in 80 m distance north from windbreak trees, and the Nos.2-6 sensors were set at 10 m, 30 m, 60 m, 100 m and 150 m for each sensor south from windbreak trees, for the purpose of clarification of the horizontal profile of meteorological data against the distance from windbreak trees (Figure 22). The photographs of sensors and windbreak trees at Al Krakat are shown in Figures 23 - 26.

2-3-2. Measurements of characteristics of trees, crops and soil

The data of trees, crops and soil were also measured at the site, such as LAI, porosity of the windbreak trees, stomatal resistance, transpiration rate, height, surface temperature, soil evaporation, soil moisture and soil thermal conductivity. The measurement of LAI was done with Canopy Analyzer (LI-2000), stomatal resistance and transpiration rate was done with Leaf Porometer (LI-1600), surface temperature was with handy surface thermometer (MINOLTA), evaporation was with Chamber method (Matsuno, 2011), soil moisture was with handheld TDR (HydroSense Ⅱ) and soil thermal conductivity was with handheld thermal conductivity meter (KD2).

The porosity of the windbreak trees was estimated by an image analysis with Image J software. A photograph of the windbreak trees taken in Al Krakat was changed into a monochrome figure as shown in Figure 27, and the ratio of black-and-white part was analyzed by image analysis software as porosity of the windbreak trees. Actually 14 windbreak trees in the Nile-Delta were analyzed their porosity in the same method in the summer of 2011. The result of estimation of the porosity of 14 windbreak trees is shown in Table 4, and the locations of 14 windbreak trees are shown in Figure 28. The porosities

of the windbreak trees at Al Krakat and Tomida farm are shown in Table 5. As these results show, it can be said that the porosities of the windbreak trees which were observed at Al Krakat and Tomida farm were general in the Nile-Delta.

The data of LAI, height, surface temperature, evaporation, soil moisture and soil thermal conductivity were measured at six points of the Vaisala sensors. The photographs of each portable sensor and measurements are shown in Figures 29 and 30. The measurements of soil evaporation were done with chamber method as follows. One term of measurement contains 5 times measurements which were done by covering with a chamber. The evaporation was estimated by averaging values of measured vapor density ratio at five times. Detailed explanation was shown in Matsuno (2011).

2-4. Estimation of evaporation and transpiration in an agricultural land

2-4-1. TOPLATS model

The TOPLATS model (TOPMODEL-Based Land Surface-Atmosphere Transfer Scheme) was first proposed by Famiglietti *et al* (1992) and modified by Crow and Wood (2003). This model is for regional and global atmospheric models and studies of macro-scale water and energy balance and it was unified explicitly distributed and statistical version in this study. Thus in this study, the part of Land Surface- Atmosphere Scheme was used to estimate soil evaporation and transpiration of crops. The part of Transfer which means base-flow, water balance in a lake and so on was not used in this study. The input data were meteorological and radiation data, such as temperature, wind velocity, net radiation and relative humidity, and some parameters of crops and soil were required. The structures of inputs and outputs of TOPLATS model are schematically shown in Figure 31, as a conceptual figure.

2-4-2. Calculation of evaporation and transpiration in an agricultural land for both cases without and with windbreak trees

The seasonal variations of evaporation, transpiration and evapotranspiration in an agricultural land without windbreak trees were estimated by inputting the measured data as measured by the AWS at Sakha. In this study, an agricultural land was assumed same as the field at Sakha. This is ok as its shape and size are standard in the Nile-Delta. In the case of an agricultural land with windbreak trees, it was assumed that Sakha field has the same windbreak trees as those at Tomida farm whose transpiration and LAI were measured. Furthermore, the windbreak trees were assumed that they were planted at only a northern edge of the Sakha field in a line at an interval of 2 ~ 3 m. The reason why the windbreak trees were assumed to be on only Northern edge of Sakha field was the main wind direction at Sakha field is north in a year, shown in Figure 32. The horizontal profile of meteorological data and the data of crops and soil at the Sakha field were assumed

Figure 21　Photograph of the AWS at Sakha
(Sakha, July 2011)

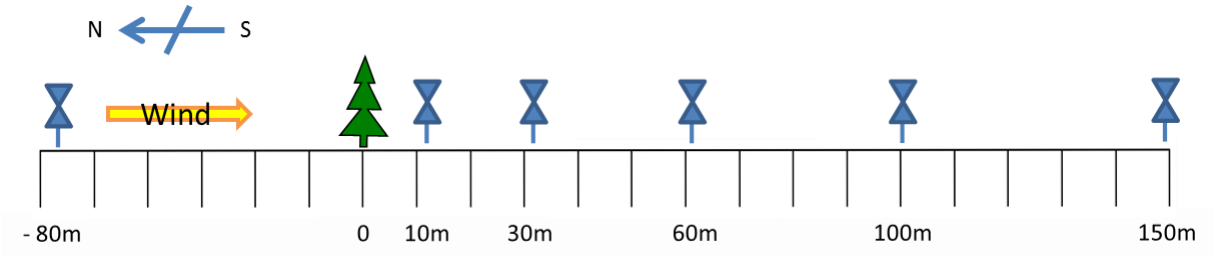

Figure 22 Figure showing sensor settings at Al Krakat. Blue figures show sensors.

Figure 23　A set of Vaisala sensor for meteorological measurements
(Al Krakat, August 2012)

Figure 24　A sensor and the windbreak trees from North side
(Al Krakat, August 2012)

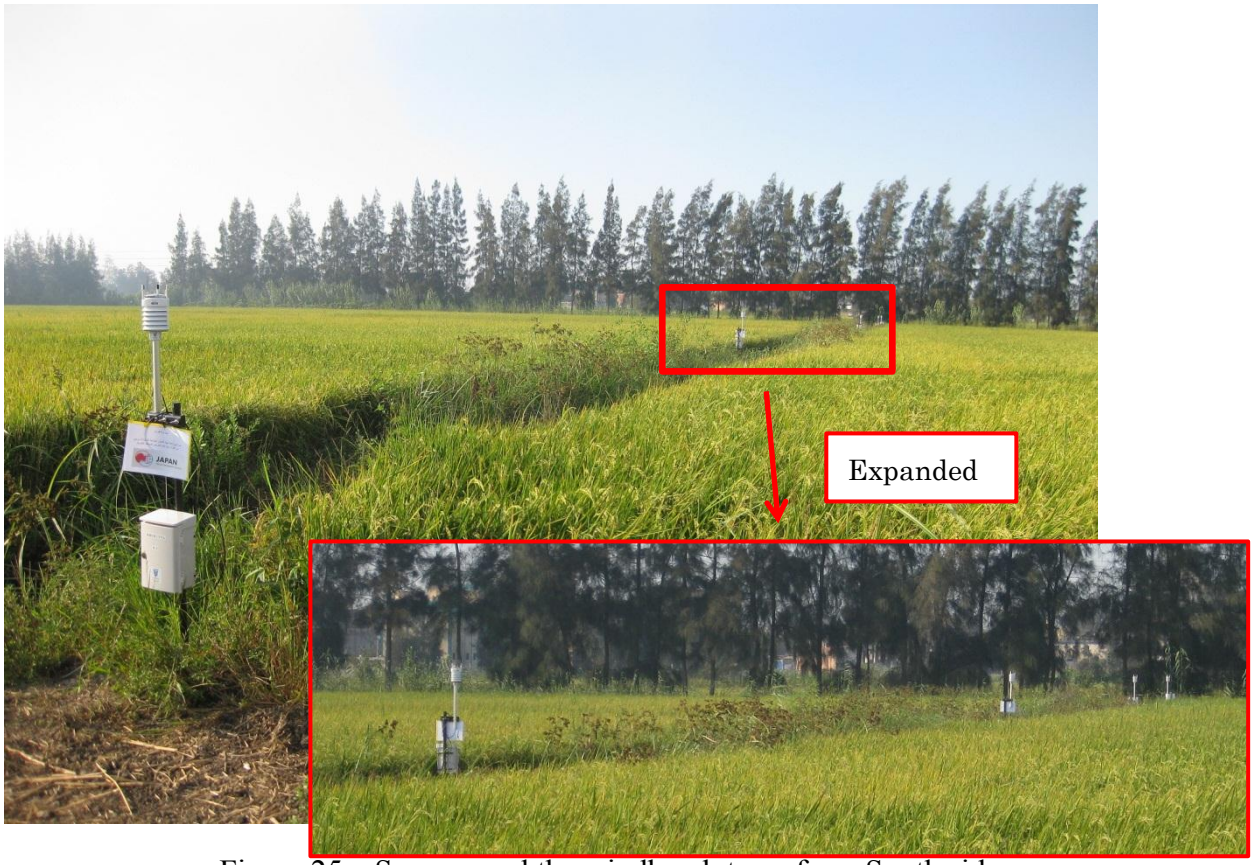

Figure 25 Sensors and the windbreak trees from South side

(Al Krakat, August 2012)

Figure 26　Target windbreak trees at Al Krakat from North side
(Al Krakat, August 2012)

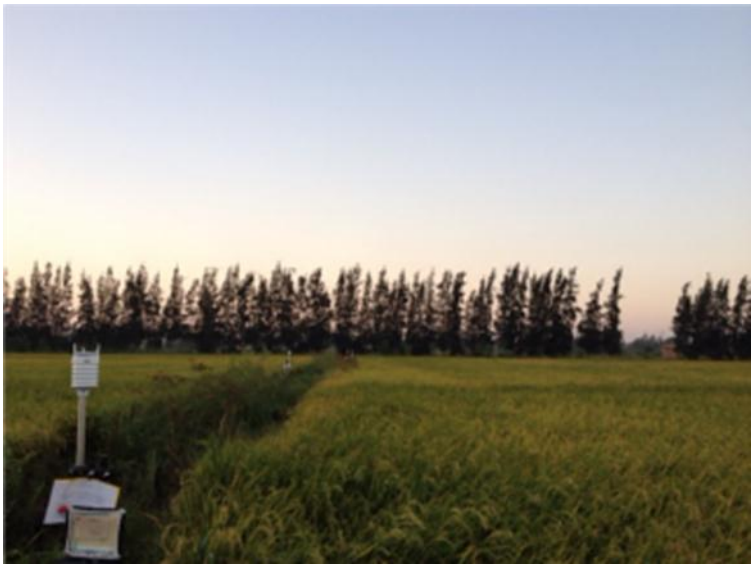

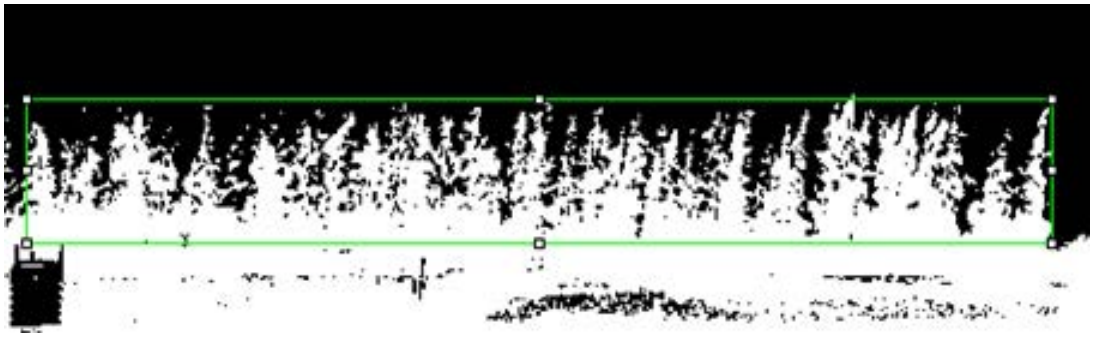

Figure 27 A black-and-white figure of the windbreak trees at Al Krakat (analyzed with Image J software). In this analysis, the porosity of the windbreak trees could be estimated as the ratio of black part and white part in the area surrounded by a green line.

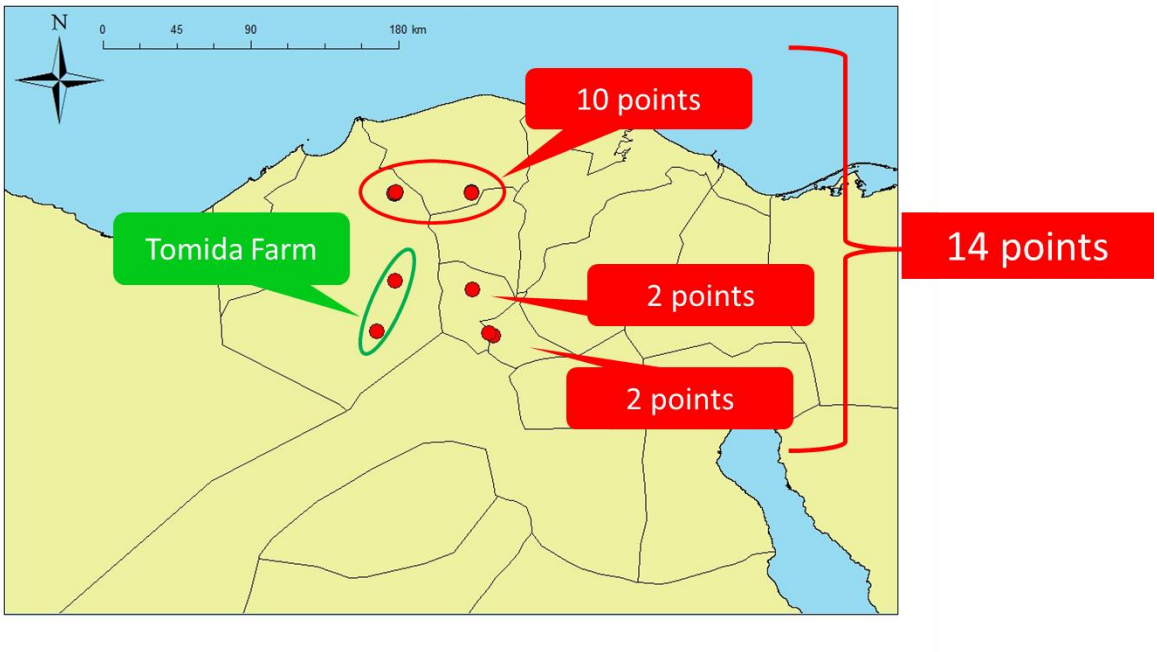

Figure 28 The locations of 14 points for estimation of porosities of windbreak trees in the Nile-Delta measured in July 2011.

Table 4　Estimated porosities of windbreak trees at 14 points in the Nile-Delta

	Porosity (%)
Place 1	41.7
Place 2	52.6
Place 3	47.7
Place 4	42.3
Place 5	51.4
Place 6	50.4
Place 7	52.6
Place 8	43
Place 9	52.4
Place 10	40.7
Place 11	46.5
Place 12	44.3
Place 13	42
Place 14	44.6
Average	46.6

Table 5　Estimated porosities of windbreak trees at Tomida farm and Al Krakat

Windbreak trees	Tomida Farm	Al Krakat
Porosity (%)	52.7	43.6

same as those measured at Al Krakat. So the inputted meteorological data, especially the data of wind velocity, was estimated based on the measured horizontal profile at Al Krakat. And the grid size was set as 10 m × 10 m. The calculation processes of TOPLATS model are shown below. The estimated transpiration E_{bs} was given in following equation.

$$E_{bs} = \min\left[E_1, E_2\right] \tag{1.24}$$

where e_1 is given in following equation by provided by Monteith and Unsworth (1990)

$$E_1 = \frac{\Delta \times \left(R_n - G\right) + c_p \times \rho \times VPD \cdot g_a}{\left(\Delta + p_s\right) \times L_e} \tag{1.25}$$

where Δ is gradient of saturated water vapor curve, R_n is net radiation, G is soil heat flux, c_p is specific heat at constant pressure, ρ is air density, r_a is aerodynamic resistance, p_s is psychrometric constant which includes consideration of soil resistance, L_e is latent heat for vaporization, and VPD is given in following equation

$$VPD = e^* - e \tag{1.28}$$

where e^* means saturated water vapor pressure and e is water vapor pressure. The air density ρ is given in Equation (1.21). The aerodynamic resistance r_a is given in following equation provided by Brutsaert and Sticker (1979)

$$g_a = \left\{ \frac{1}{0.4^2 \times u} \log\left(\frac{z_a - z_{pd}}{z_{0h}} \right) \log\left(\frac{z_w - z_{pd}}{z_{0m}} \right) \right\}^{-1} \tag{1.32}$$

where u is horizontal wind velocity, z_a is the height of measurement of meteorological data, z_{pd} is zero-plane displacement, z_{0h} is roughness length for heat transfer, z_w is the height of measurement of wind velocity, z_{0m} is roughness length for momentum transfer. The psychrometric constant which includes consideration of soil resistance p_s is given in following equation

$$p_s = \gamma \left(1 + \frac{r_s}{r_a} \right) \tag{1.33}$$

Figure 29　Measurement of tree's stomatal resistance by LI-1600
(Tomida farm, August 2012)

Figure 30　Measurement of soil moisture and soil thermal conductivity by HydroSense Ⅱ and KD2 (Sakha, September 2012)

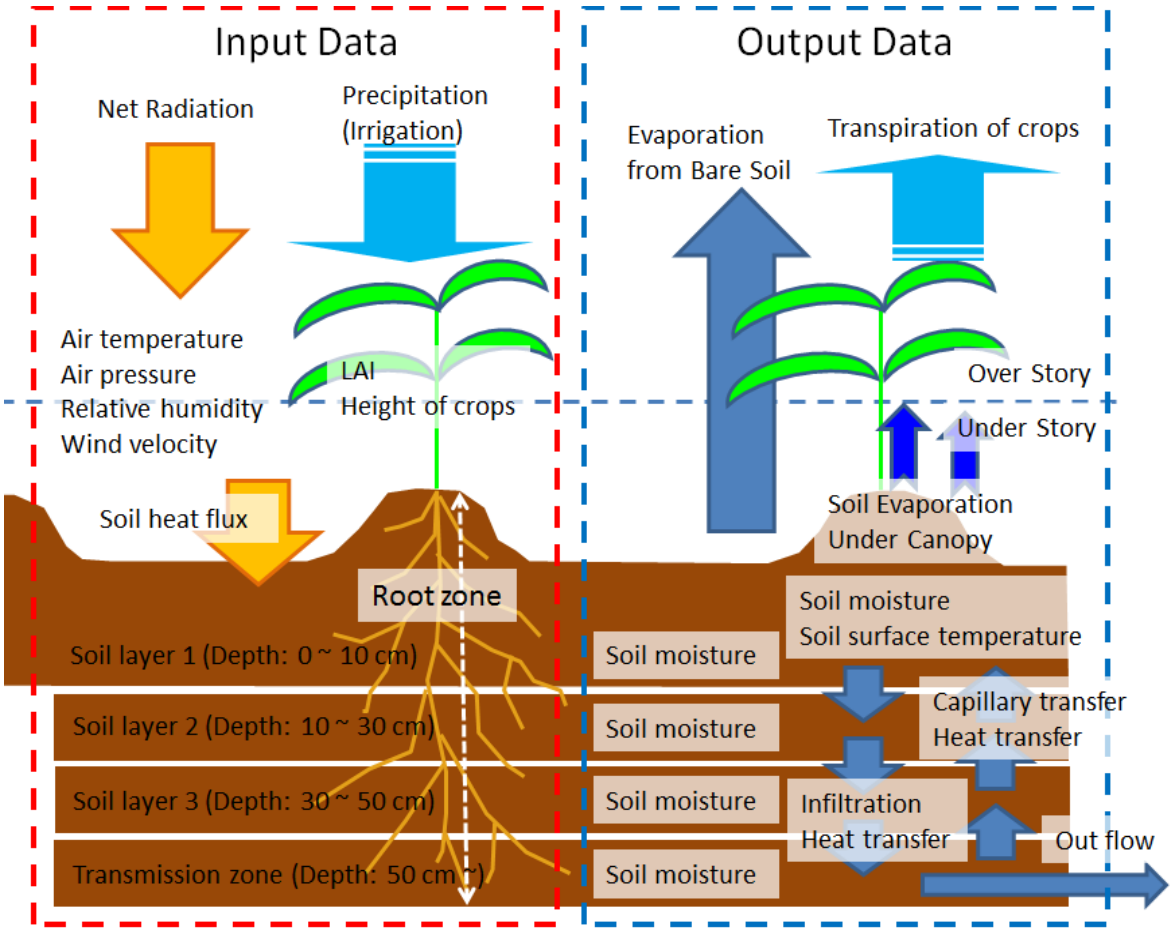

Figure 31 Conceptual figure of TOPLATS model (Input and Output data)

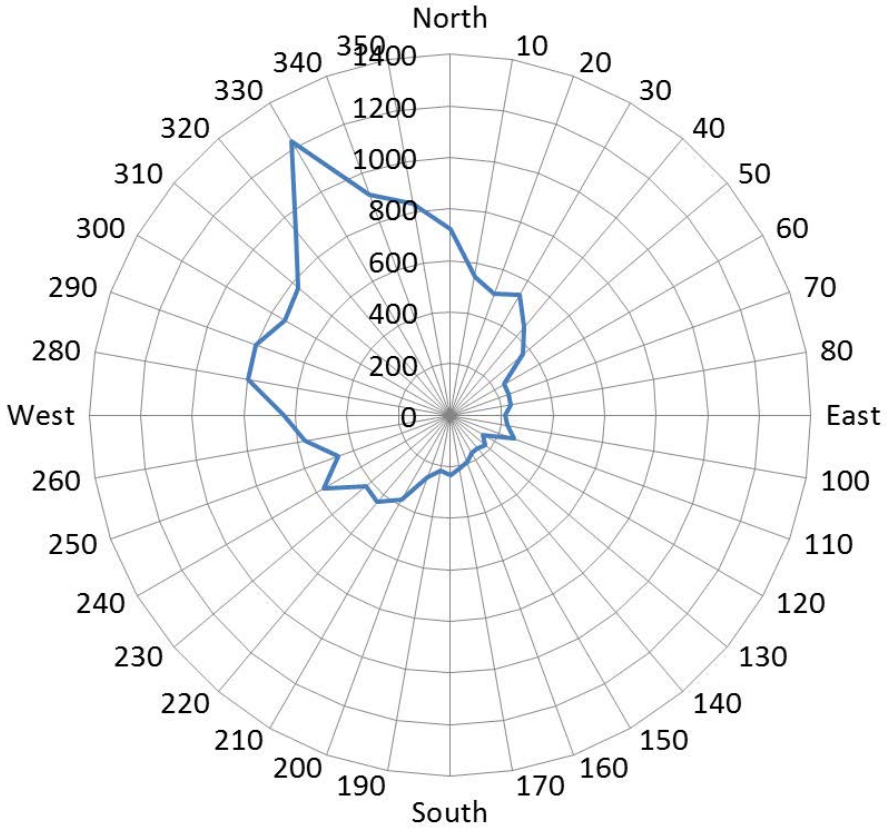

Figure 32 Annual wind rose at Sakha field (2010/10/1 ~ 2011/9/30). Main wind direction is from North to South.

where γ is psychrometric constant, r_s is soil resistance, and γ is given in Equation (1.15). In this study, the soil resistance r_s is given in following equation provided by Sun (1982)

$$r_s = 3.5\left(\frac{\theta_s}{\theta}\right)^{2.3} + 33.5 \tag{1.35}$$

The e_2 equals to e_1 when soil resistance r_s assumed to be 0. Next, the transpiration of crops is given in following equation

$$E_{dc} = \min\left(E_3, E_4\right) \tag{1.40}$$

where e_3 is given in following equation provided by Feyen *et al*. (1980)

$$E_3 = \frac{P_{soil} + P_{leaf}}{R_{soil} + R_{plant}} \tag{1.41}$$

where P_{soil} is soil water potential, P_{leaf} is leaf critical water potential, R_{soil} is resistance from soil, R_{plant} is resistance from plants. The soil water potential P_{soil} is given in following equation

$$P_{soil} = -\frac{\psi_b}{R_s^{1/B}} \tag{1.42}$$

where ψ_b is air incursion, R_s is valid soil saturation, B is Brooks-Corey pore size distribution reference. The valid soil saturation R_s is given in following equation

$$R_s = \frac{\theta - \theta_r}{\theta_s - \theta_r} \tag{1.43}$$

where θ is soil water content, θ_r is residual soil moisture, θ_s is saturated soil moisture. The resistance from soil R_{soil} is given in following equation provided by Feyen et al. (1980)

$$R_{soil} = \frac{1}{A \times K \times D} \tag{1.44}$$

where A is root activity factor, K is unsaturated hydraulic transmissivity, D is root density. The unsaturated hydraulic transmissivity K is given in following equation provided by Famiglietti et al. (1994)

$$K = K_z \times R_s^{\frac{2+3B}{B}} \tag{1.45}$$

where K_z is saturated hydraulic transmissivity, ff is TOPMODEL parameter, z_{rz} is depth from soil surface, and K_z is given in following equation

$$K_z = K_s \times \exp\left(-ff \times z_{rz}\right) \tag{1.46}$$

The resistance from plants R_{plant} is given in following equation provided by Feyen et al. (1980)

$$R_{plant} = \frac{r_t}{D} \tag{1.47}$$

where r_t is root resistance. Next, e_4 is given in following equation

$$E_4 = \frac{v_p \times \left(R_n - G\right) + c_p \times \rho \times VPD / \left(f_1 f_3 f_4 / g_e + 1/g_a\right)}{\left(v_p + p_s\right) \times L_e} \tag{1.48}$$

where f_1 is limiting factor due to PAR to canopy resistance, f_3 is limiting factor due to vapor pressure deficit to canopy resistance, f_4 is limiting factor due to air temperature to canopy resistance and r_e is plant resistance. The plant resistance r_e is given in following equation provided by Jacquemin and Noilhan (1990)

$$g_e = \left(\frac{r_{s\min}}{LAI}\right)^{-1} \tag{1.49}$$

where r_{smin} is minimum stomatal resistance, LAI is leaf area index. The limiting factor due to PAR to canopy resistance f_1 is given in following equation provided by Jacquemin and Noilhan (1990)

$$f_1 = \frac{1+f}{f + r_{s\min}/r_{s\max}} \tag{1.50}$$

where r_{smax} is maximum stoamtal resistance and f is given in following equation

$$f = 0.55 \times \frac{R_g}{R_{gl}} \times \frac{2}{LAI} \tag{1.51}$$

where R_{gl} is radiation parameter. The limiting factor due to vapor pressure deficit to canopy resistance f_3 is given in following equation provided by Jacquemin and Noilhan (1990)

$$f_3 = \frac{1}{1 - f_{3par} \times VPD} \tag{1.52}$$

where f_{3par} is parameter due to vapor pressure deficit by plant resistance r_e. The limiting factor due to air temperature to canopy resistance f_4 is given in following equation provided by Jacquemin and Noilhan (1990)

$$f_4 = \frac{1}{1 - f_{4par} \times \left(t_{ref} - t_c\right)^2} \tag{1.53}$$

where f_{4par} is parameter due to air temperature by plant resistance r_e, t_{ref} is reference air temperature due to plant resistance.

2-4-3. Parameters

In TOPLATS model analysis, some parameters of the canopy, soil and aerodynamic factors had to be determined. The time constant parameters are shown in Tables 6 and 7 with units, values and their sources. The time varying parameters, such as LAI of crops, roughness length for momentum transfer, roughness length for heat transfer and zero-plane displacement are shown in Table 8.

2-5. Definition of the effectiveness of windbreak trees

In the consideration of the effectiveness of windbreak trees, the addition of outputs of water in the water balance of an agricultural land and the growth of crops must be

Table 6　Time constant parameters in TOPLATS model settings

Parameters	**Value**	**Characteristics**	**Source**
Brooks-Corey pore size distribution index	0.25	Adopting similar soil	Ino (2002)
Bubbling pressure (m)	0.01	From measurement at local fields	Hoshino (personal communication)
Saturated soil moisture	0.63	From measurement at local fields	Hoshino (personal communication)
Residual soil moisture	0.35	Adopting similar soil	Sugita and Kotoda (1985)
Surface saturated hydraulic conductivity (m/s)	1.66×10^{-5}	From measurement at local fields	Hoshino (personal communication)
Depth of deep soil temperature (m)	0.4	From measurement at local fields	Fukuda (2012)
Temperature for deep soil layer (K)	302.15	From measurement at local fields	Fukuda (2012)
Depth of mid soil temperature (m)	1	From measurement at local fields	Fukuda (2012)
Initial mid soil temperature (K)	281	From measurement at local fields	Fukuda (2012)
Heat capacity of dry soil ($J/kg/m^3$)	2.26×10^{-6}	Adopting similar soil	Tani (1982)
Quartz content (%)	0.35	From measurement at local fields	Tsuchihira (2011)
Root fraction in each layer (Sakha)	0.53, 0.47, 0	From measurement at local fields	Tsuchihira (2011)
LAI for canopy storage	0	From measurement at local fields	Tsuchihira (2011)
Albedo for dry surface	0.11	From measurement at local fields	Fukuda (2009)
Albedo for wet surface	0.11	From measurement at local fields	Fukuda (2009)
Emissivity	0.95	Adopting similar soil	Tsuchihira (2011)

Table 7　Time constant parameters in TOPLATS model settings

Parameters	Values	Characteristics	Sources
Minimum stomatal resistance (s/m)	87	From measurement at local fields	Fukuda (2012)
Maximum stomatal resistance (s/m)	5000	From measurement at local fields	Chen and Dudhla (2001)
Radiation parameter for PAR adjustment to canopy resistance (W/m^2)	30	Adopting similar vegetation	Jacquemin and Noilhan (1990)
Parameter for vapor pressure deficit adjustment to canopy resistance	0.06	Adopting similar vegetation	Jacquemin and Noilhan (1990)
Parameter for temperature adjustment to canopy resistance	0.0016	Adopting similar vegetation	Jacquemin and Noilhan (1990)
Reference temperature used in temperature adjustment to canopy resistance	298	Adopting similar vegetation	Jacquemin and Noilhan (1990)
Parameter for calculation of vegetation transmission factor used to calculate ground heat flux under vegetation	0.4	Adopting similar vegetation	Choudhury et al. (1987)
Root activity factor	250	Adopting similar vegetation	Hanawa (2007)
Root density ($1/m^2$) (Sakha)	87.3	From measurement at local fields	Tsuchihira (2011)
Root resistivity (s/m)	6.00×10^8	Adopting similar vegetation	Hanawa (2007)
Critical leaf water potential (m)	-210	Adopting similar vegetation	Famiglietti et al. (1994)
Extinction coefficient of solar radiation in the canopy (Sakha)	0.44	From measurement at local fields	Tsuchihira (2011)
Flux in saturated soil (m^3/s)	2000	Adopting similar soil	Hanawa (2007)
TOPMODEL parameter ff	3.8	Adopting similar soil	Hanawa (2007)
Depth of initial average groundwater table (m)	1.27	From measurement at local fields	Tsuchihira (2011)

Table 8　Time varying parameters in TOPLATS model settings

Parameter	Range	Source
LAI for energy balance	0 - 4.38	Fukuda (2009) Maruyama (personal communication)
Roughness length for momentum transfer (m)	0.01 - 0.32	Estimated with Measured data
Roughness length for heat transfer (m)	0.001 - 0.032	Estimated with Measured data
Zero plane displacement (m)	0.2 - 1.09	Estimated with Measured data

specified. First, it was assumed that windbreak trees reduce certain amount of evaporation in an agricultural land, and the amount of reduced evaporation must be larger than that of the transpiration of windbreak trees to regard the windbreak trees be effective against reduction of evaporation. If the transpiration of windbreak trees is larger than the amount of reduced evaporation, it is better not to plant the windbreak trees in an aspect of water balance of an agricultural land. However, if the amount of transpiration of windbreak trees equals to the amount of reduced evaporation, the windbreak trees are also effective against reduction of evaporation, because *Casuarina* can be used as a useful material such as building materials in architecture industries. These mechanisms of evaporation reduction are shown in Figure 33 as a conceptual figure. On the other hand, even if the transpiration of windbreak trees is less than or equal to the amount of reduced evaporation, windbreak trees must not prevent the crops from growing by reducing the transpiration of crops which support the growth of crops. According to the mechanism of windbreak trees which reduce evaporation, certain amount of the transpiration of crops also is simultaneously reduced. Therefore, it must be considered whether the reduction of crops' transpiration does not prevent crops from growing. After these considerations, the effectiveness of windbreak trees can be validated for the reduction of evaporation.

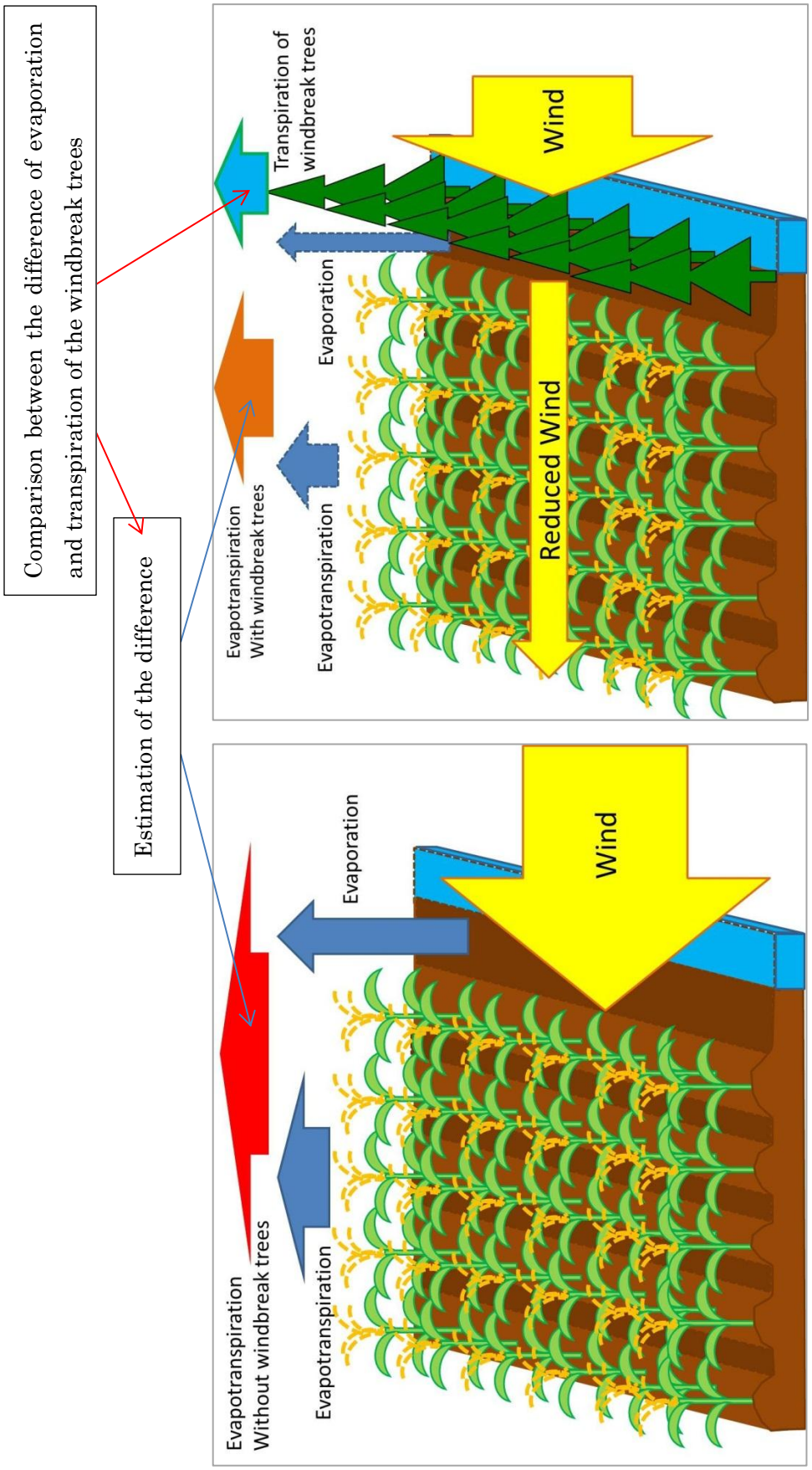

Figure 33 How to validate the effectiveness of windbreak trees

3. Results

3-1. Estimation of annual transpiration of windbreak trees

3-1-1. Measured transpiration at Tomida farm

The seasonal variations of difference of temperature between probes of sapflow sensors are shown in the Figure 34 for each sensor and the result of measurements of projected leaf areas and sapwood areas of samples at Tomida farm are shown in Table 6. As Table 6 shows, these values suggest the size of trees, such as DBH which means diameter at bust height, height of trees and projected leaf area. DBH was measured in 2010 with a scale for each sample. The reason why these five trees were chosen as samples is the frequency distribution of trees at Tomida farm. In Tomida farm, there a lot of *Casuarina*, and the frequency of size of trees is scattered. Thus the frequency distribution of DBH was made, and the classes of ranks of DBH of trees were divided into five classes. Therefore, these five samples represent the classes for each sample well.

The projected leaf areas of samples were measured by walking under the tree crown with holding GPS, and recorded data of GPS were appeared as circles in map software, e. g., MapSource. Then the circles which mean the projected leaf areas of samples were estimated their areas on the map software. At the same time, projected leaf areas were measured by another method as follows. Two people hold each edge of a scale, and one stays beside the stem of a sample, another person walks under the edge of tree crown. Then the distances from the tree stem in eight directions were measured. Therefore, the brief shapes of projected leaf areas of each sample appeared as five octagons in a map. Then the areas of five octagons were estimated and treated as the projected leaf areas.

The seasonal variations of the transpiration of each sample are shown in Figure 35. These variations of transpiration were estimated by the multiplication of sapflow and sapwood area from the measurements against each five samples, and transpiration (mm/day) was calculated by division of transpiration (volume) by projected leaf area. In these charts of transpiration of each tree sample, the values of transpiration are different from each other, and small scale sample seemed to have small transpiration. Daily variations of transpiration of No.6, 4 and 3 were much smaller than that of No.11 and 6. This result also implies that there seemed to be some correlation between scale of tree and its amount of transpiration. Especially, the variation of transpiration of No.3 was the smallest, and the amount was remarkably small. The results of consideration of the correlation between transpiration and trees' characteristics, such as projected leaf area, LAI, DBH and tree height for each tree sample are shown in Figures 36 - 41. According to these characteristics which represent the size of each tree, as these characteristics get larger, transpiration of each tree get larger at the same time. Additionally, these results were similar to Fujiyama et al. (2005) and Poyatos et al. (2005) which clarified the correlation between transpiration or sapflow velocity of trees and DBH and projected leaf

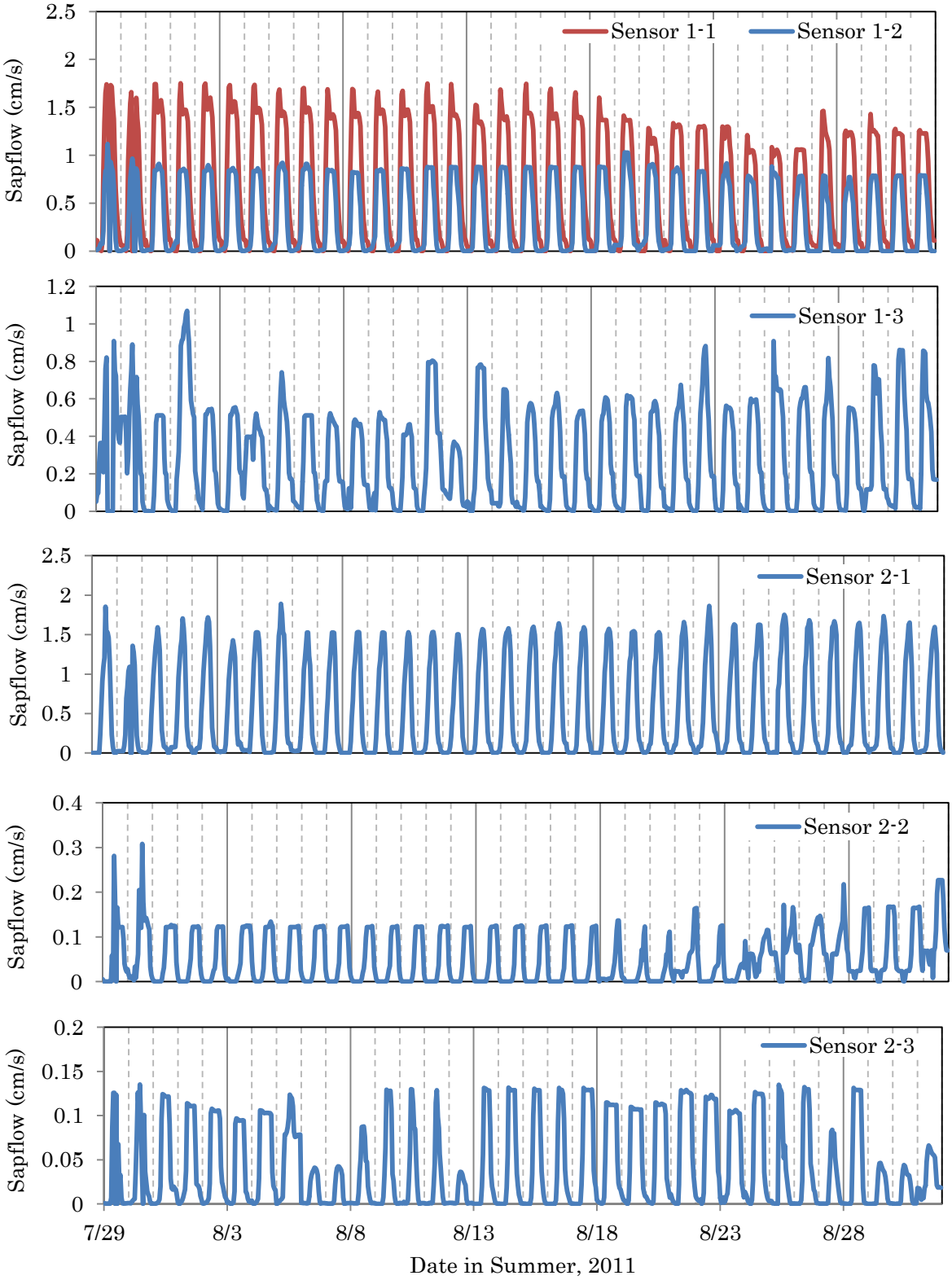

Figure 34　Daily variation of sapflow (cm/s) of 5 samples

Table 9　Characteristics of each tree sample

Samples	No. 11	No. 6	No. 5	No. 4	No. 3
DBH (cm)	51.6	27.8	67.6	82.8	43.4
Height (m)	12.9	9.8	16	11	6.3
Sapwood area (cm^2)	766	411	1057	1693	705
Projected Leaf area (m^2) in 2011	141.2	20.2	211.9	274.2	19.9

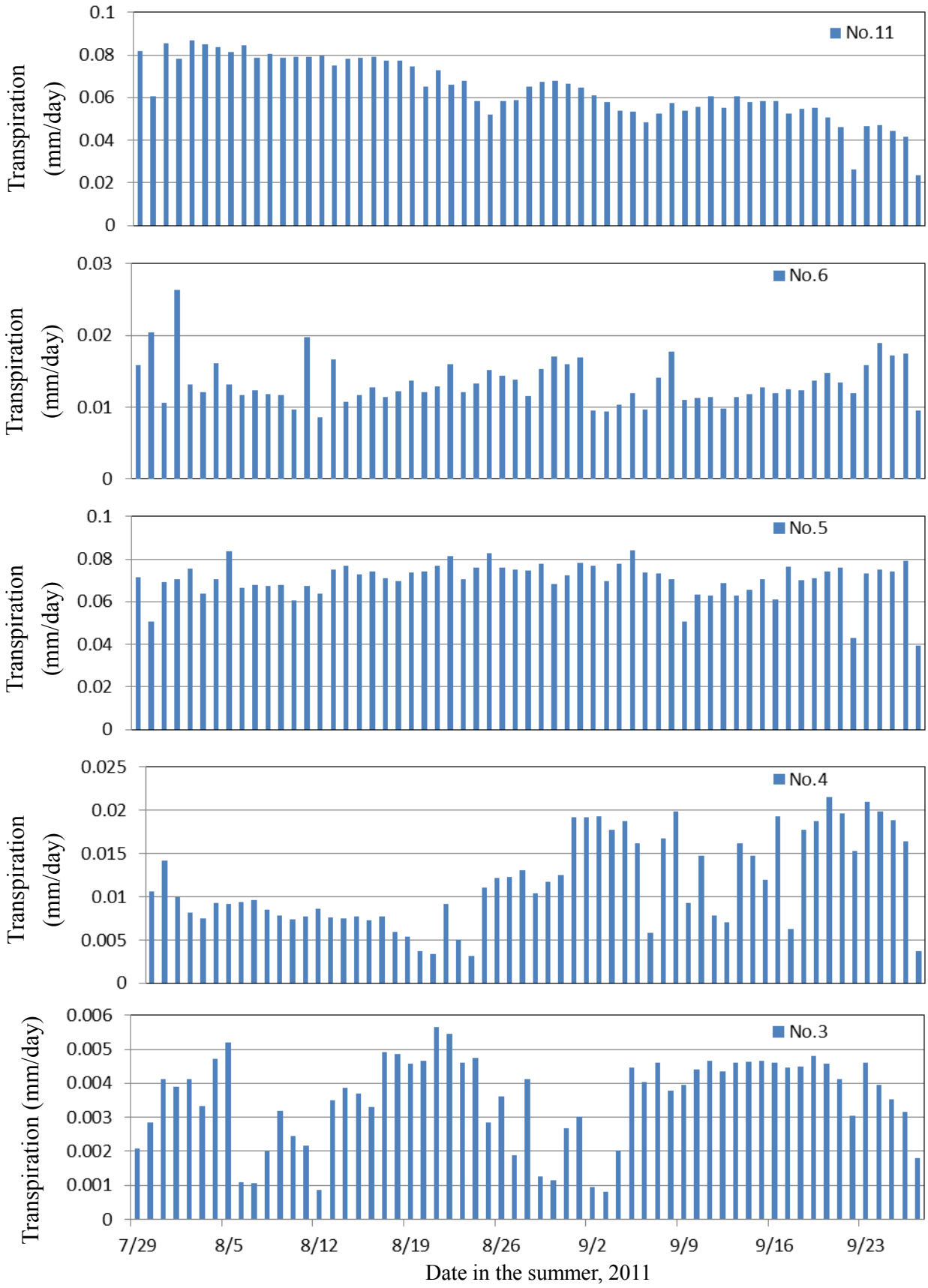

Figure 35 Variation of daily integrated transpiration per unit projected leaf area of each sample in the summer of 2011

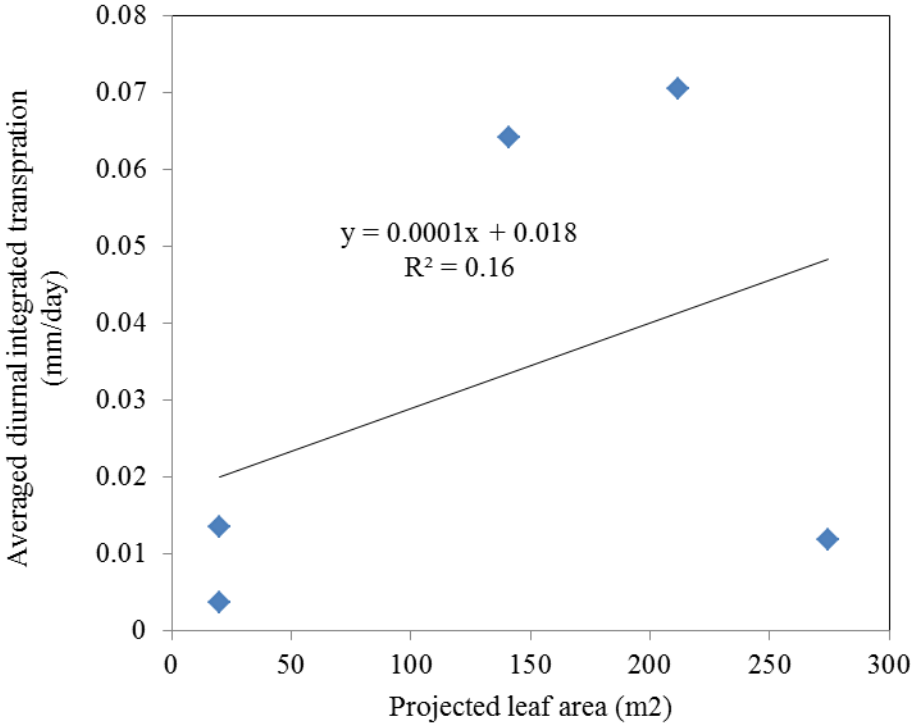

Figure 36　The correlation between transpiration and projected leaf areas of 5 tree samples at Tomida farm. Diurnal integrated transpiration was averaged in the measurement period.

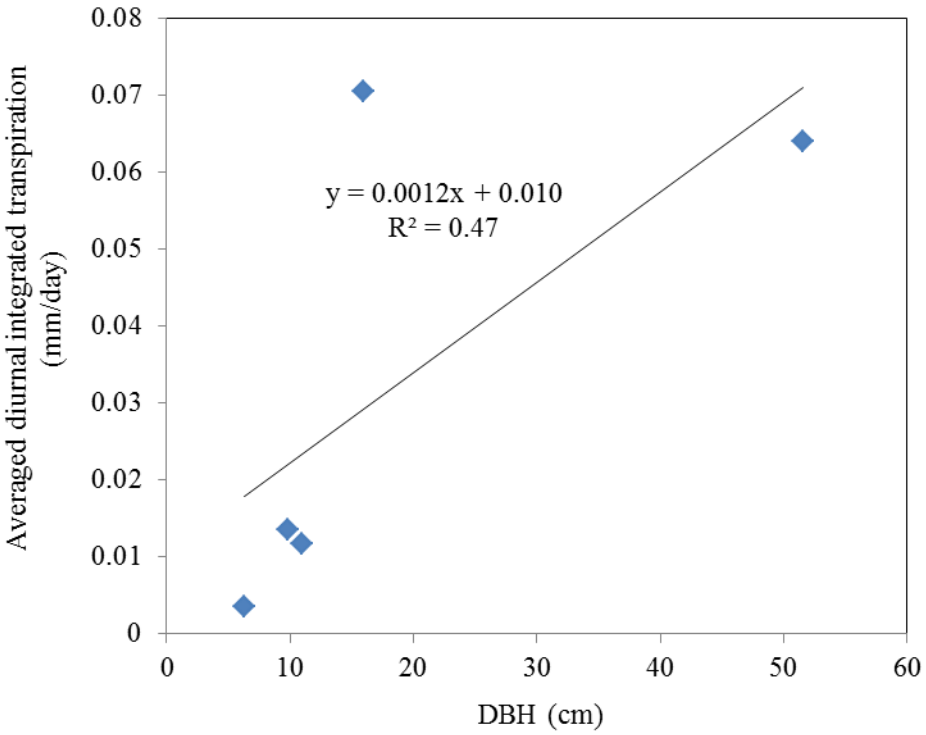

Figure 37　The correlation between transpiration and DBH (diameter at breast height) of 5 tree samples at Tomida farm. Diurnal integrated transpiration was averaged in the measurement period.

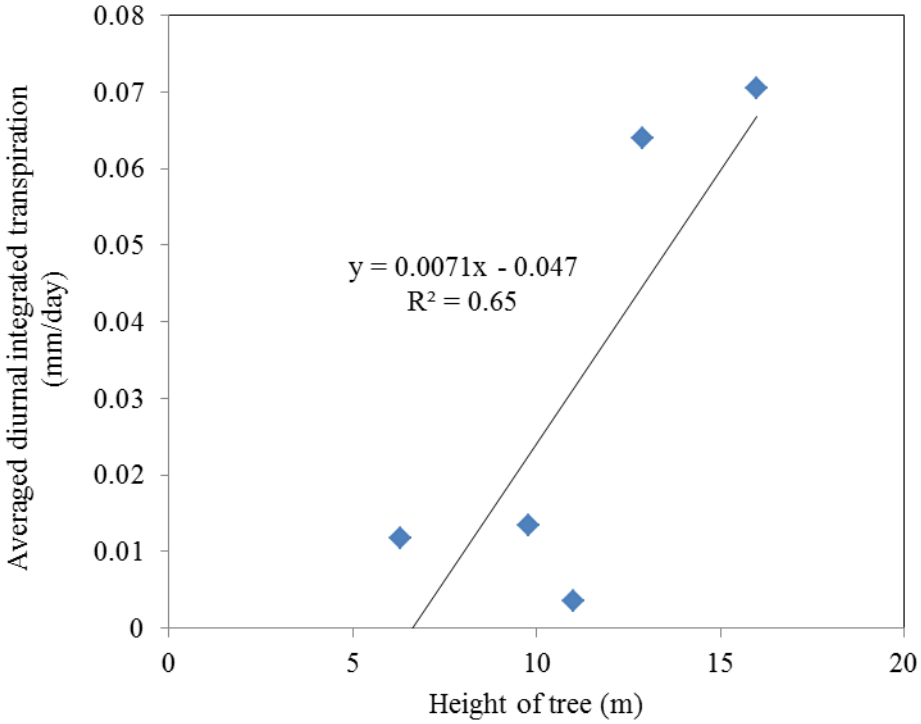

Figure 38 The correlation between transpiration and height of 5 tree samples at Tomida farm. Diurnal integrated transpiration was averaged in the measurement period.

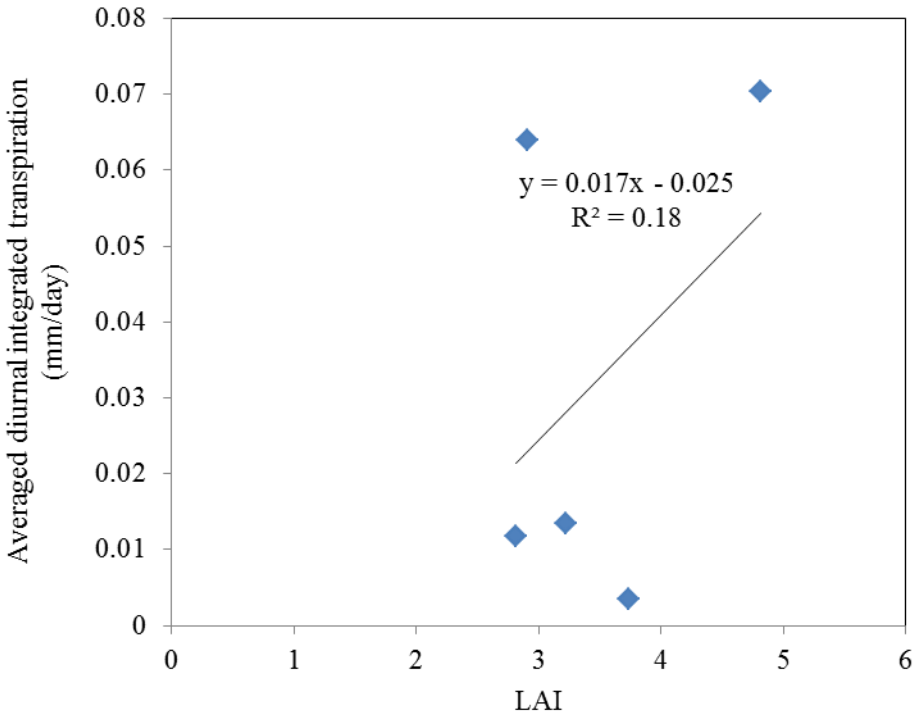

Figure 39　The correlation between transpiration and LAI of 5 tree samples at Tomida farm. Diurnal integrated transpiration was averaged in the measurement period.

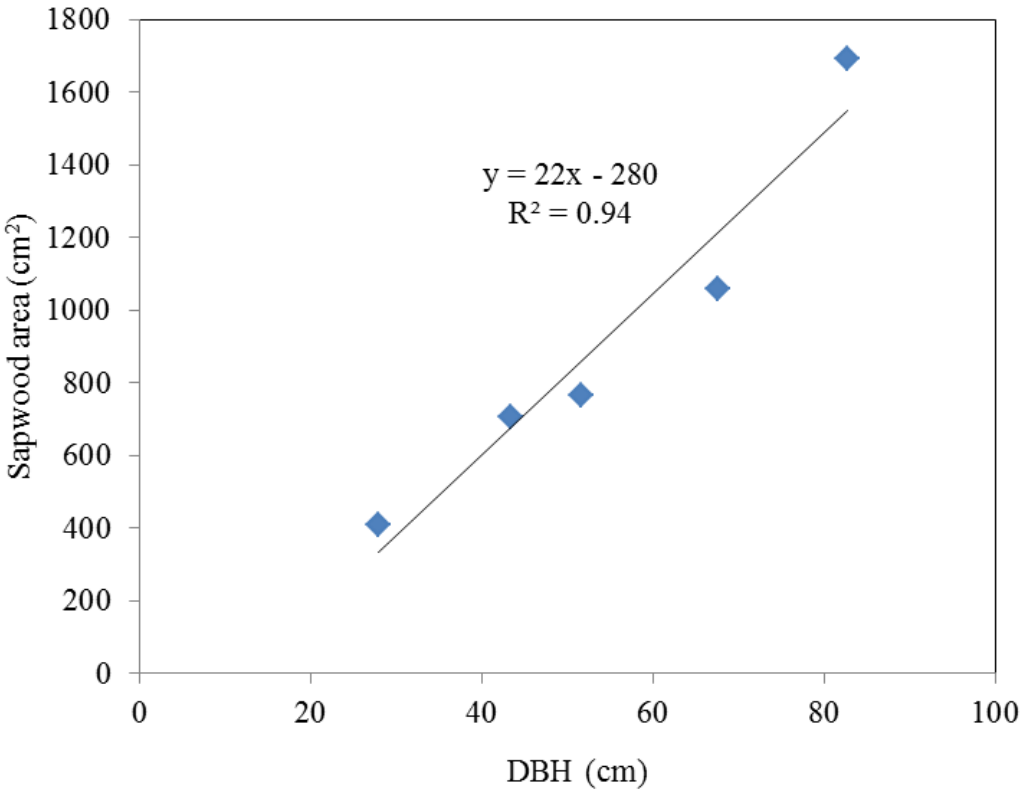

Figure 40 The correlation between DBH (cm) and sapwood area (cm^2) of 5 tree samples at Tomida farm.

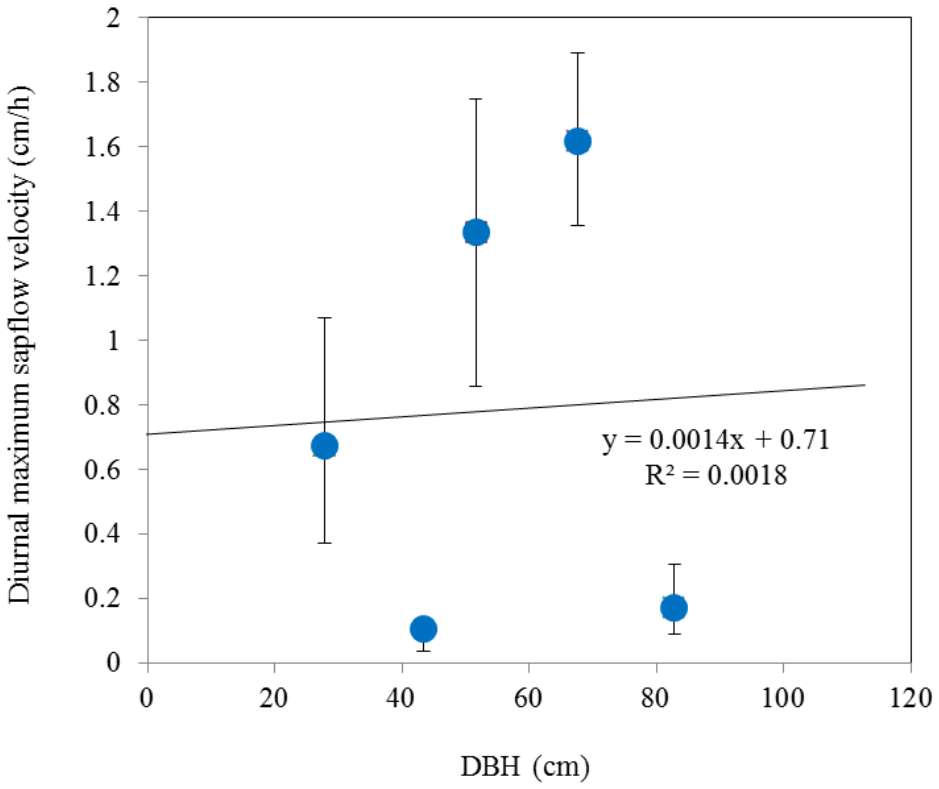

Figure 41 The correlation between DBH (cm) and sapflow velocity (cm/h) of 5 tree samples at Tomida farm. The error bar means maximum and minimum in the measurement period.

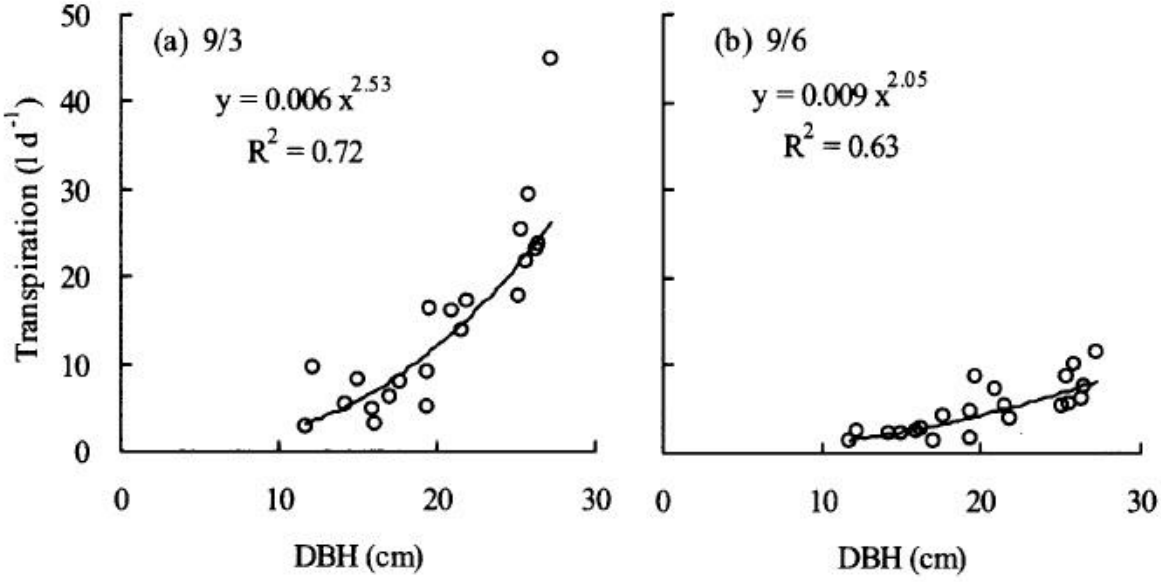

Figure 42 Correlation between transpiration and DBH from Fujiyama et al. (2005). Transpiration of trees were measured by Granier method against *Chamaecyparis obtuse* in Japan.

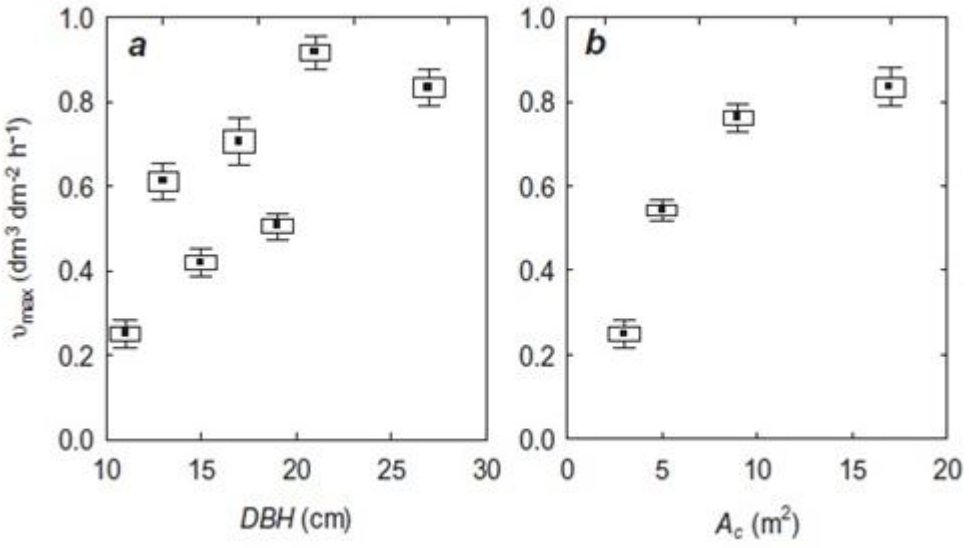

Figure 43 Correlation between maximum sapflow velocity and DBH, projected leaf areas (crown projected area) from Poyatos et al. (2005). Sapflow of trees were measured by Granier method against *Pinus sylvestris* in north-east Spain.

area of trees, as shown in Figures 42 and 43. In both theses, sapflow of trees were measured by Granier method. In spite of the results mentioned by Fujiyama et al. (2005) that the correlation between transpiration and DBH could be represented by exponential function, similar result could not be found in this study, because the plots of measurement seemed to be not enough. Furthermore, the correlation between DBH and diurnal maximum sapflow velocity could not provide obvious positive linear function in this study. Thus the reason why exponential function was not discovered in this study could be thought that obvious positive linear correlation was not found between DBH and sapflow velocity from few measurement samples. On the other hand, the variation of transpiration of No.11 implies that it had seasonal change in Figure 44. The amount of daily integrated value of transpiration of No.11 was getting smaller gradually in the end of the summer in 2011.

The daily variations of transpiration of five samples from 9/10 to 9/20 are shown in Figure 35. This chart has a purpose of focusing on diurnal variation. The variations of transpiration of No.11, No.6 and No.5 had similar shape. For example, the maximum value of peak of transpiration appears at around 13:00 or 14:00 (local time), and the speed of the variation of transpiration in the morning is somehow larger than that in afternoon. Transpirations of all samples became zero in every night, and these characteristics are usually general in measurements of Granier method.

3-1-2. Estimation of surface conductance with Jarvis model

According to Stewart (1988) who modified Jarvis (1976), surface conductance generally has correlations with four environmental factors, such as air temperature, solar radiation, specific humidity deficit and soil moisture deficit. In Jarvis (1976), it was shown that surface conductance has correlations with five environmental factors, such as air temperature, photon flux density, vapor pressure, leaf water potential and CO_2 concentration. Observing Jarvis (1976), surface conductance could be estimated as in a tree system. On the other hand, in Stewart (1988), surface conductance could be estimated as in small environmental systems surrounding the trees, not only tree characteristics or data, but also microclimate and meteorological data. In this study, assumed system of Stewart (1988) was more suitable for the purpose of estimation of surface conductance. Thus estimation of surface conductance was basically by means of Stewart (1988) rather than Jarvis (1976). The results of the correlation between measured five environmental factors and surface conductance calculated by Penman-Monteith equation with measured meteorological data are shown in Figures 46 - 51. The interactions between surface conductance which was estimated from Penman-Monteith equation and photon flux density, air temperature, specific humidity deficit and soil moisture deficit are shown. These correlations had similar results to those of Stewart

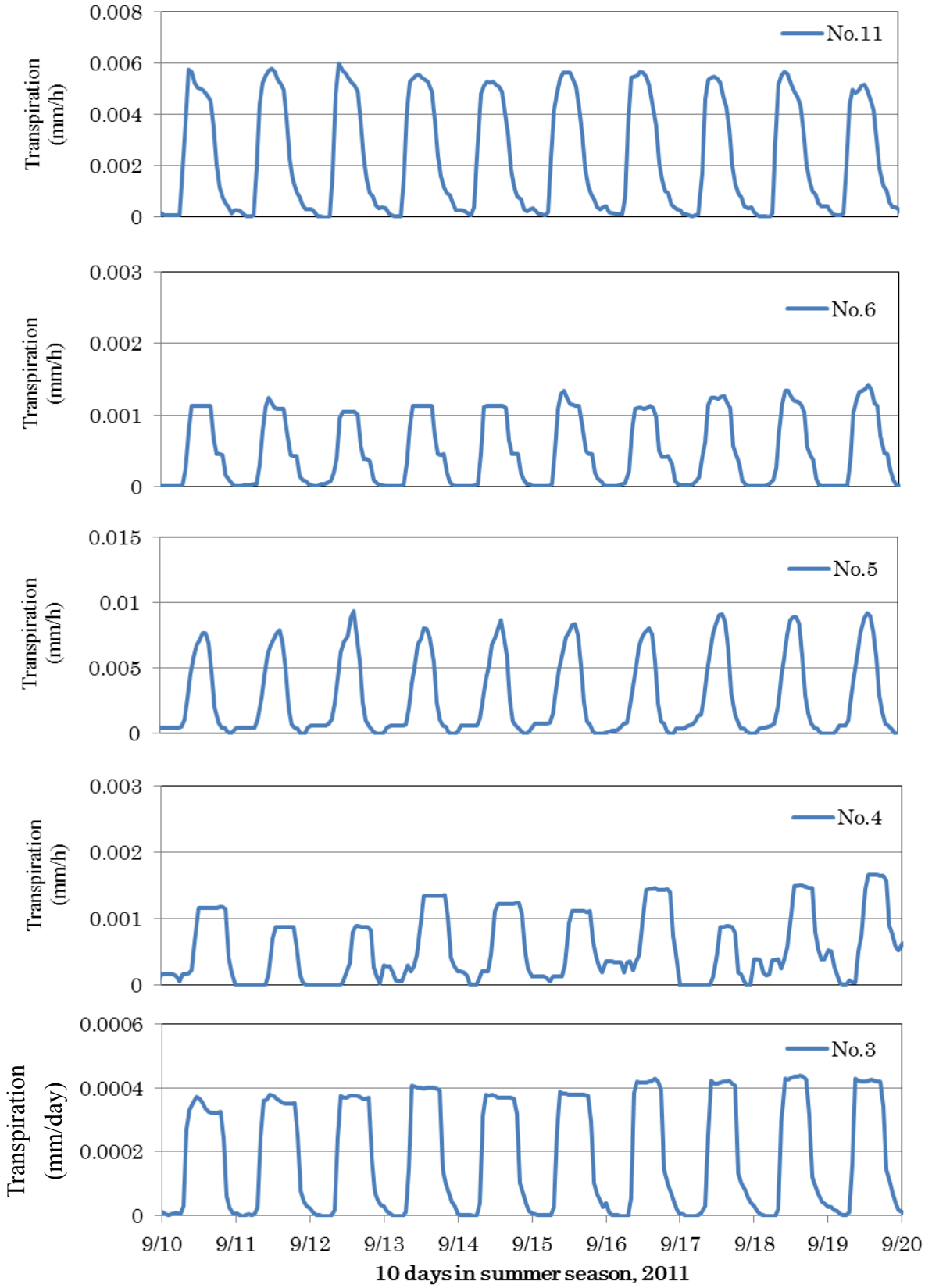

Figure 44 Daily variation of transpiration per unit projected leaf area of each sample in the summer of 2011. (Date means 0:00 UTL of each date)

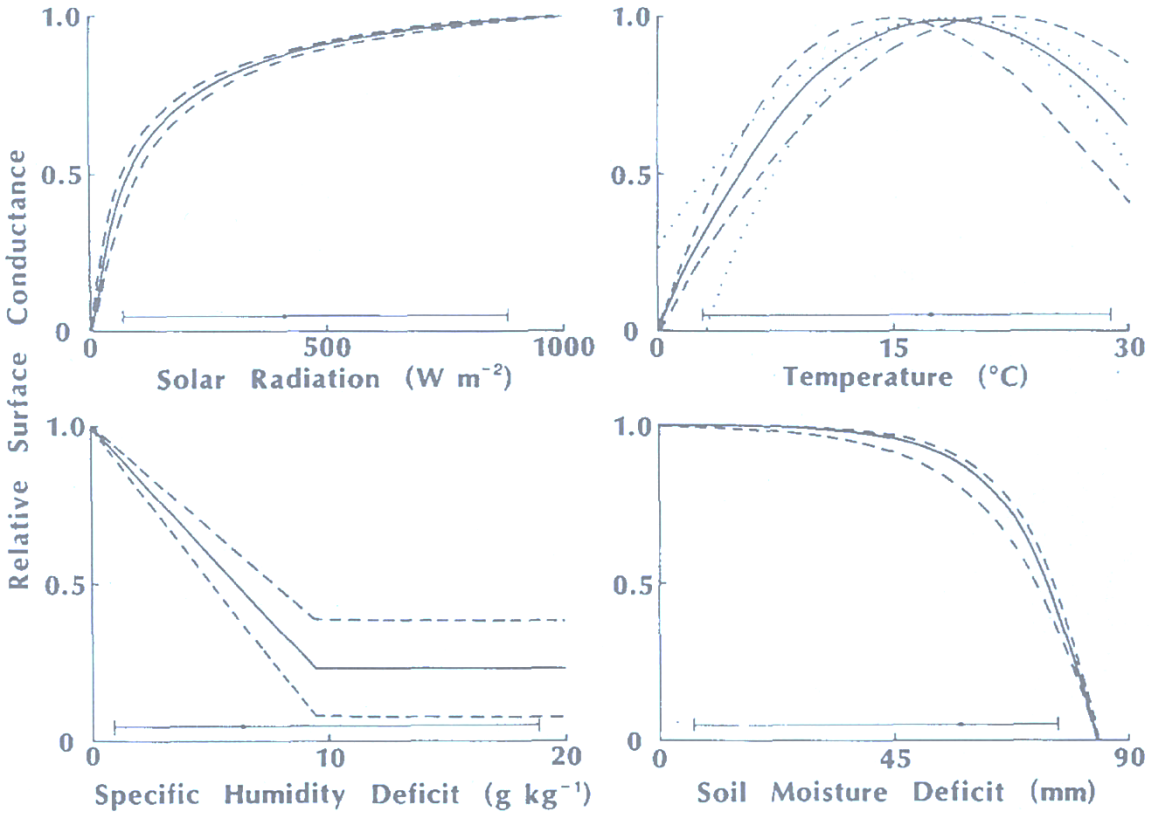

Figure 45 Interaction between relative surface conductance and four environmental factors, such as solar radiation (W/m^2), air temperature (℃), specific humidity deficit (g/kg) and soil moisture deficit (mm) (from Stewart, 1988)

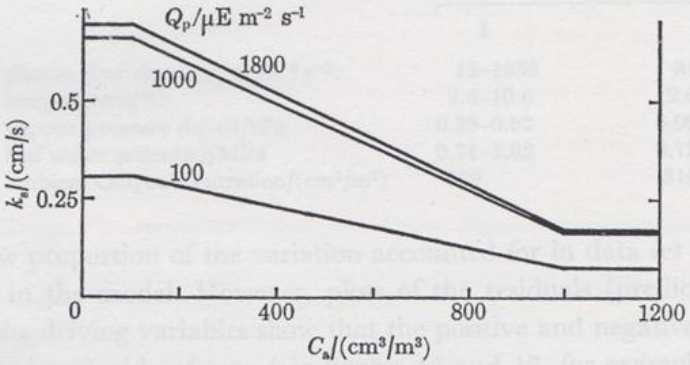

FIGURE 15. The relation between stomatal conductance (k_s) and ambient CO_2 concentration (C_a) at three levels of photon flux density (Q_p) as given by equations (8) and (9). Other conditions assumed: $\delta e = 0.5$ kPa; $\Psi_l = -0.5$ MPa; $T_a = 10$ °C.

Figure 46 Correlation between stomatal conductance (cm/s) and CO_2 concentration (cm^3/m^3) from Jarvis (1976).

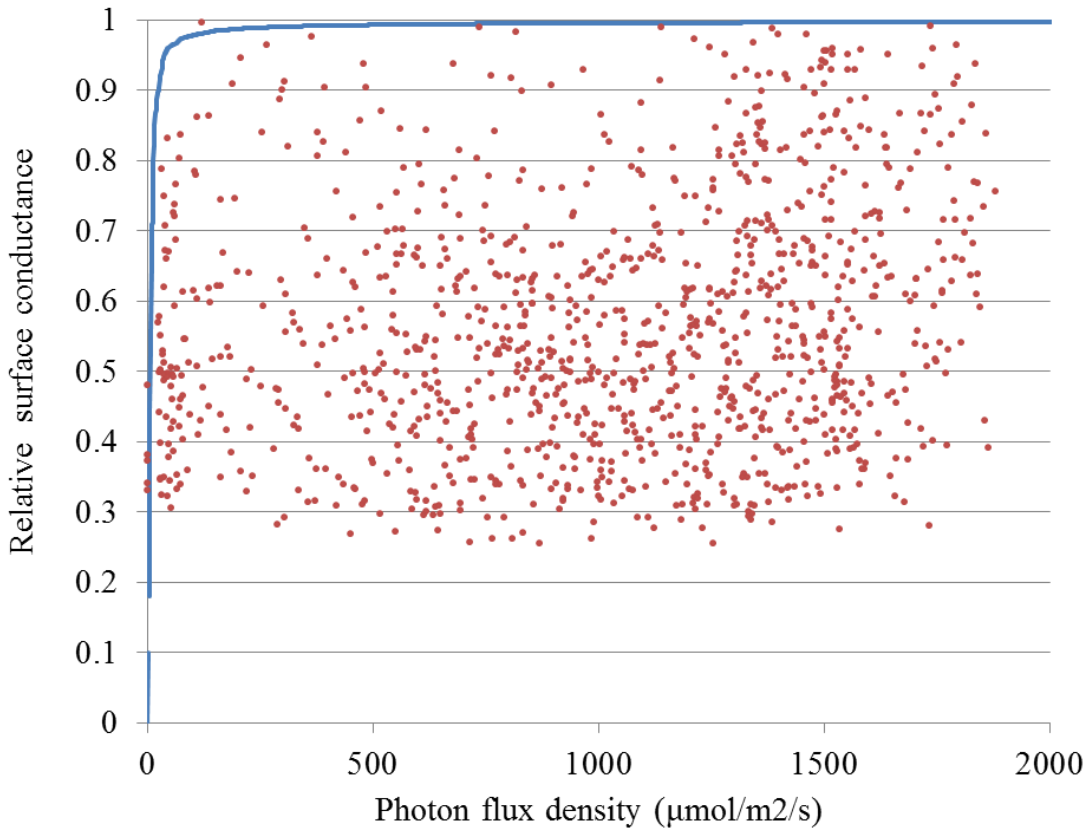

Figure 47 Correlation between measured relative surface conductance and photon flux density (µmol/m^2 /s). Relative surface conductance was calculated measured surface conductance per maximum surface conductance of the measurement period.

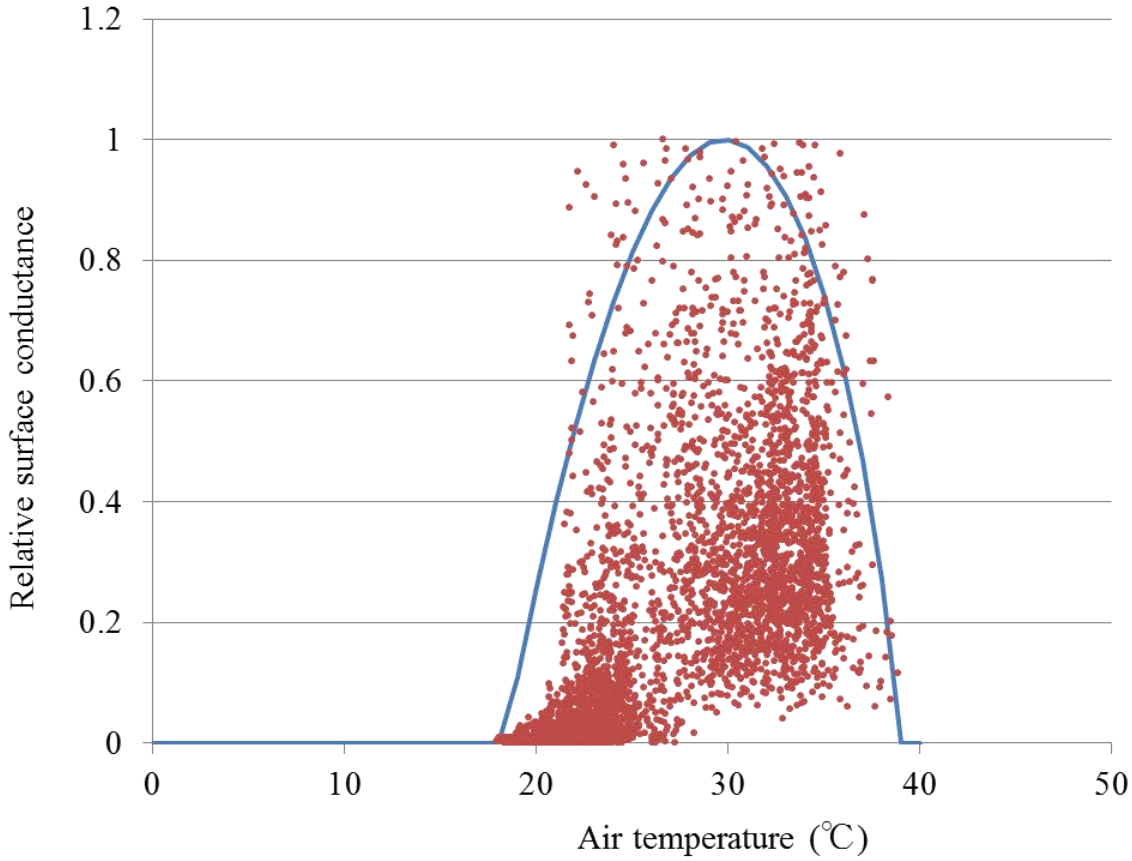

Figure 48　Correlation between measured relative surface conductance and air temperature (℃) Relative surface conductance was calculated measured surface conductance per maximum surface conductance of the measurement period.

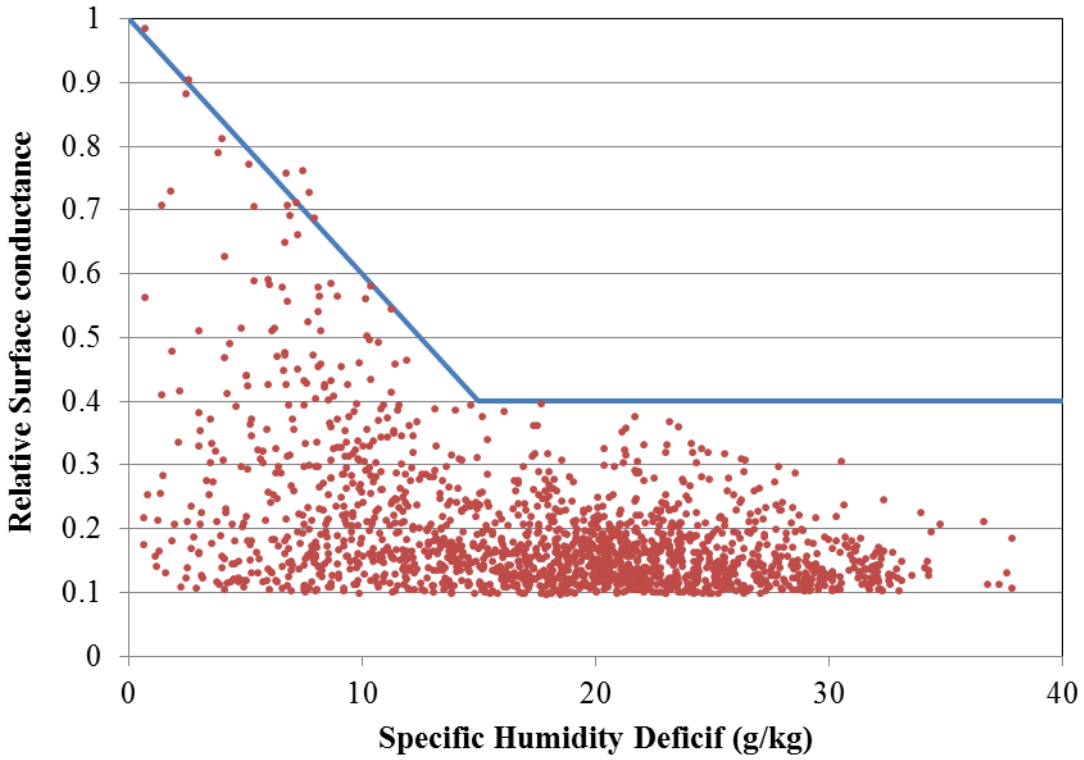

Figure 49 Correlation between relative surface conductance and specific humidity deficit (g /kg) Relative surface conductance was calculated measured surface conductance per maximum surface conductance of the measurement period.

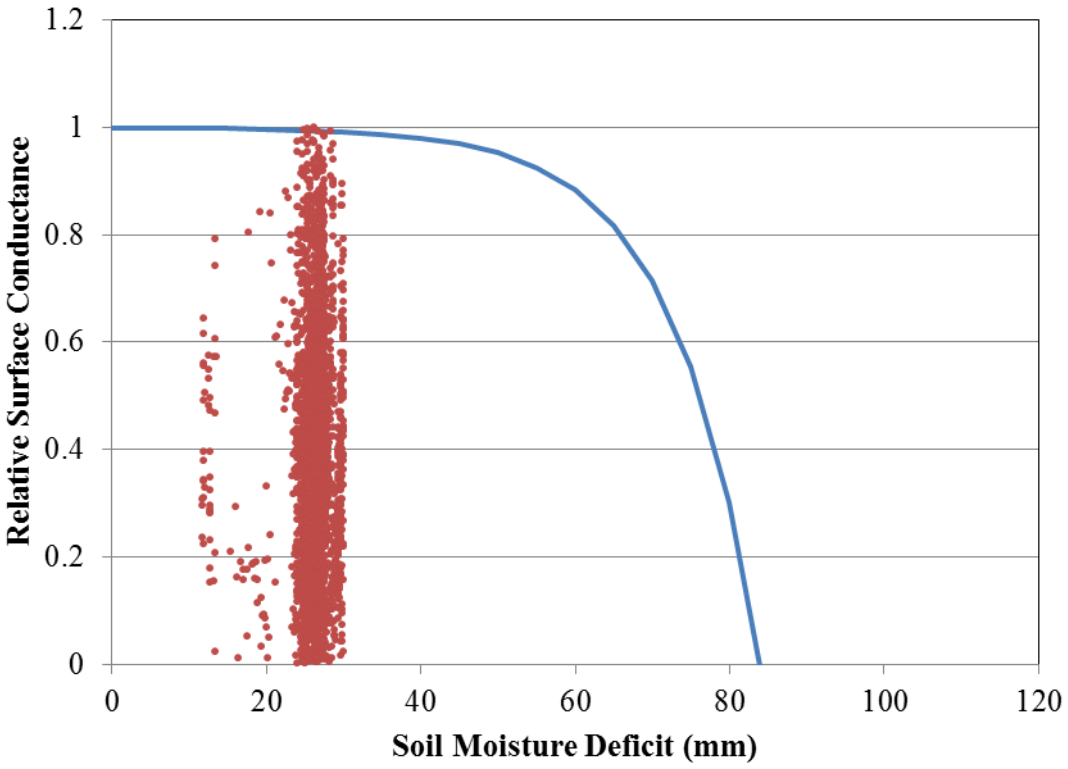

Figure 50 Correlation between relative surface conductance and soil moisture deficit (mm) Relative surface conductance was calculated measured surface conductance per maximum surface conductance of the measurement period.

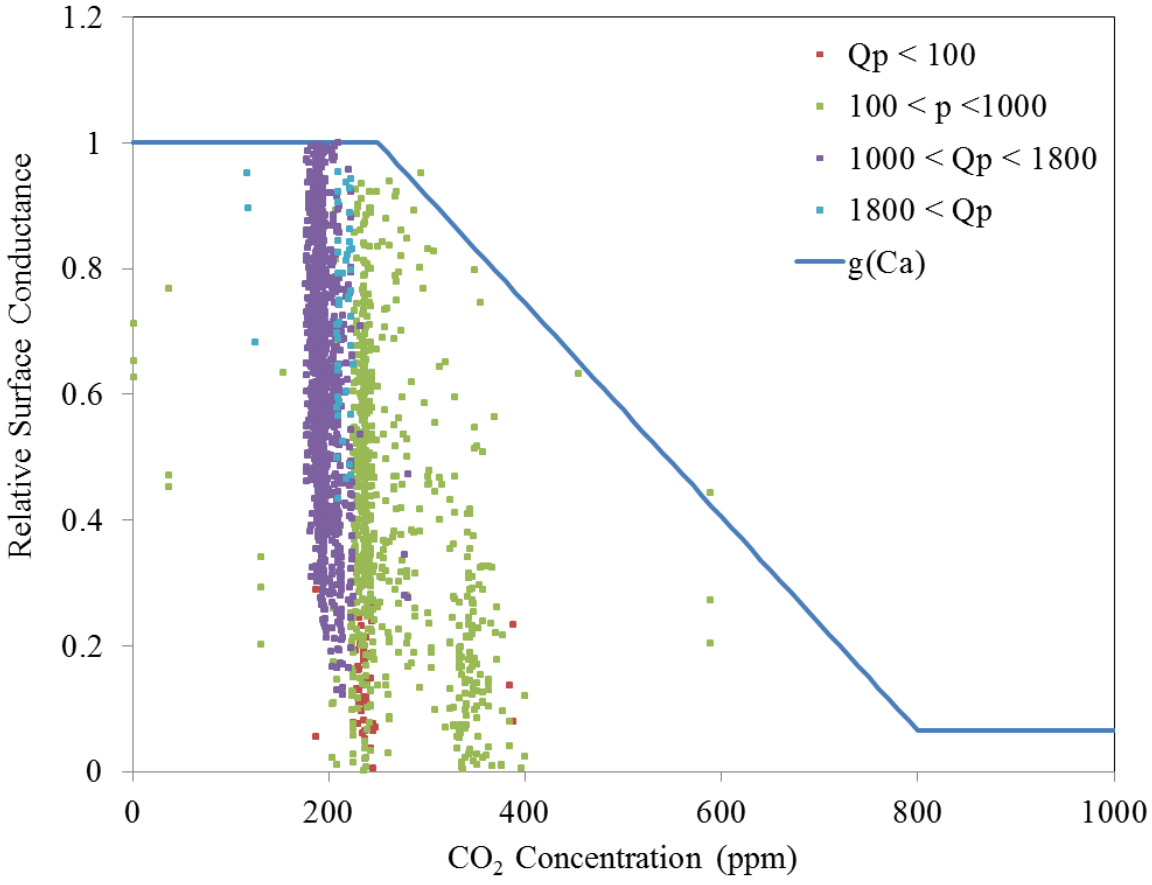

Figure 51 Correlation between relative surface conductance and CO_2 concentration (ppm) Relative surface conductance was calculated measured surface conductance per maximum surface conductance of the measurement period.

Table 10 Results of parameterization of each function in Jarvis model (Stewart, 1988)

Parameters	Values	Parameters	Values	Parameters	Values
K_1	1.98	b_1	1	LAI (No.11)	2.91
K_2	156.3	b_2	0.00221	LAI (No.6)	3.22
K_3	0.04	b_3	0.005	LAI (No.5)	4.81
K_4	15	b_4	0.69	LAI (No.4)	2.81
K_5	-	b_5	0.02	LAI (No.3)	3.73
K_6	0.0897	b_6	-	LAI (Whole windbreak trees)	2.22
K_7	1.086	b_7	0.0017	q	50
K_8	-	b_8	0.065	T_h	38.88
K_9	K_6 ($\delta\theta$-$\delta\theta_m$)	b_9	-	T_l	18.05
θ_{fc}	0.47365	b_{10}	100	T_0	30.23

(1988), and functions of each correlation could be applied for the results of this study. The functions are shown in figures as a blue line with scatter diagrams.

Overviewing these results, it can be said that a kind of tree *Casuarina* could be applied for Jarvis model, even in such semi-arid region of Egypt. However, the correlations of soil moisture deficit of this study did not have enough range of measurements. In parameterization of function of soil moisture deficit, parameters are basically same with those of Stewart (1988) in this study. Other functional forms of Stewart (1988) completely included measured value of three environmental factors in this study, so the same functional forms were regarded to be applicable for this study. The result of calibration is shown in Table 10.

3-1-3. Estimation of transpiration with Penman-Monteith equation and Jarvis model

The seasonal variation of the surface conductance which was estimated by the meteorological data measured by the AWS at Tomida farm with Jarvis model is shown in Figure 52. The calibrated parameters and LAI of each sample are shown in Table 7. The bottom graph shows the variation of surface conductance which was estimated by the meteorological data measured by the AWS at Tomida farm with Penman-Monteith equation. The scatter diagram of the correlation between estimated surface conductance with Jarvis model and calculated surface conductance with Penman-Monteith equation is shown in Figure 53. The coefficient of the correlation was 0.49, and estimated surface conductance tended to under-estimate against the real values.

However, in this study's case, the most important point is comparison between transpiration of windbreak trees and soil evaporation from the land. If the transpiration of windbreak trees were much smaller than soil evaporation from the land, the results shown in section would not influence the conclusion. Thus it can be said that the most important result is representation of the seasonal variation of measured transpiration by estimation of transpiration by Penman-Monteith equation and Jarvis model, rather than searching for higher determination coefficient of correlation between measured and estimated surface conductance itself. Thus, it is ok for this study that the correlation between measured and estimated surface conductance was not good.

The seasonal variation of estimated transpiration of windbreak tree No.11 from July 15th to Sep. 26th in 2011 is shown in Figure 54. This variation was estimated by Penman-monteith equation and Jarvis model (modified by Stewart, 1988) by equation (1. 4) with the meteorological data measured in same period recorded by the AWS at Tomida farm. The data from AWS at Tomida farm were not available during the period from July 29th to August 24th.

3-1-4. Validation of estimated transpiration with measured transpiration

The daily variations of estimated transpiration of the tree No.11 and measured transpiration of the tree No.11 are shown in Figures 54 and 55 in the growing period in 2011. From the variation of estimated and measured transpiration, analysis period could be divided into two periods, the first period and the latter period, because of the difference of agreements between estimated and measured transpiration. At a same time, the scatter diagrams (Figures 57 and 58) which represents the correlation between estimated and measured transpiration are different between estimation with four environmental factors and five environmental factors. Figure 58 shows the result of estimation by four environmental factors without CO_2 concentration, and Figure 57 shows the result of estimation by five environmental factors which include CO_2 concentration between estimated and measured transpiration was also high ($R^2 = 0.79$), but Penman-Monteith equation and Jarvis model overestimated the measured transpiration in this case. In the whole period, the determination coefficient was 0.51. Thus it can be said that estimated transpiration by Penman-Monteith equation and Jarvis model coud represent the seasonal change of measured transpiration in the summer period in 2011. Actually, this result was a modified version from previous analysis. Previous analysis of Jarvis model in this study did not contain CO_2 concentration, and photon flux density could not represent the seasonal change of measured transpiration. Thus it can be said that the final reasonable result of estimated transpiration of windbreak trees which represents seasonal change of measured transpiration was given by some modification, such as addition of CO_2 concentration and modification of the function of photon flux density. The improvement can be seen in Figure 57 and 58.

In the same method, other variations of transpiration of tree samples No.6, 5, 4, 3 were estimated with the meteorological data measured by the AWS at Tomida farm by Penman-Monteith equation and Jarvis model, and they are shown in Figure 59 with measured seasonal variations of transpiration at Tomida farm. The variations of the transpiration of each sample were estimated by Penman-Monteith equation and Jarvis model. In the process of estimation of surface conductance, same parameters were set for each samples, except for LAI of the trees were used. In general, the surface conductance should not change much, if the samples are same kind of trees. Thus, in the parameterization of Jarvis model for each tree sample, only L (LAI) of samples were changed. However, the results did not reflect such general assumption. The results of estimation of transpiration of all samples overestimated the variations of actual transpiration, which can be seen in scatter diagrams in Figures 60 - 63. The correlations were high (No.6: $R^2 = 0.66$, No.5: $R^2 = 0.83$, No.3: $R^2 = 0.65$) except for No.4 ($R^2 = 0.13$). In spite of well representation transpiration estimation by Penman-Monteith equation and Jarvis model against measured transpiration of No. 11, representations

against No.6, 5, 4 and 3 were not reasonable. As results, estimated transpirations of each sample were over-estimated against measured transpiration. As the reasons against this result, in the situation at Tomida farm, the tree samples named No.6, 4 and 3 were standing beside high and big tree crown trees. The tree crowns of trees which stood side by side were overlapping each other. Therefore, measurement of projected leaf areas by walking under the tree crowns might bear some error. Thus it can be said that these results were influenced by choice of samples and measurement of projected leaf areas easily.

3-2. Measurements of meteorological data, crops and soil

3-2-1. Measurements of meteorological data

The components of meteorological data are shown in Table 8, and the horizontal wind profiles before and after harvesting are shown in Figure 64. The horizontal line means the relative distance from the windbreak trees which was calculated by dividing the distance (m) by the height of the windbreak trees (m). The vertical line means relative values of meteorological data which was calculated by dividing the data of each sensor by the data of No.1 by treating No.1 as a reference. Against the horizontal wind profile, two kinds of curves were tried to fit by using TableCurve2D (curve fitting software) shown in Figure 65.

The horizontal profile of relative wind velocity leeward of the windbreak trees in the period of after harvesting was very similar to that in period of before harvesting, shown in Figure 64. The data of wind velocity profile which are larger than 1 m/s were picked up in Figure 65, and the function of the profile of relative wind velocity was given by TableCurve2D as follow.

$$\frac{u}{u_0} = \frac{a + cx^{0.5} + ex}{1 + bx^{0.5} + dx + fx^{1.5}} \tag{1.26}$$

where u is measured wind velocity of the sensors No. 2 - 6, u_0 is measured wind velocity of the sensor No. 1, a - f are parameters and x is relative distance from the windbreak trees. In this study, a was determined as 100.66, b was -0.5387, c was -84.1766, d was 0.13818, e was 23.9287 and f was 0.0079, and the determination coefficient R^2 was 0.707. As a result, the horizontal profile of wind velocity leeward of the windbreak trees is not affected by the crops, and represented by a function (1.24).

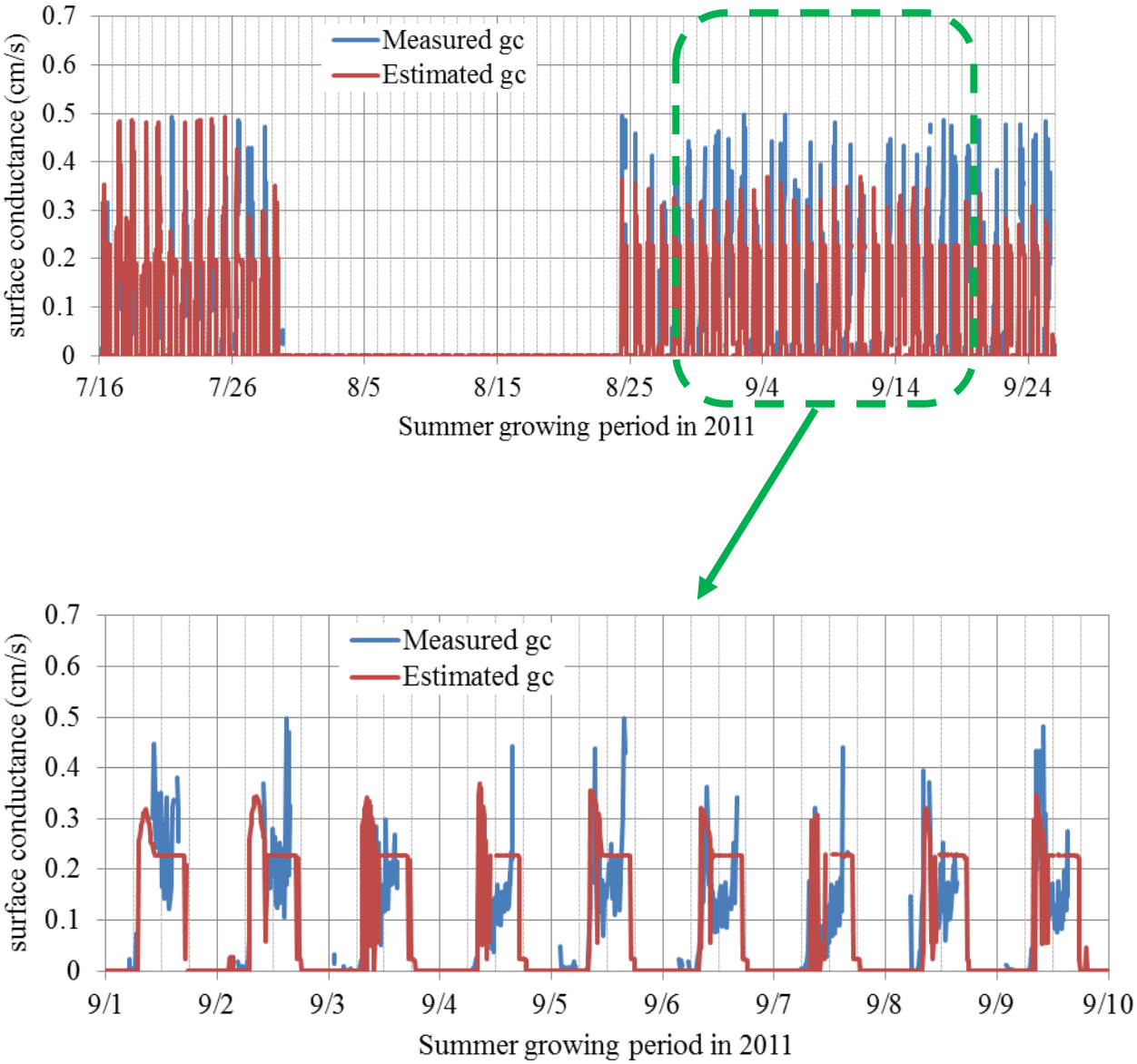

Figure 52 Daily variation of measured and estimated surface conductance (cm/s), above: in a growing period of crops (from July 15th to September 26th in 2011, below: focusing on 15 days in September, 2011

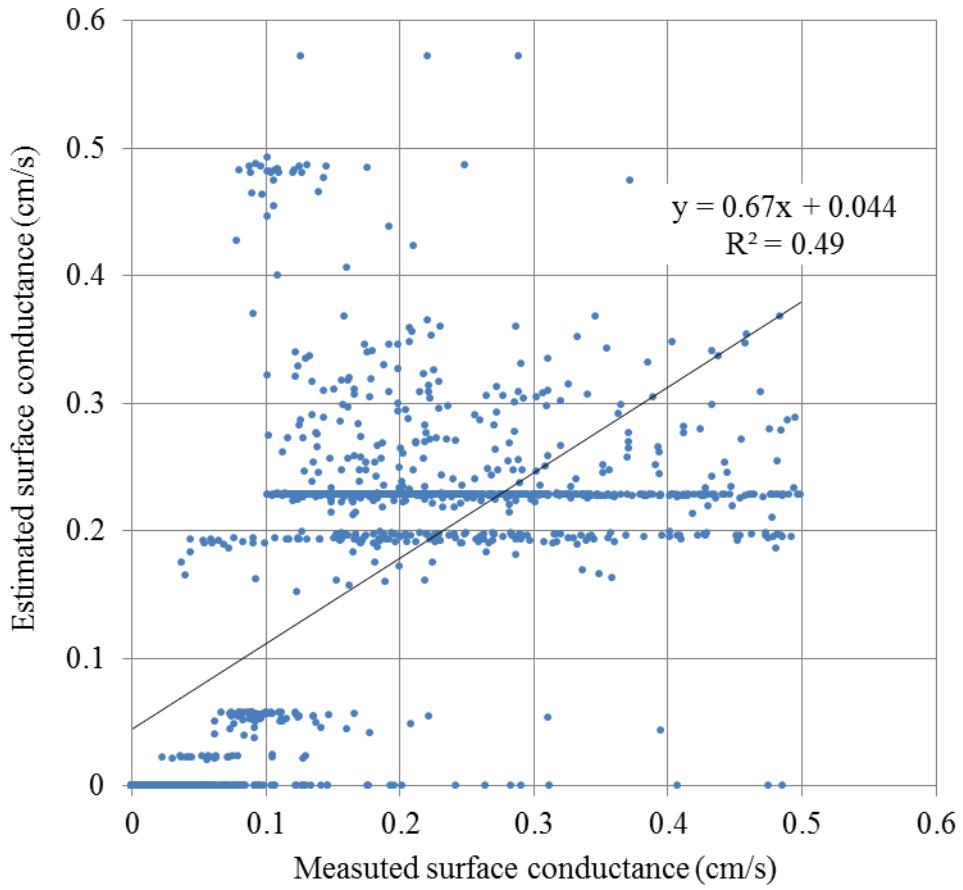

Figure 53 Correlation between measured and estimated surface conductance (cm/s) (measured surface conductance was calculated by Penman-Monteith equation, estimated surface conductance was estimated by Jarvis model)

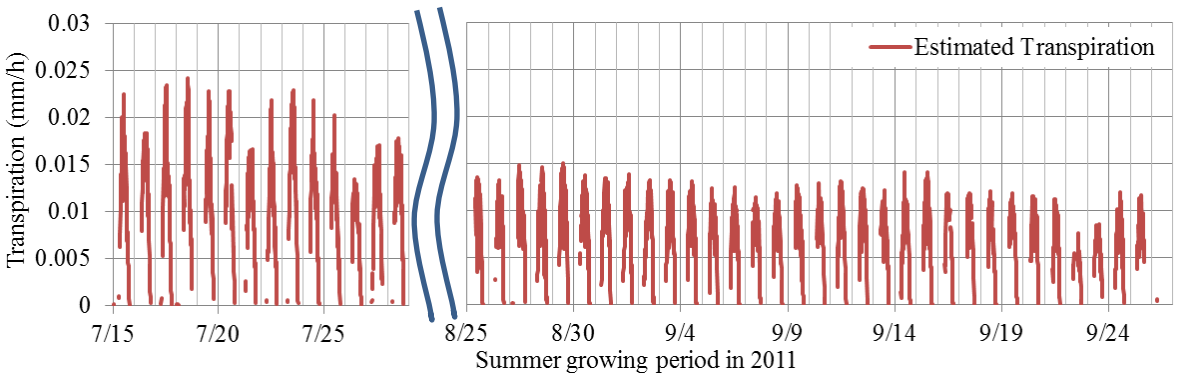

Figure 54　Daily variation of estimated Epm: transpiration (mm/h) of No.11 by Penman-Monteith equation and Jarvis model (modified by Stewart, 1988)

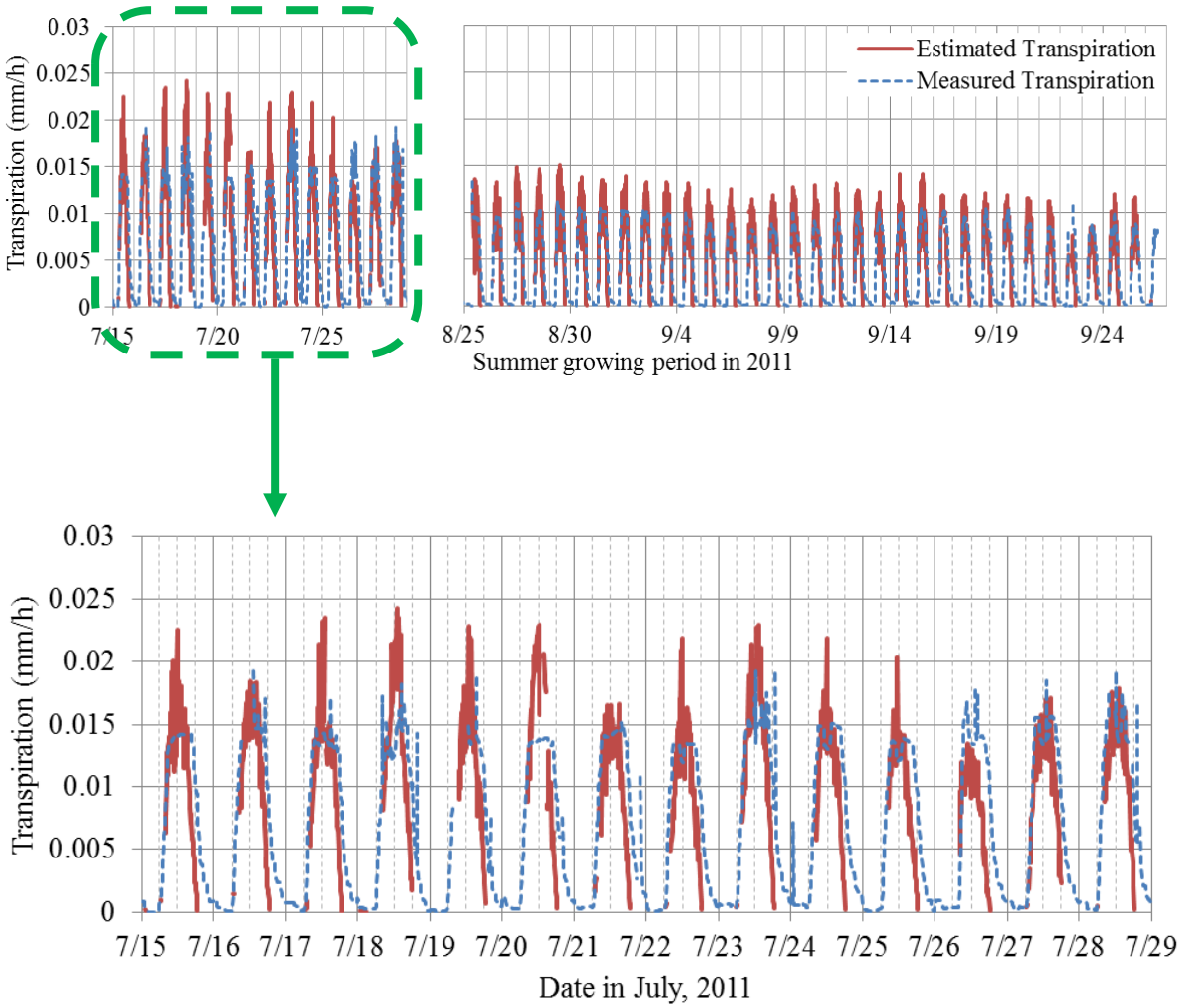

Figure 55 Daily variations of estimated and measured transpiration of No.11 in the summer growing period. (focused on the first period)

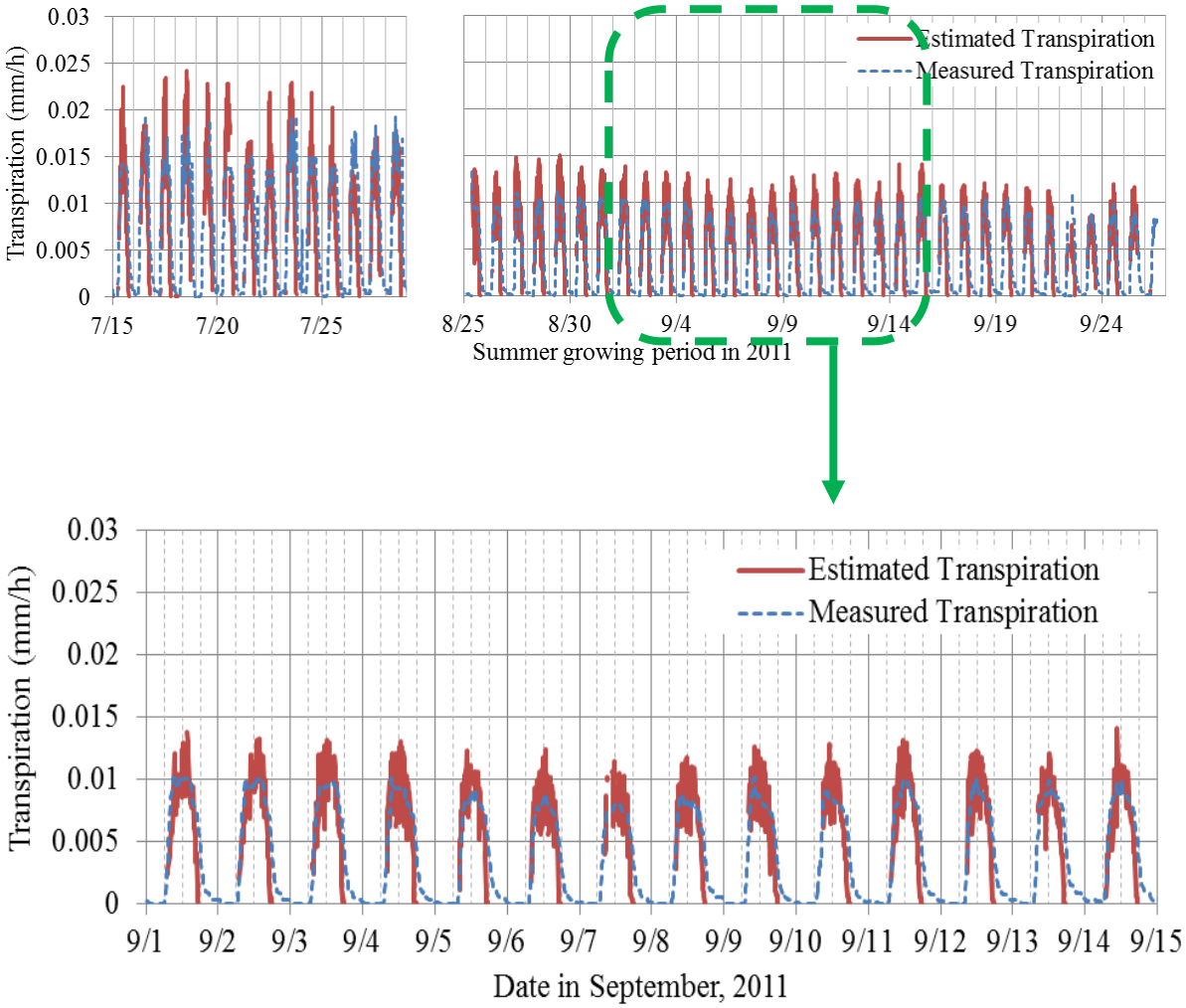

Figure 56 Daily variations of estimated and measured transpiration of No.11 in the summer growing period. (focused on the latter period)

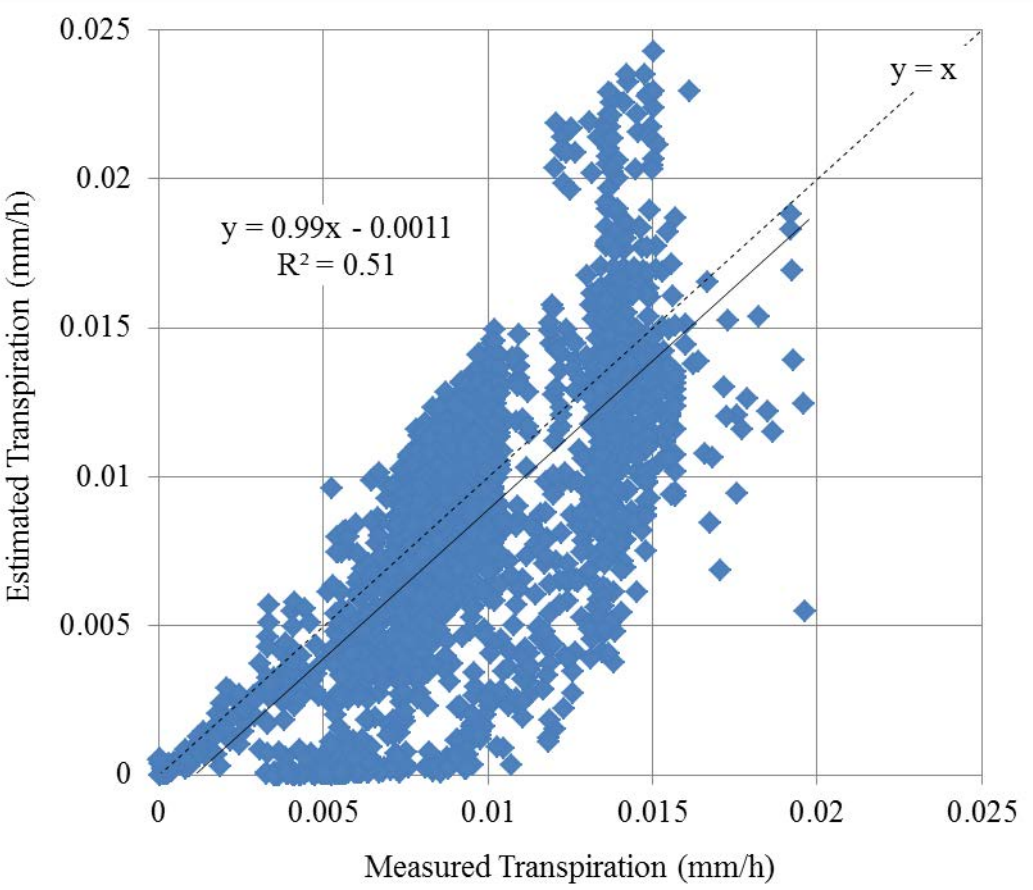

Figure 57　Correlation between measured and estimated transpiration (mm/h) (measured transpiration was from data of No.11 at Tomida farm, estimated transpiration was from Penman-Monteith equation with estimated surface conductance by Jarvis model)

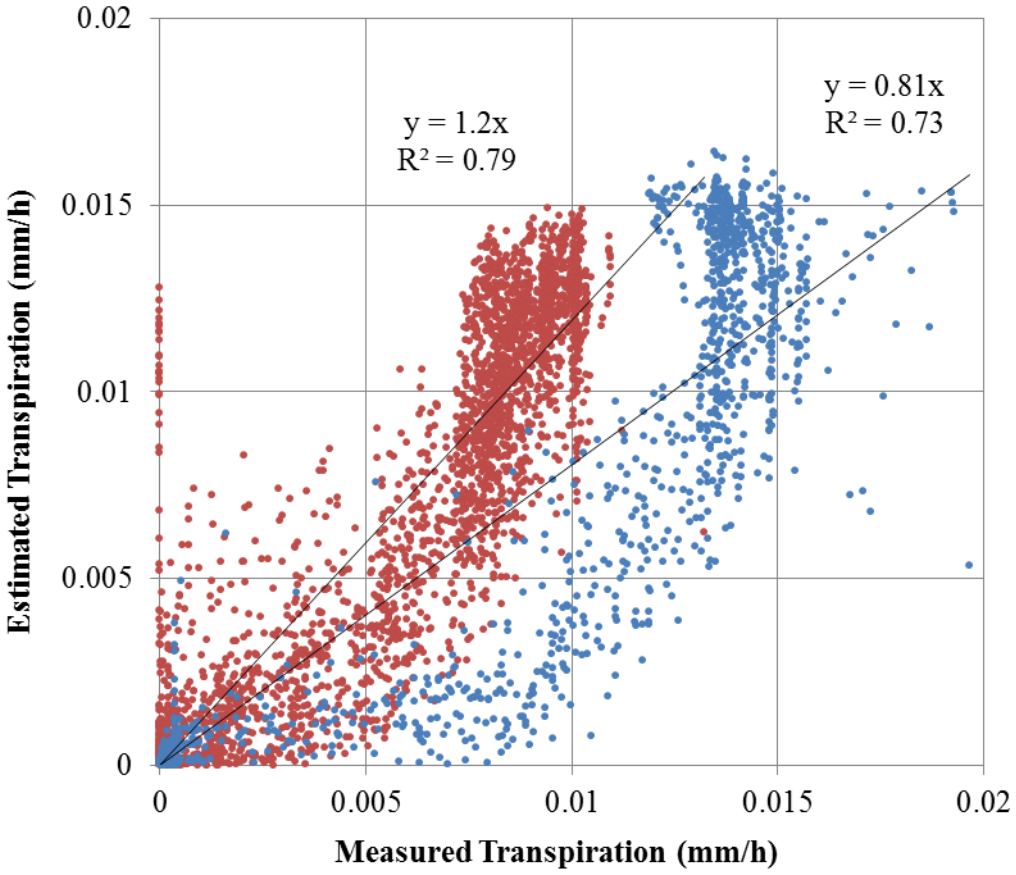

Figure 58 Difference of correlation between estimation in July and September in 2011 (blue: estimation in July, red: estimation in September) The transpiration was estimated by Jarvis model without CO_2 concentration (ppm) and before modification of photon flux density part.

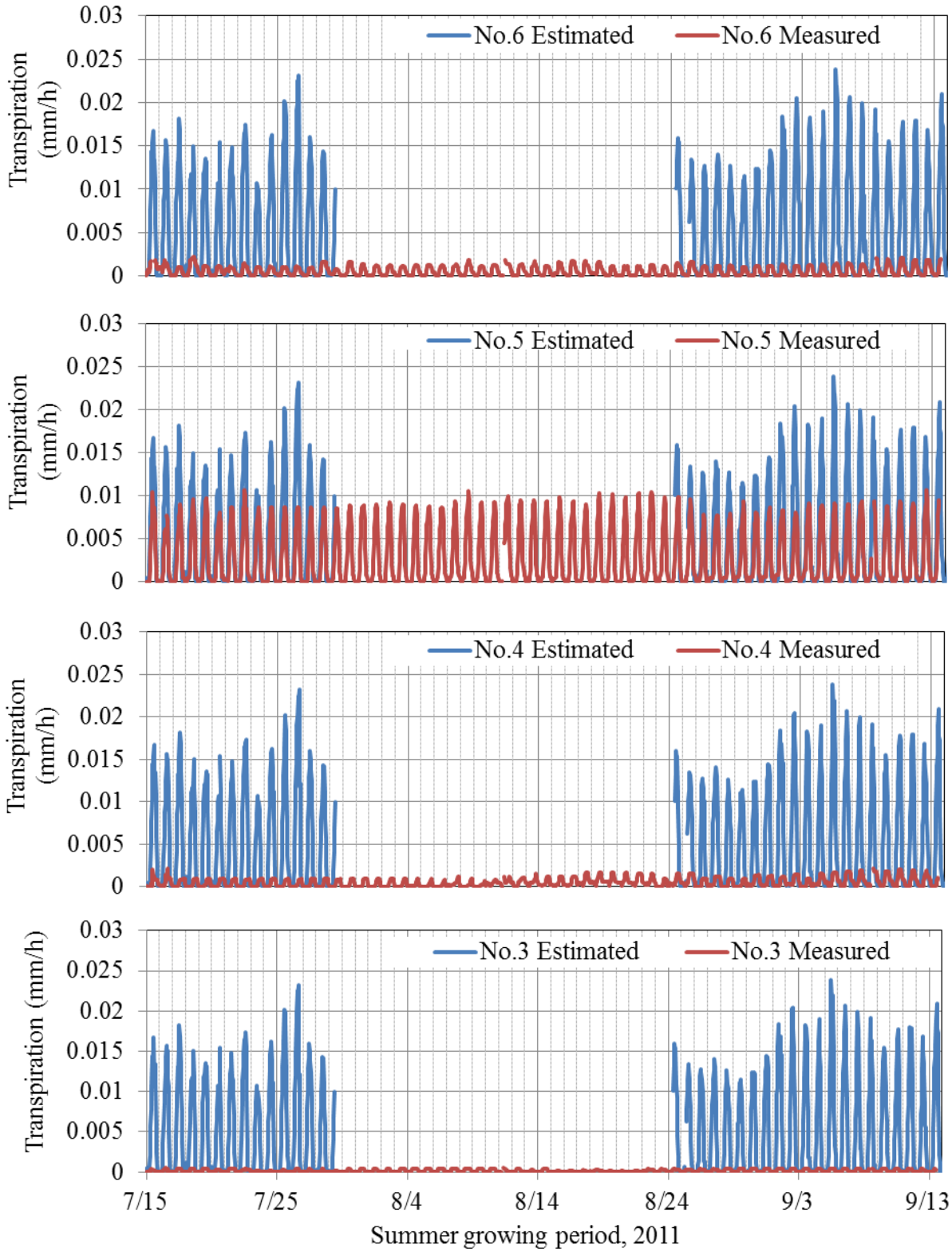

Figure 59 Daily variations of measured and estimated transpiration (mm/h) of each sample (No.6, 5, 4 and 3) at Tomida farm. (Measured transpiration was calculated from measured data at Tomida farm, estimated transpiration was estimated from Penman-Monteith equation with estimated surface conductance by Jarvis model)

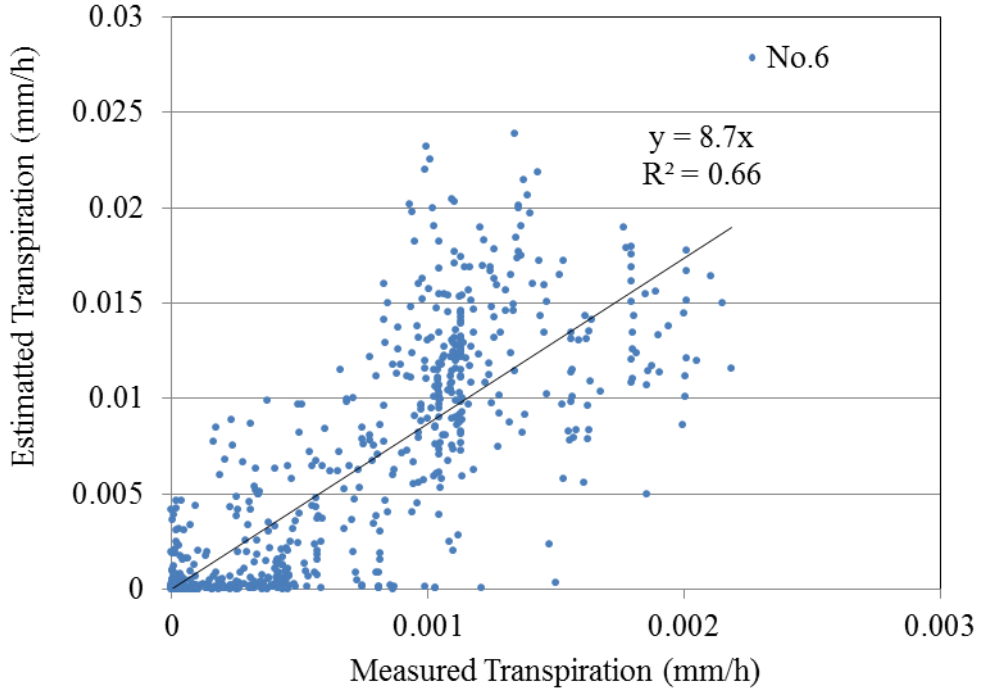

Figure 60　Correlation between measured and estimated transpiration (mm/h) of No.6.

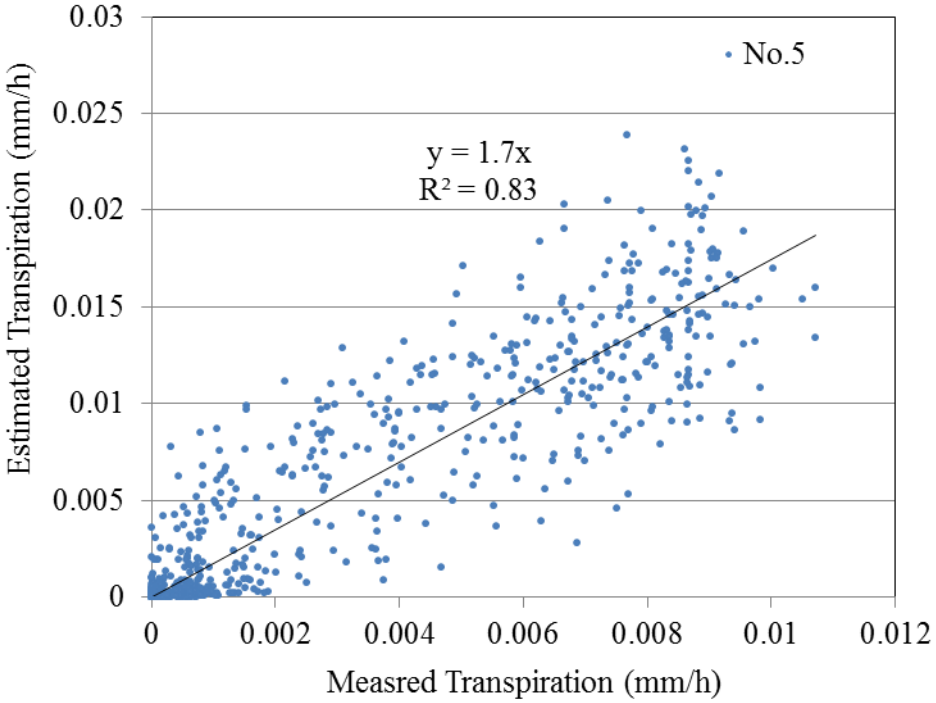

Figure 61 Correlation between measured and estimated transpiration (mm/h) of No.5.

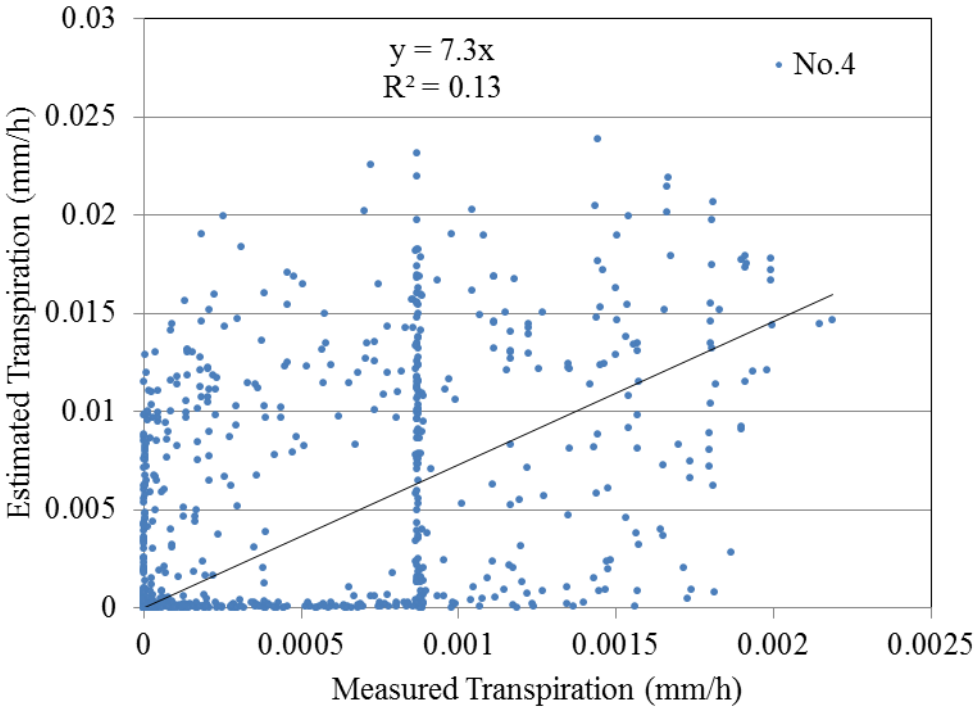

Figure 62　Correlation between measured and estimated transpiration (mm/h) of No.4.

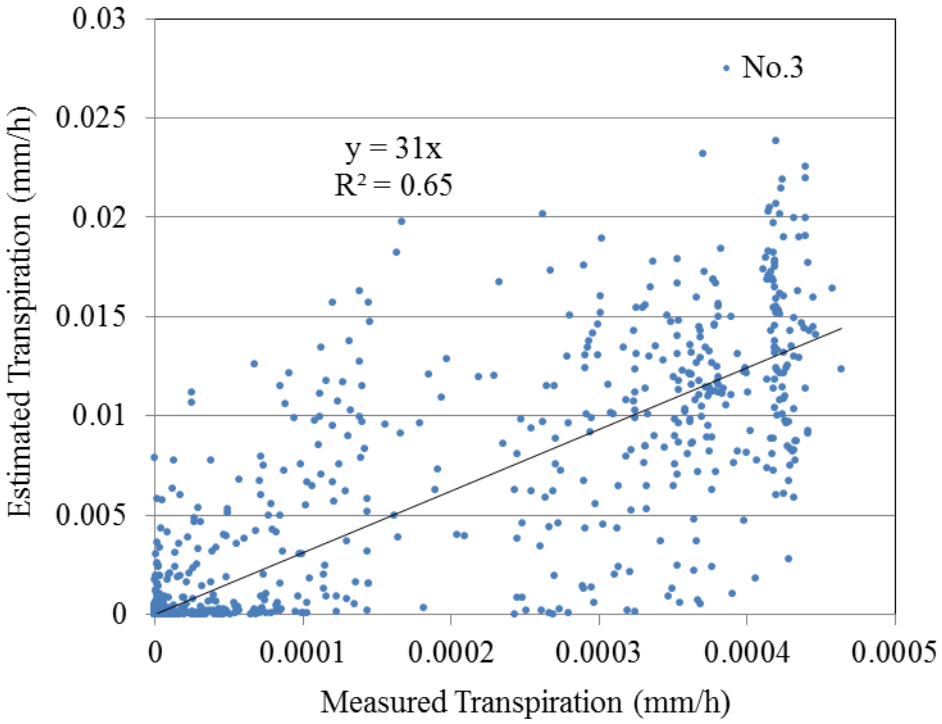

Figure 63 Correlation between measured and estimated transpiration (mm/h) of No.3.

Another function of curve fitting was given by TableCurve2D (Figure 66). The function is

$$\frac{u}{u_0} = \left(a + cx + ex^2 + gx^3 + ix^4\right) \Big/ \left(1 + bx + dx^2 + fx^3 + hx^4\right) \tag{1.27}$$

where u is measured wind velocity of the sensors No. 2 - 6, u_0 is measured wind velocity of the sensor No. 1, a - f are parameters and x is relative distance from the windbreak trees. In this study, a was determined as 100.78, b was -1.34, c was -144.62, d was 1.414, e was 121.7, f was -0.22, g was -25.32, h was 0.028 and i was 2.97, and the determination coefficient R^2 was 0.715. These functions seemed to be the best functions to represent wind profile, and latter function (1.28) was adopted in this study, because of the higher determination coefficient than former function.

Diurnal variation of the meteorological data (air temperature, wind velocity, wind direction, relative humidity and air pressure) which were measured by Visala sensors in the period before harvesting are shown in Figures 67, 68 and the wind rose of each measurement points is shown in Figure 69. The measurement period before harvesting was from August 25th to September 6th in 2012. The differences of diurnal variations of three meteorological data, such as air temperature, relative humidity and air pressure at six points seemed to be very small. The diurnal variations of air temperature at six points got largest value around noon every day. On the other hand, the diurnal variations of relative humidity at six points got largest value around midnight. The range of diurnal variations of air pressure at six points was very small (minimum: 1005, maximum: 1013). Therefore the seasonal variations or annual trends could not be seen during this short period. As shown in Figure 68, wind velocity got maximum value around noon, and from sunset to sunrise, wind velocity got less than 1 m/s every day in this period. Furthermore, diurnal variations of wind direction during night time look like wave. Thus before drawing out the wind rose (Figure 69), the data of wind direction during night time when the value of wind velocity got less than 1 m/s were rejected as error.

Diurnal variations of the meteorological data (air temperature, wind velocity, wind direction, relative humidity and air pressure) which were measured by Visala sensors in the period after harvesting are shown in Figure 70, 71 and the wind rose of each measurement points is shown in Figure 72. The measurement period after harvesting was from September 12th to September 19th in 2012. The trends of diurnal variations of meteorological data were very similar to the diurnal variations of meteorological data before harvesting, and the diurnal variations of wind velocity and wind direction were also similar to that before harvesting. Therefore, the values of wind direction during night

Table 11 Characteristics of windbreak trees at Al Krakat and Tomida farm

Characteristics of windbreak trees	Height (m)	LAI (no unit)	Porosity (%)	Maximum stomatal resistance: r_{smax} (s/cm)	Minimum stomatal resistance: r_{smin} (s/cm)
Al Krakat	14	4.92	43.6	54.6	35.2
Tomida farm	11	2.22	52.7	762	38.5

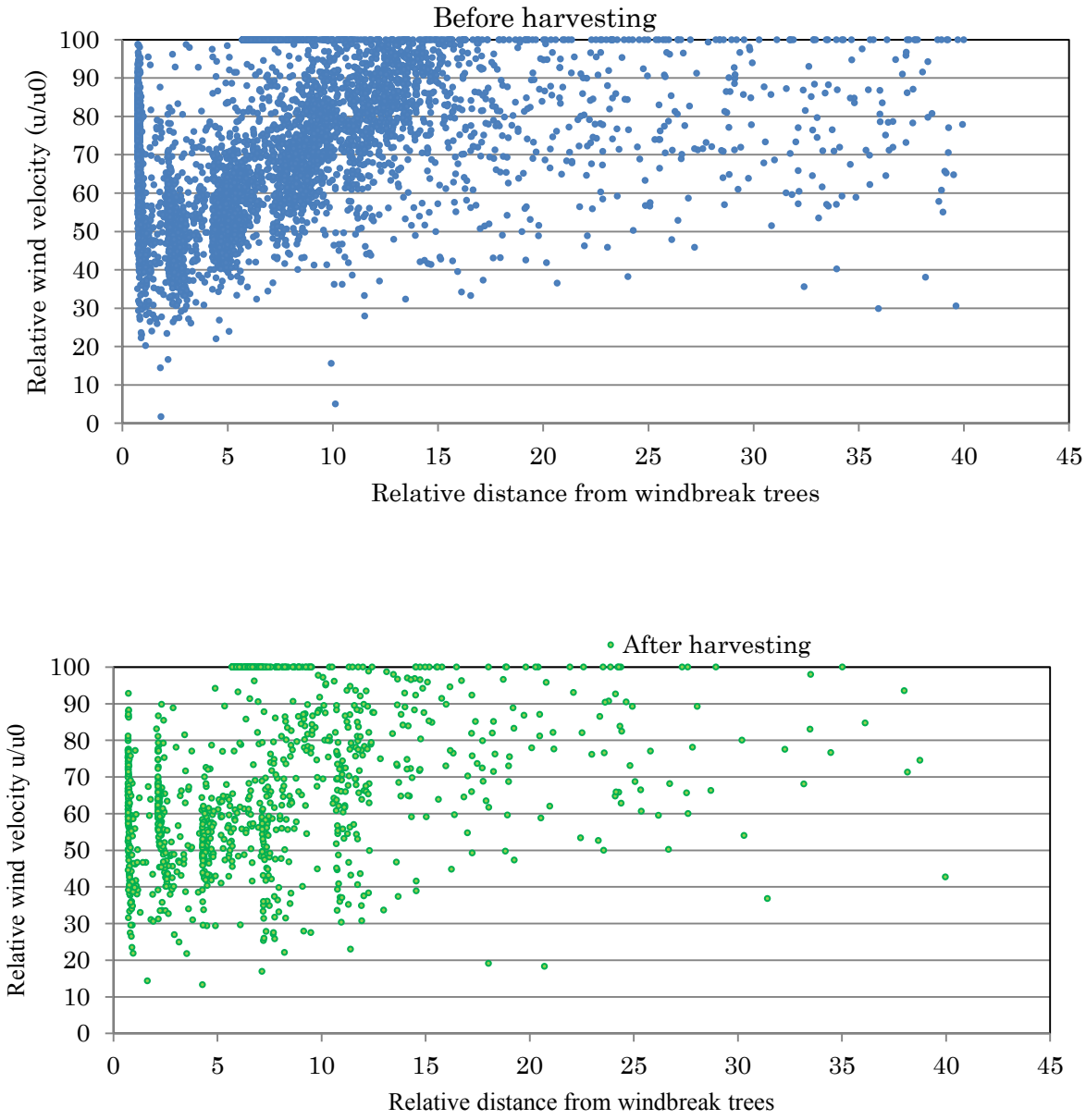

Figure 64　Horizontal relative wind profile
(above: before harvesting, below: after harvesting)
Measurement period: 2012/8/25 ~ 9/6 (before harvesting),
2012/9/12 ~ 9/19 (after harvesting)

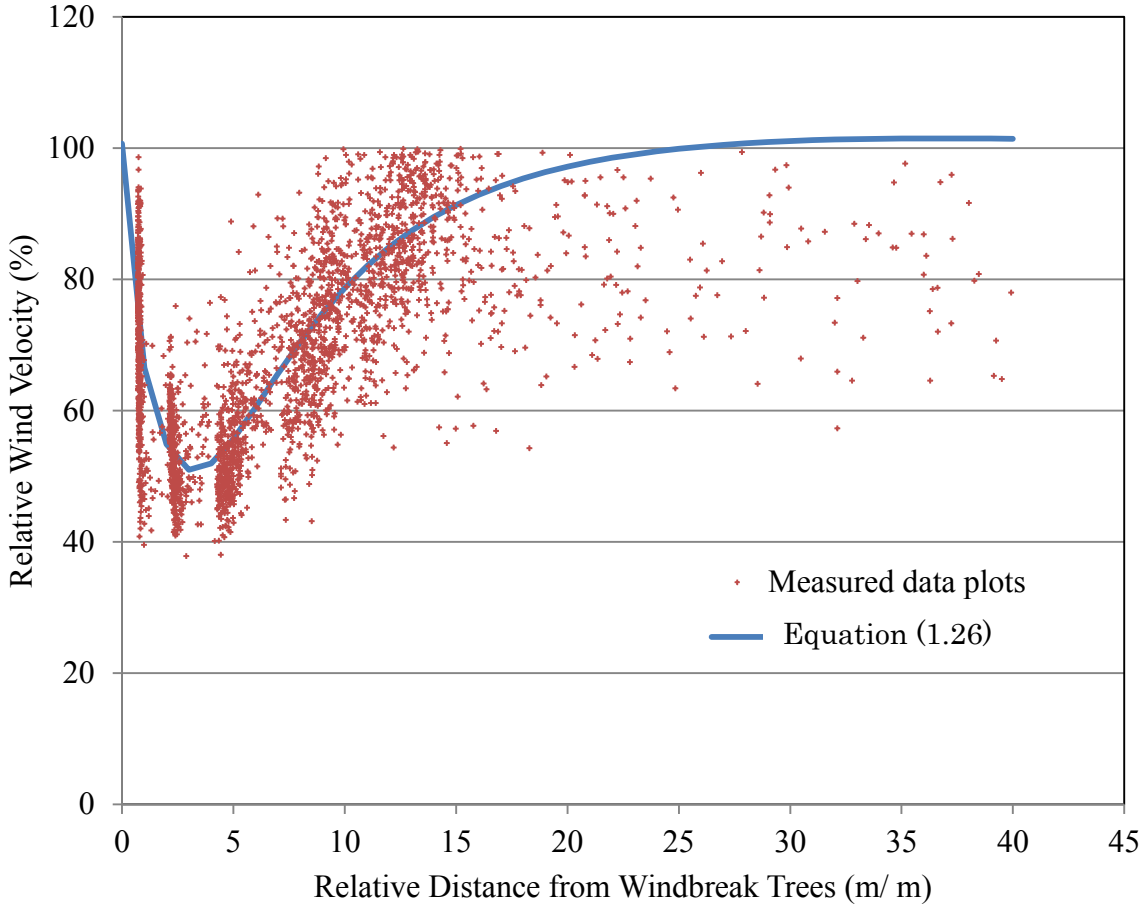

Figure 65 Measured horizontal wind profile (%) against the relative distance from the windbreak trees (m/ m), and a Function1 (R^2= 0.707) given by a result of curve fitting software (TableCurve2D)

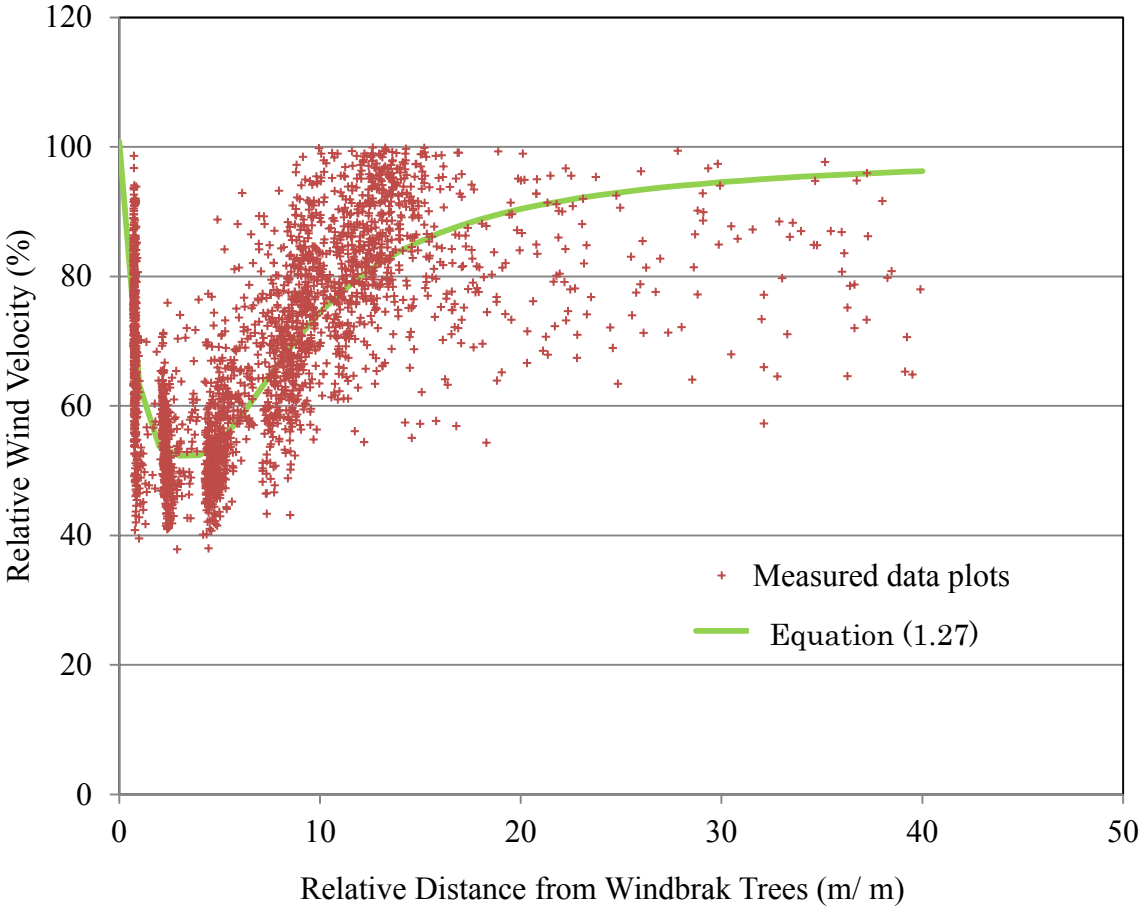

Figure 66 Measured horizontal wind profile (%) against the relative distance from the windbreak trees (m/ m), and a Function2 (R^2= 0.715) given by a result of curve fitting software (TableCurve2D)

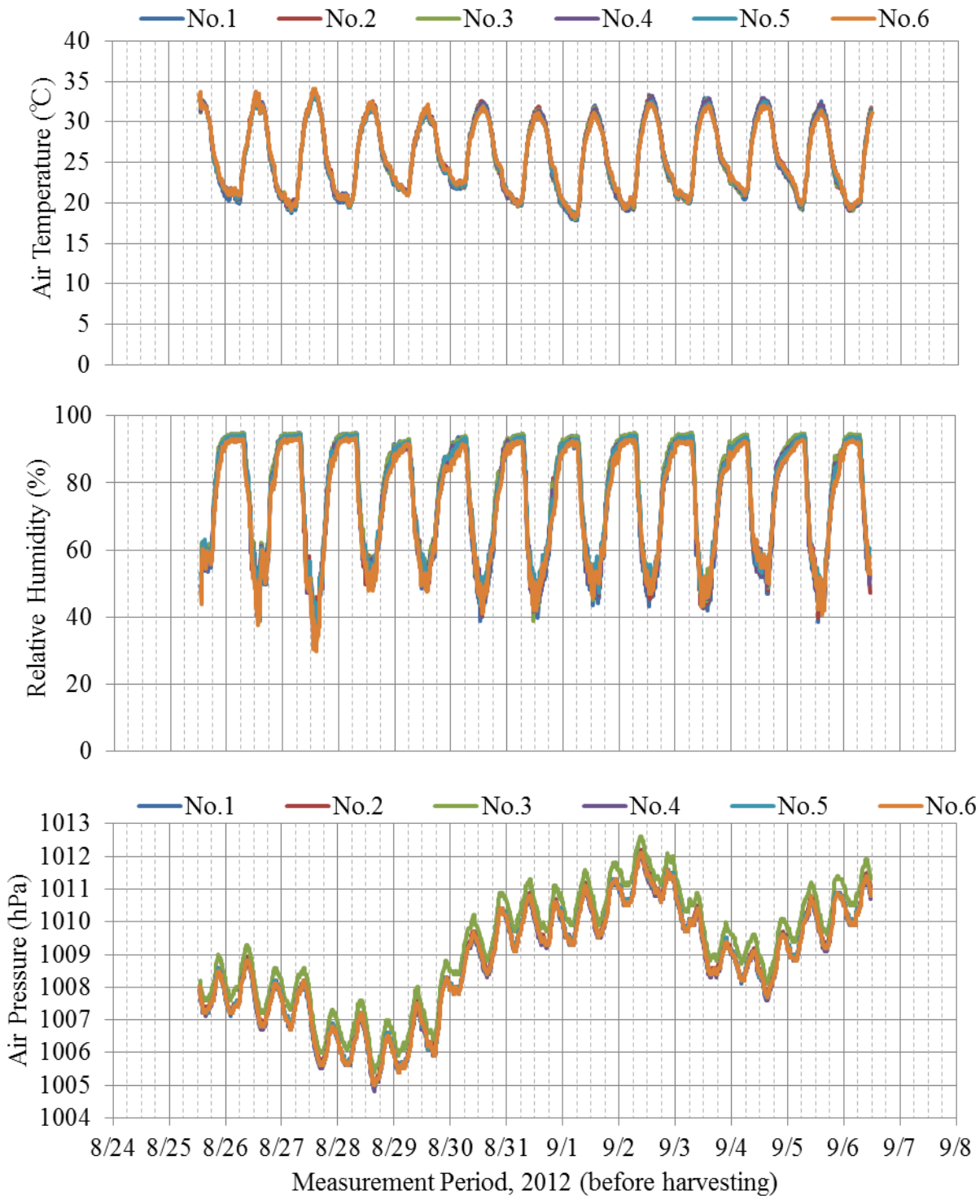

Figure 67　Daily variations of air temperature(℃), relative humidity (%) and air pressure (hPa), in the measurement period before harvesting.

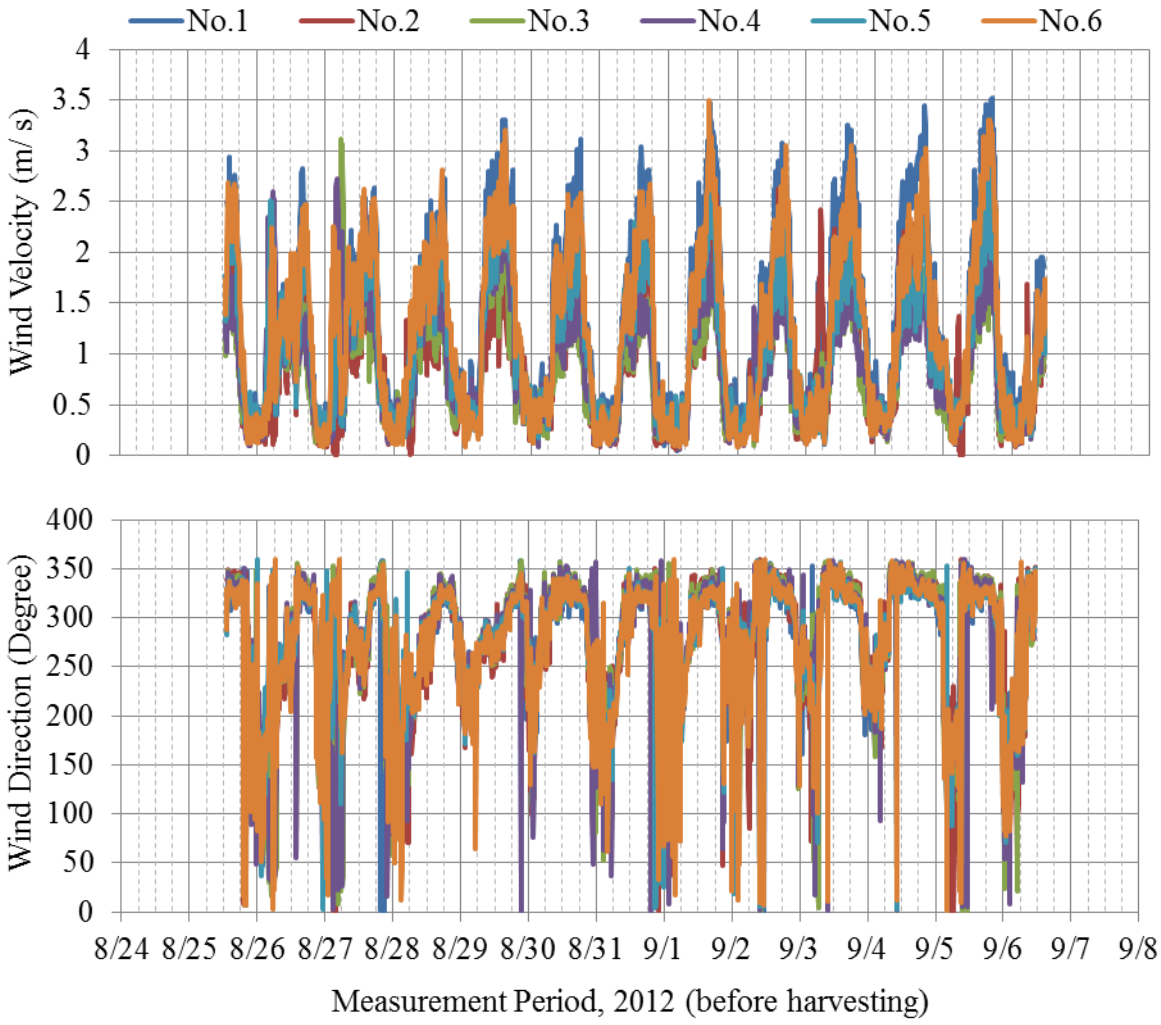

Figure 68 Daily variations of wind velocity (m/s) and wind direction (degree), in the measurement period before harvesting.

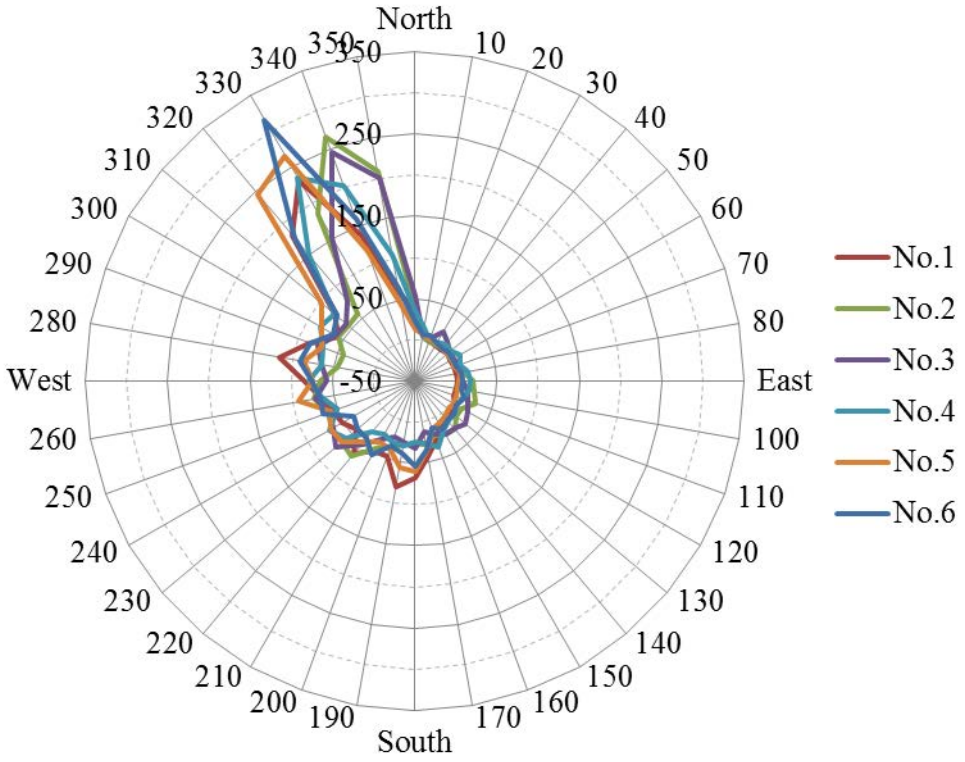

Figure 69 Wind rose of each measurement points at Al Krakat before harvesting, from August 25th to September 6th in 2012

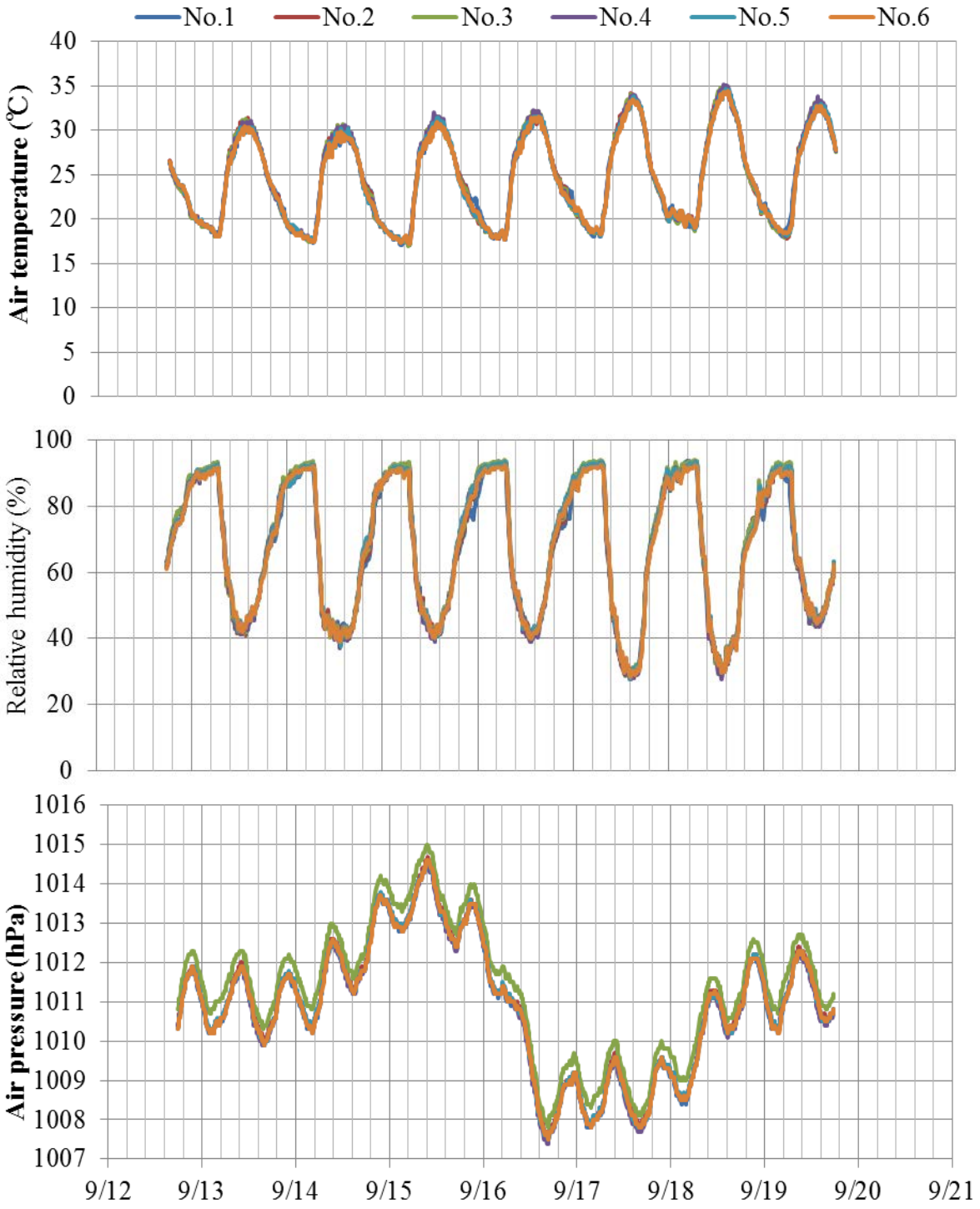

Figure 70 Daily variations of air temperature(℃), relative humidity (%) and air pressure (hPa), in the measurement period after harvesting.

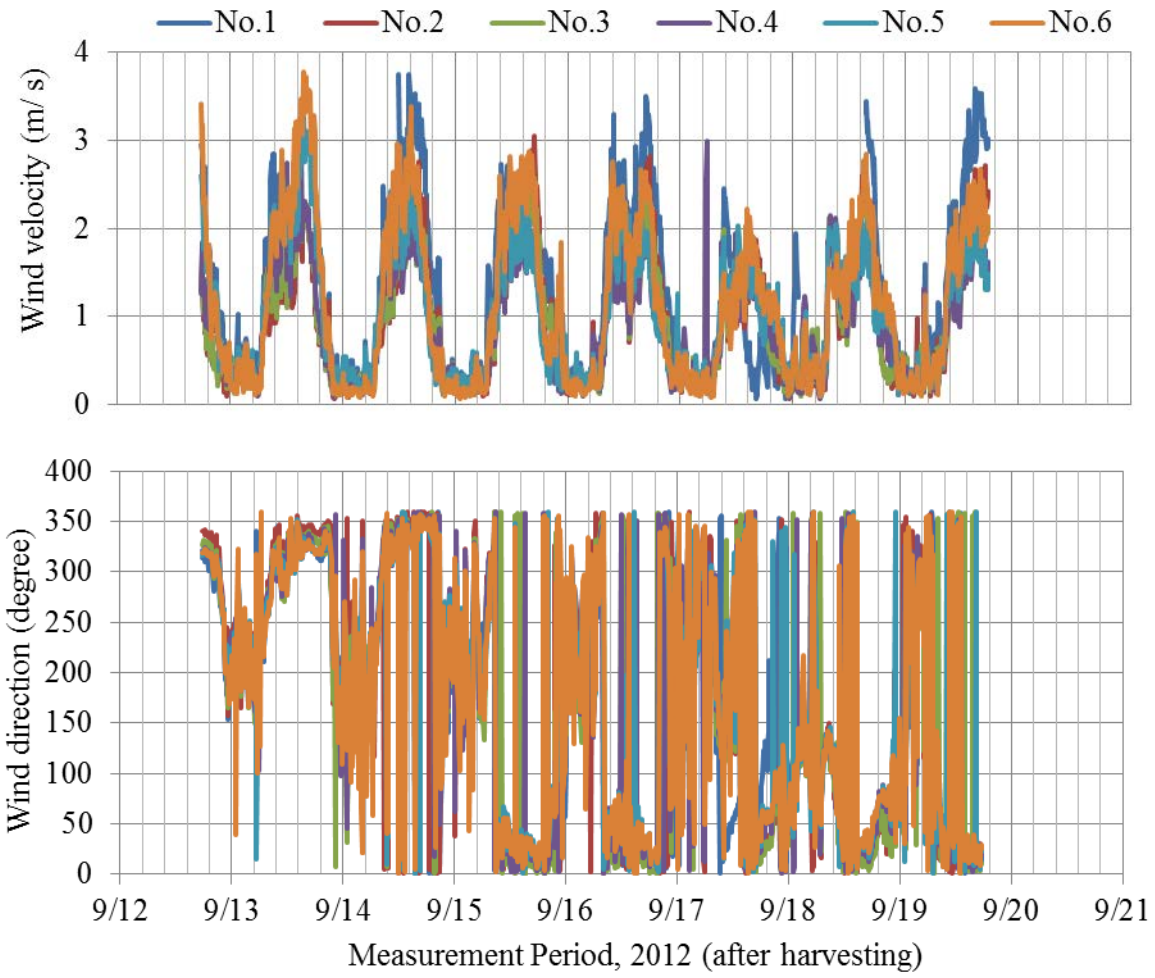

Figure 71 Daily variation of wind velocity (m/s) and wind direction (degree), in the measurement period after harvesting.

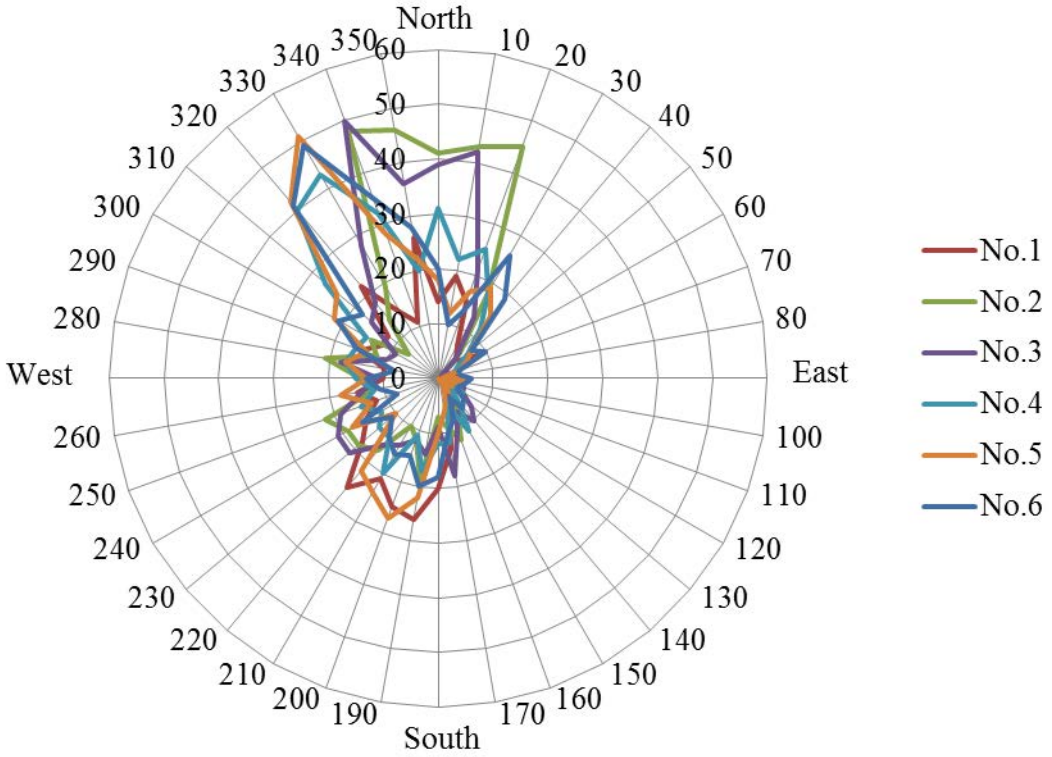

Figure 72 Wind rose of each measurement points at Al Krakat after harvesting, from September 12th to 19th in 2012

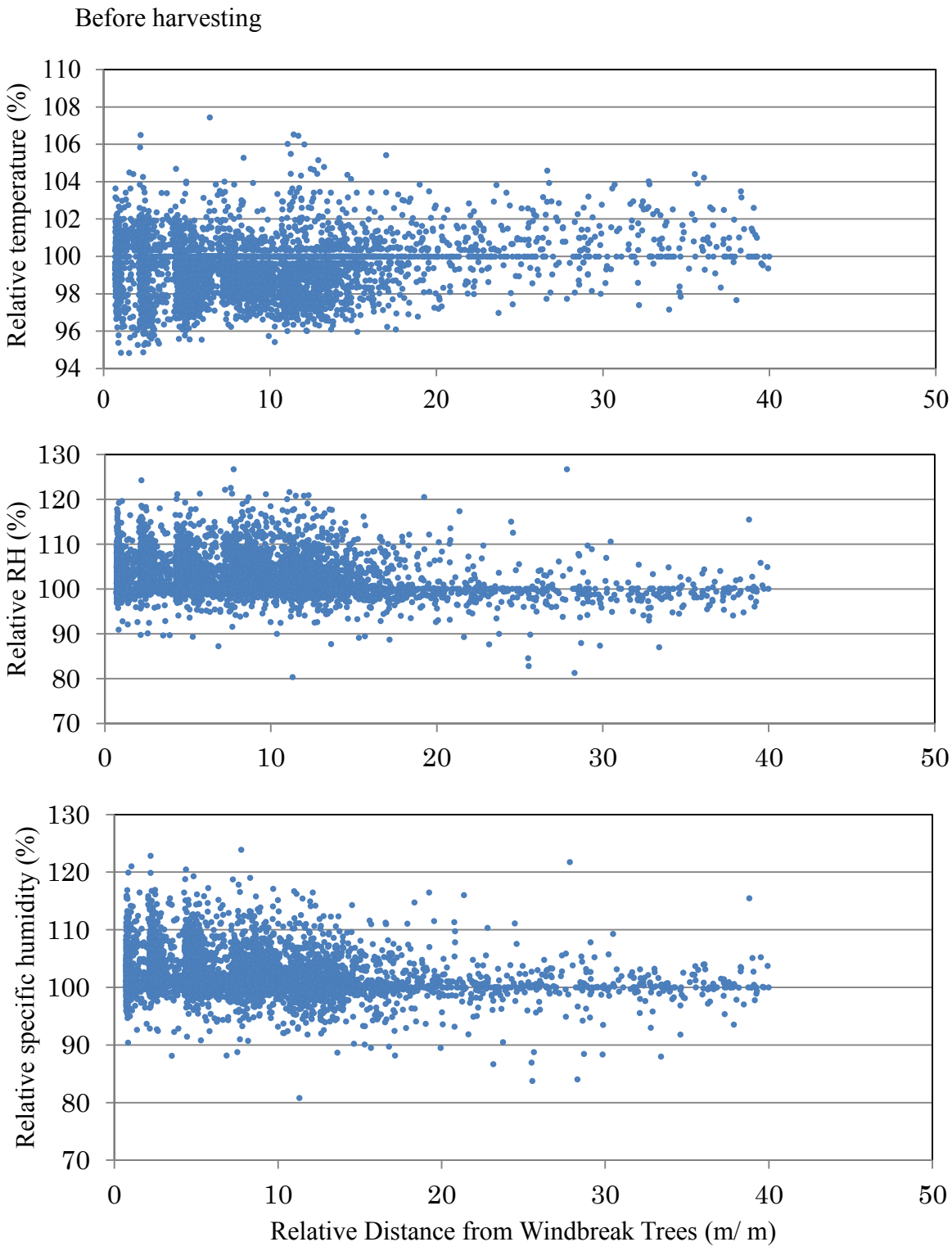

Figure 73 Relative data profiles of air temperature, relative humidity and specific humidity leeward of the windbreak trees at Al Krakat in the summer of 2012 (before harvesting)

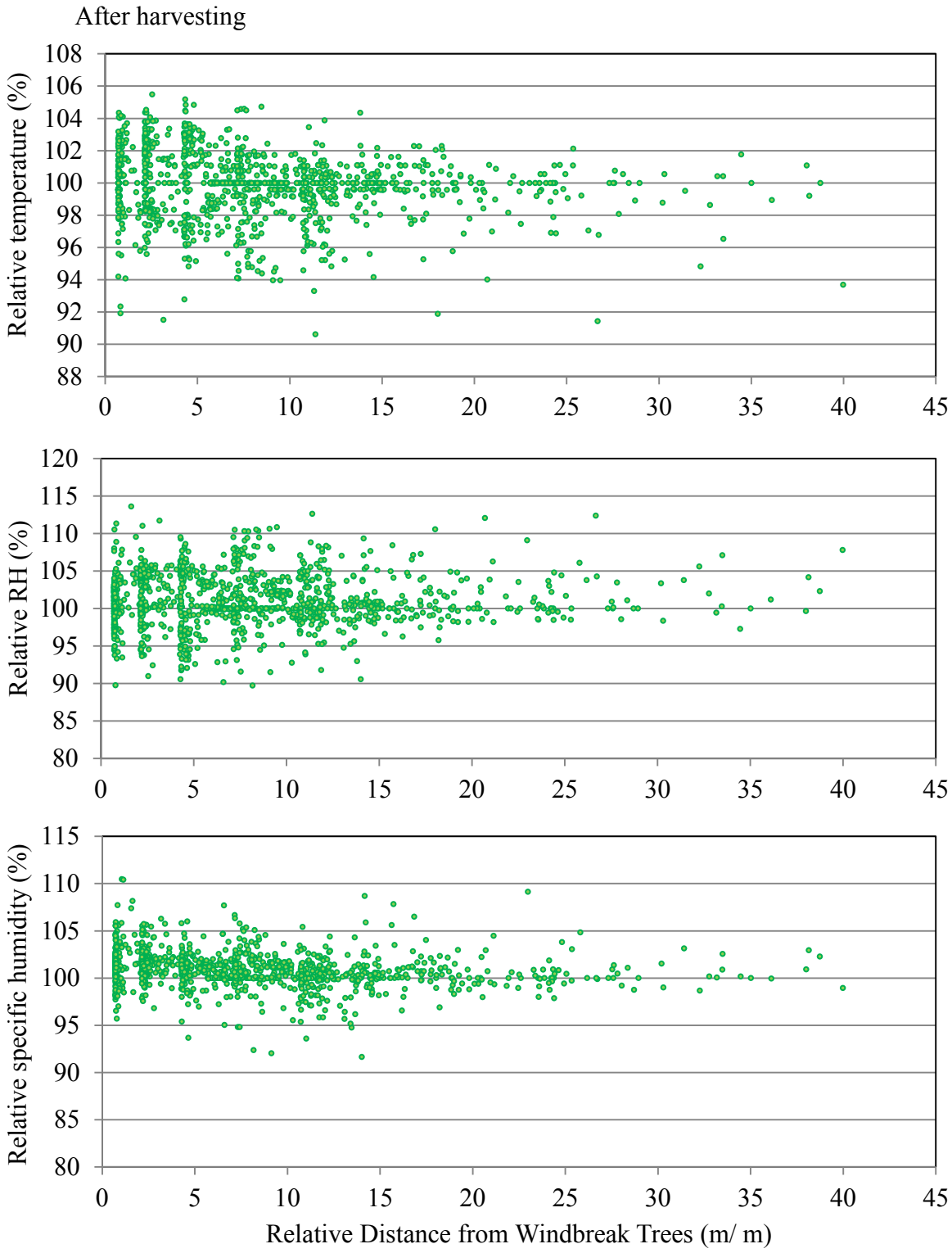

Figure 74 Relative data profiles of air temperature, relative humidity and specific humidity leeward of the windbreak trees at Al Krakat in the summer of 2012 (after harvesting)

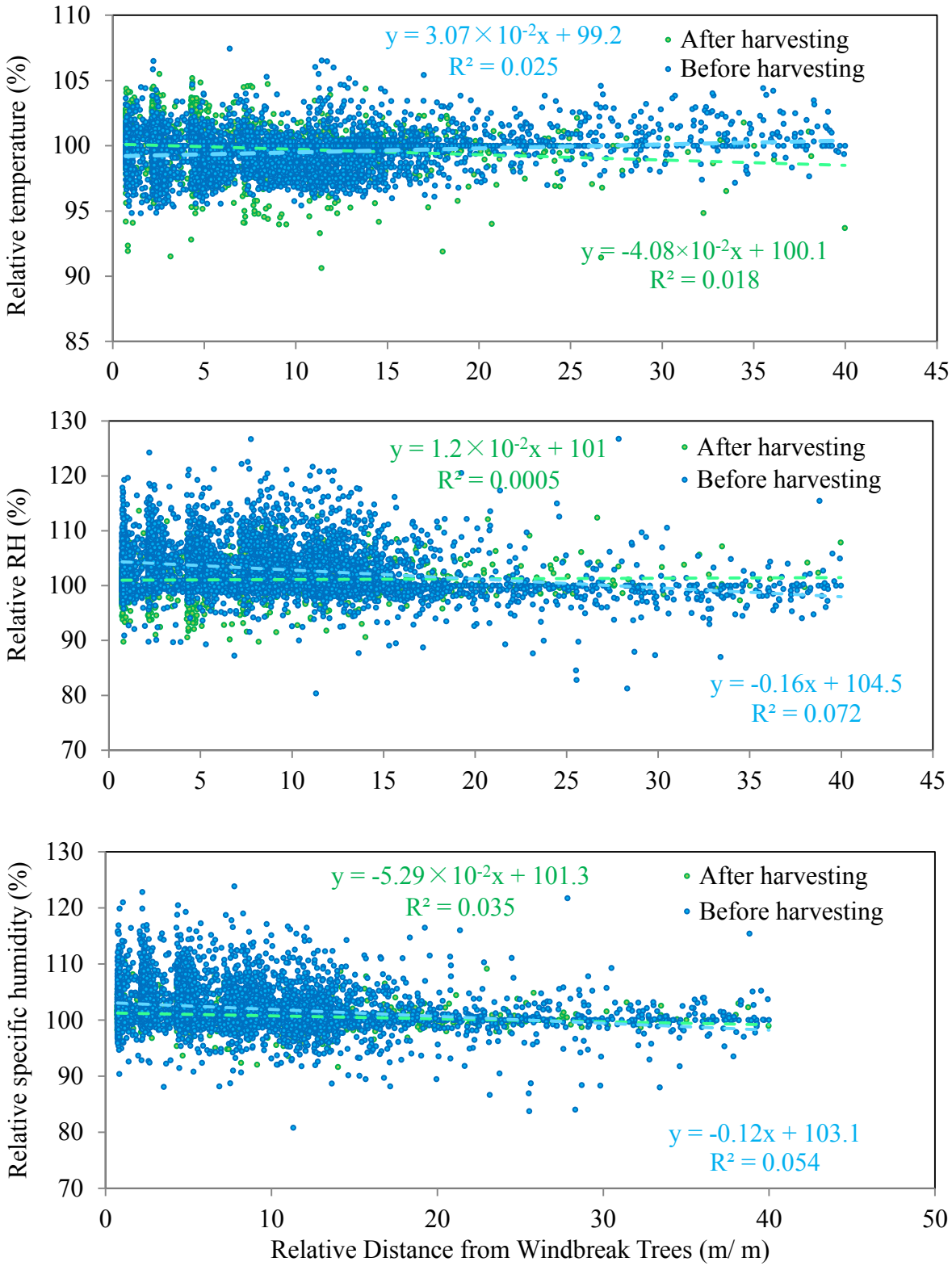

Figure 75 Comparison of the relative profiles of meteorological data, such as air temperature, relative humidity and specific humidity, between before and after harvesting.

time when the value of wind velocity got less than 1 m/s were similarly rejected. After this data transaction, wind rose after harvesting was drawn out. Comparing the wind roses between before and after harvesting, both data have similar trend which main wind directions were north-west regardless before or after harvesting. Thus, it can be decided suitable for that the horizontal variations of some meteorological data in south field would be measured as the variations leeward of windbreak trees.

Other horizontal profiles of meteorological data (such as air temperature, relative humidity and specific humidity) in period of before and after harvesting are shown in Figure 73 and Figure 74. Horizontal profiles of meteorological data both before and after harvesting are shown in Figure 75 together, and compared the functions each other. These horizontal variations seemed to have no trend against relative distance from the windbreak trees. However, some statistical analysis should be done against the horizontal variations of meteorological data, such as air temperature, relative humidity and specific humidity to evidence that they have no trends.

The correlations between relative distance and relative meteorological data (air temperature, relative humidity and specific humidity) were considered if they have a trend by Mann-Kendall rank statistic. Mann-Kendall rank statistic is a nonparametric test, thus frequency distribution of time-series data was not necessary to be considered. Test statistic τ is generally defined by following equation.

$$\tau = 4\left(\sum_{i=1}^{N} n_i \Big/ \left[N\left(N-1\right) \right] \right) - 1 \tag{1.28}$$

where n_i is the number of values latter of i which are larger than the value of the turn of i, N is the number of samples. In this case, the null hypothesis was “the variations do not have trends”.

For validation of significance, τ should be compared with τ_g given by following equation.

$$\tau_g = \pm t_g \left[\left(4N+10\right) \Big/ 9N\left(N-1\right) \right]^{1/2} \tag{1.29}$$

where t_g is value from a t-test (level of significance is 1% or 5%). In this case, null hypothesis is “the variations do not have trends”, so if τ was larger than τ_g, the hypothesis should be rejected. In other ward, if τ is smaller than τ_g ($\tau_g - \tau > 0$), the hypothesis “the

Table 12 Results of Mann-Kendall Rank Statistic

	Relative values	τ	τ_g	τ_g - τ	Proposition
Before harvesting	Air temperature	-9.38×10^{-2}	6.17×10^{-14}	+	no trend
	Relative humidity	-7.35×10^{-2}	1.03×10^{-13}	+	no trend
	Specific humidity	-1.38×10^{-2}	-6.5×10^{-14}	+	no trend
After harvesting	Air temperature	-9.90×10^{-2}	3.17×10^{-14}	+	no trend
	Relative humidity	-9.98×10^{-3}	-8.2×10^{-15}	+	no trend
	Specific humidity	-3.01×10^{-3}	2.28×10^{-14}	+	no trend

variations do not have trends" would be accepted. The values of τ and τ_g and each proposition are shown in Table 9 for each horizontal variation.

By Mann-Kendall rank statistic, the correlations between relative distance from windbreak trees and meteorological data have no trend. In other ward, it was validated that meteorological data leeward of windbreak trees are not affected by the distance from the windbreak trees. According to this result, horizontal variations of meteorological data, such as air temperature, relative humidity and specific humidity leeward of the windbreak trees were treated as constant in this study. Thus, finally it can be said that leeward of windbreak trees, there is only one horizontal variation of wind velocity in meteorological aspect, and other meteorological data, such as air temperature, relative humidity and specific humidity can be treated that the horizontal variations of them have no trend against relative distance from the windbreak trees. Furthermore, these results can be applied for an agricultural land regardless of crop existence, in other words, difference of the trends of horizontal variations of meteorological data between an agricultural land with and without crops could be ignored.

3-2-2. Measurements of characteristic of crops and soil

The horizontal profiles of the data of crops and soil before harvesting are shown in Figure 76. The horizontal line means relative distance from the windbreak trees and the vertical line means the real measured data of each crop. The horizontal profiles of soil data after harvesting are shown in Figure 77. Measured data at Al Krakat are shown in Table 3. In case of data before harvesting (Figure 76), all horizontal profiles could be said that these environmental factors (such as soil thermal conductivity, soil water content and soil surface temperature) were not affected by the horizontal wind profile, except for LAI of the crops. Actually as the ecosystem in an agricultural land, these soil physics and crop characteristic data showed the result affected by meteorological conditions. For example, the soil water content might be affected by soil evaporation, and at the same time, soil evaporation might be affected by the horizontal variation of wind velocity. If soil water content were affected by evaporation, soil thermal conductivity also might be affected. Thus, the horizontal variation of wind velocity might affect to soil evaporation, soil water content and finally soil thermal conductivity. However, the range of the variations of soil water content was small. Furthermore, horizontal variations of soil water content and soil thermal conductivity seemed not to have correlation with horizontal variation of wind velocity very much. On the other hand, horizontal variations of LAI, soil surface and leaf surface temperature seemed to have some correlation with horizontal variation of wind velocity, because of its shape of the horizontal variation.

In case of after harvesting (Figure 77), these environmental factors were also not affected by the horizontal wind profile, similar to before harvesting. Thus, regardless of

cases before or after harvesting, all environmental factors could be treated as constant values in direction of leeward. The daily variations of measured soil surface temperature before and after harvesting are shown in Figures 78 and 79. According to these result, it can be said that daily variations of environmental factors in a day are more important leeward of windbreak trees, rather than the horizontal profiles, and this is mentioned in the result of daily variation of evaporation which measured by Chamber method (Matsuno, personal communication) shown in Figures 80 and 81. The range of horizontal variations of soil water content, soil thermal conductivity and soil surface temperature seemed to get smaller than these data before harvesting. The horizontal variation of soil surface temperature seemed to have some correlation with the horizontal variation of wind velocity, because of the trend of the variation. The diurnal variation of soil evaporation measured by Chamber method seemed that most of measurement of soil evaporation got largest value around noon, except for No. 1. Because the north field where No. 1 sensor was set was harvested earlier than south field by four days. The horizontal variations of soil evaporation at each time steps have different horizontal variations. As the sun got lower, the peak of the variation shifted from far point to near point against the trees.

In the environmental factors, there are two components which have highly correlation each other in surface soil, soil thermal conductivity and soil water content. In this study, the correlation between soil thermal conductivity and soil water content which were measured the depth of 6.5 cm in the Nile-Delta was clarified. Additionally, the soil contains much organic matters. The correlation between soil thermal conductivity and soil water content was used to set parameters in TOPLATS model. In TOPLATS model, soil moisture is calculated as an output, and soil thermal conductivity would be calculated. At the same time, soil surface temperature and soil heat flux would be calculated by TOPLATS model. Figure 82 shows the correlation between soil thermal conductivity and soil water content of soil surface layer (6.5 cm depth) at three fields (Sakha, Al Krakat and Zankalon in September, 2012) and one previous measurement (personal communication, Matsuno in March, 2012), and in Figure 83, all data at three fields were put together. However, the plots of data appear scattered. Thus the first maximum value of soil thermal conductivity against soil water content was estimated to pre-screen data by a method of Hillel (2001). In Hillel (2001), general functional form between soil moisture and soil thermal conductivity is given as the following equation

$$x_c = \frac{f_w x_w + k_s f_s x_s + k_a f_a x_a}{f_w + k_s f_s + k_a f_a} \tag{1.30}$$

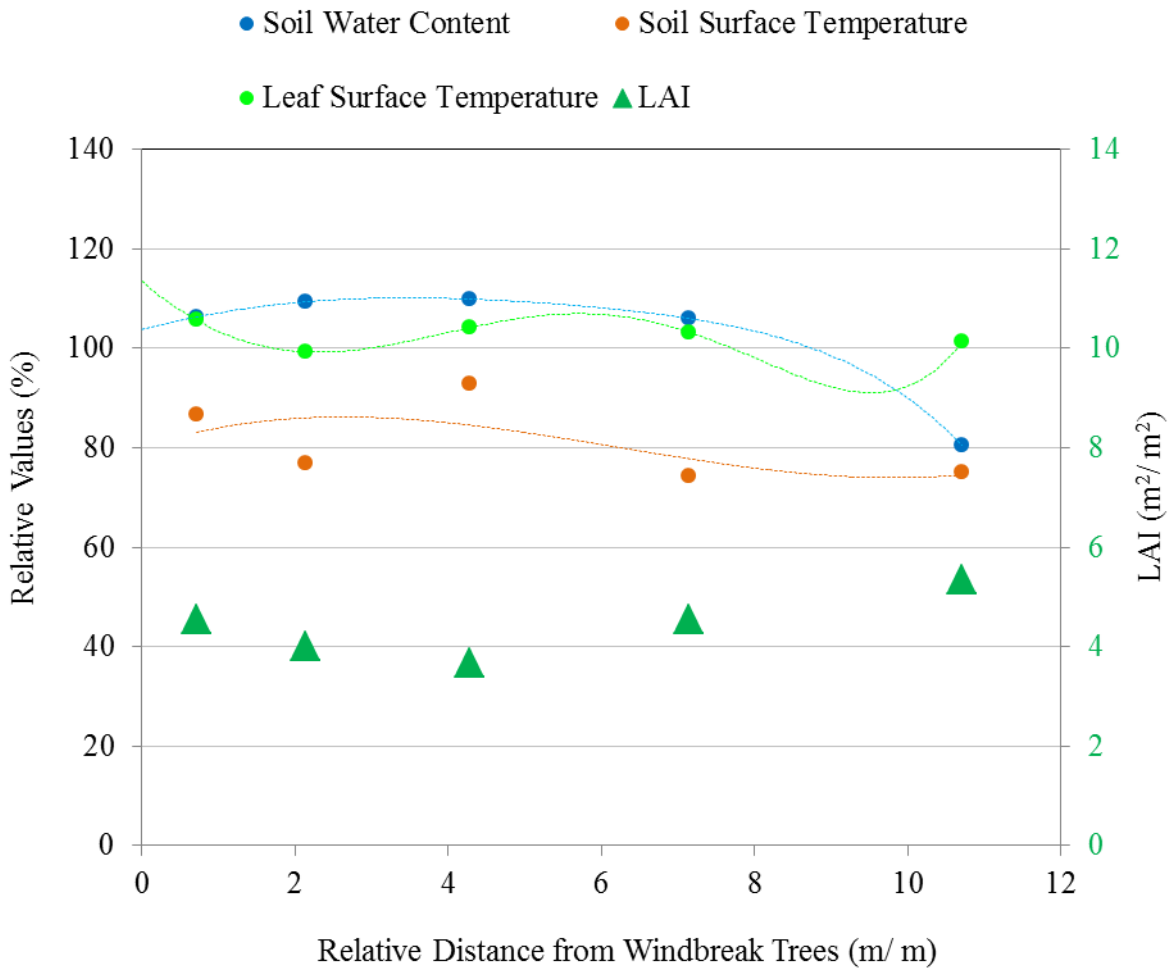

Figure 76 Horizontal profiles of the data of soil and crops at Al Krakat. (before harvesting). x-axis: relative distance means the distance from windbreak trees (m) scaled by average height of windbreak trees (14 m), y-axis: relative means the values of each variables measured at point 2-6 scaled by the values measured at point 1 at Al Krakat

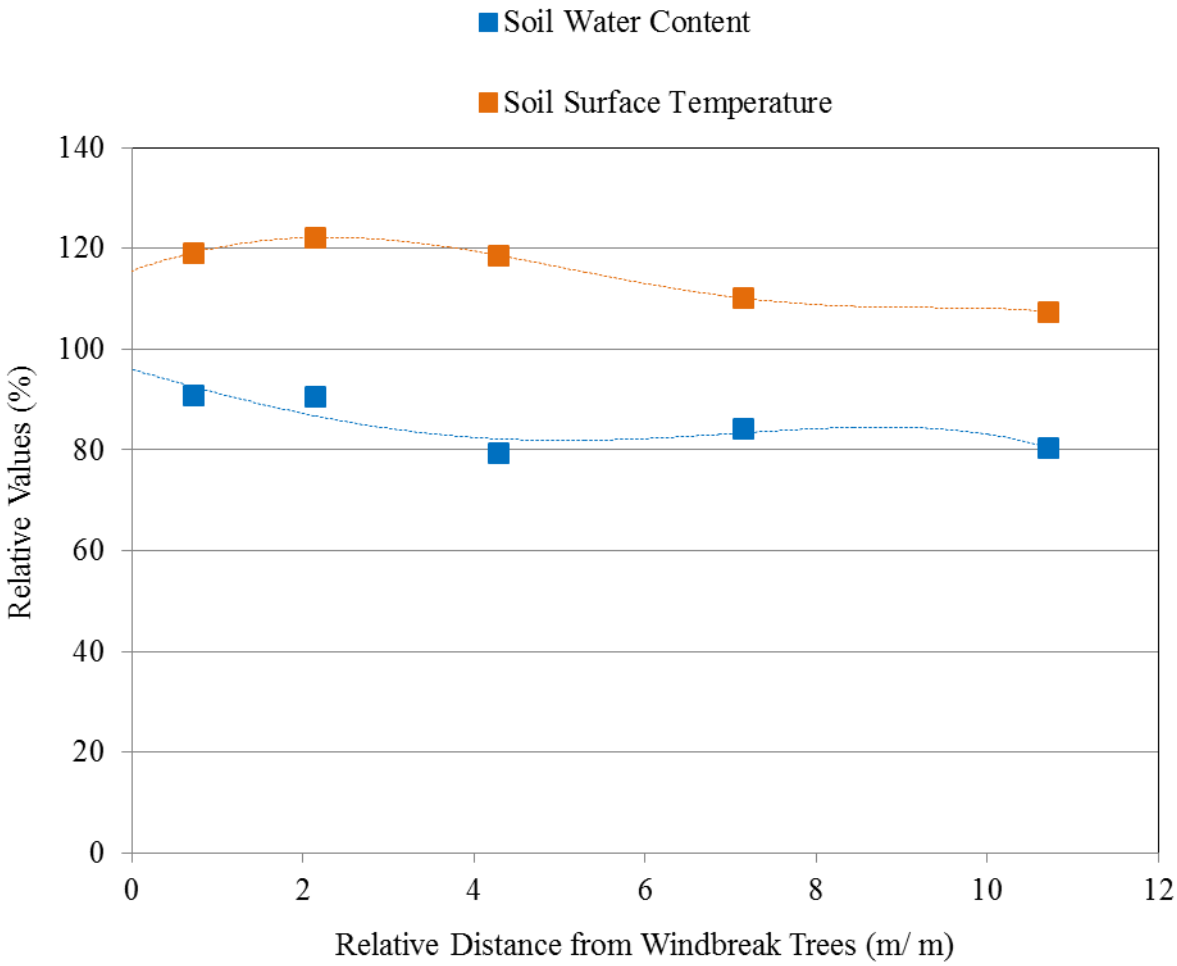

Figure 77 Horizontal profiles of the data of soil and crops at Al Krakat. (after harvesting) x-axis: relative distance means the distance from windbreak trees (m) scaled by average height of windbreak trees (14 m), y-axis: relative means the values of each variables measured at point 2-6 scaled by the values measured at point 1 at Al Krakat

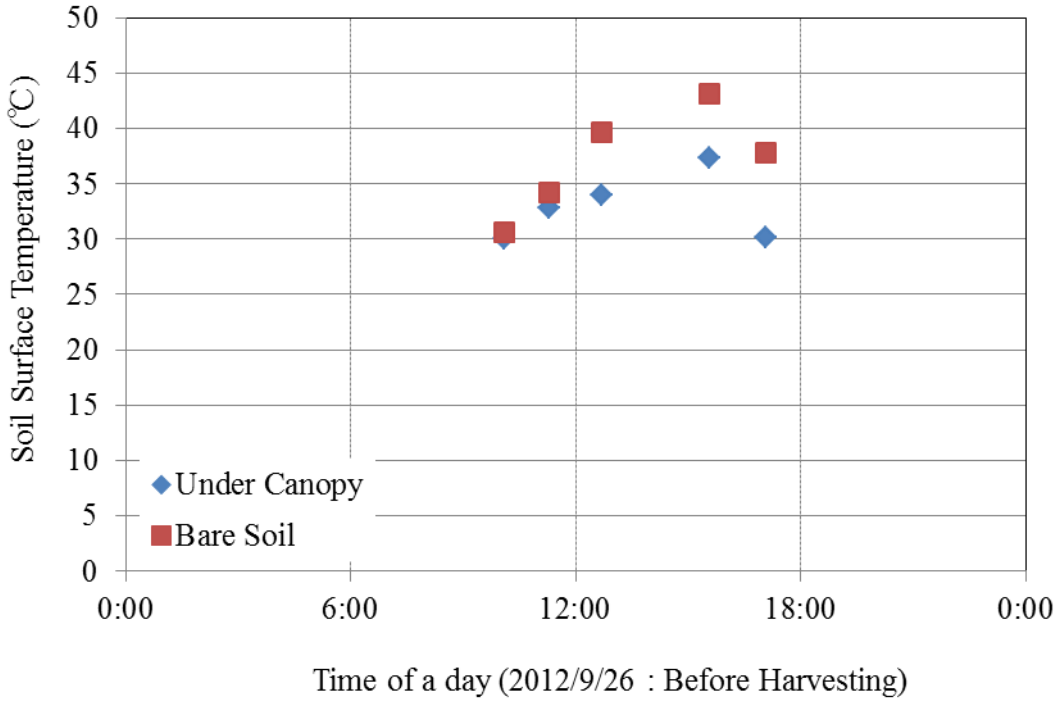

Figure 78 Measured daily variations of surface temperature of soil and canopy at Al Krakat. (before harvesting)

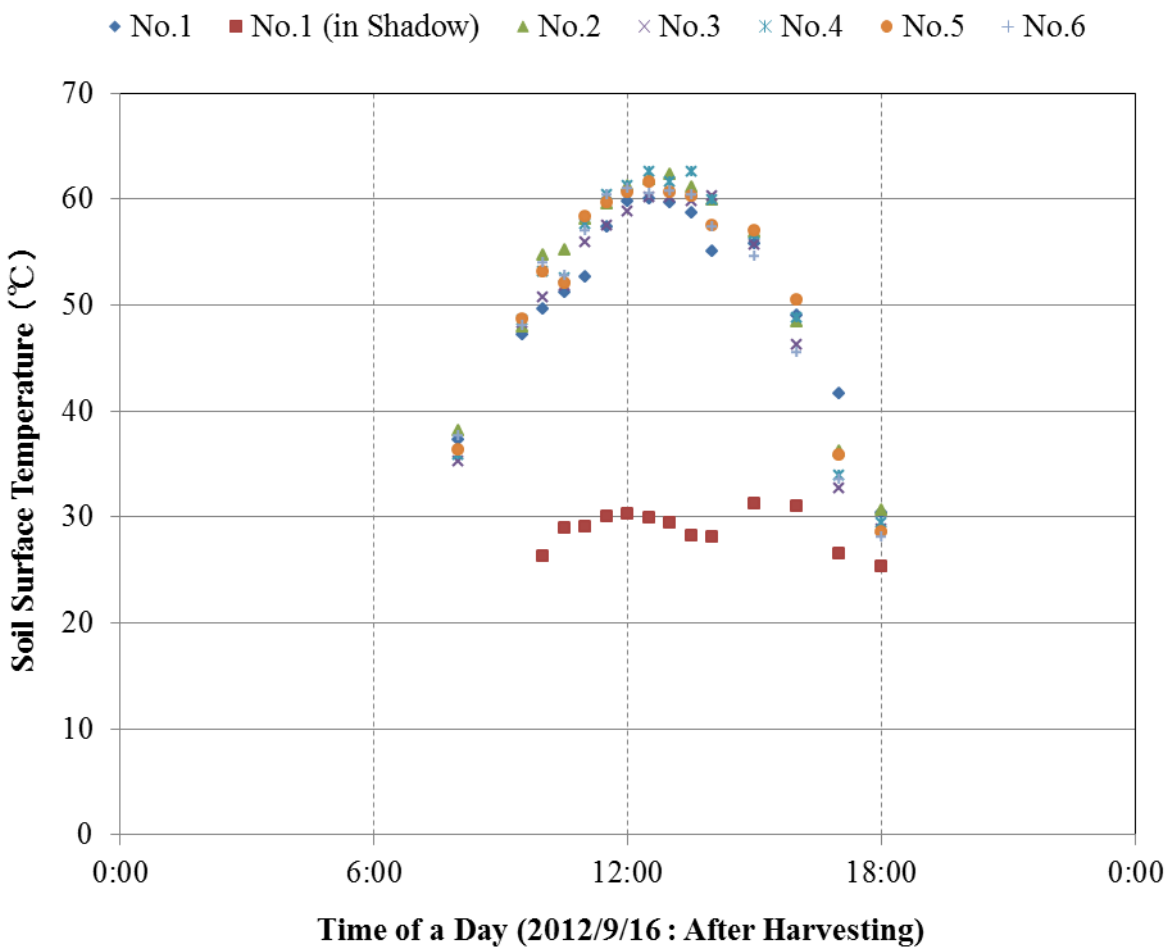

Figure 79　Measured daily variations of surface temperature of soil and canopy at Al Krakat. (after harvesting). No.1 (in Shadow) means measurements in the shadow of windbreak trees in North field, not at the point of No.1.

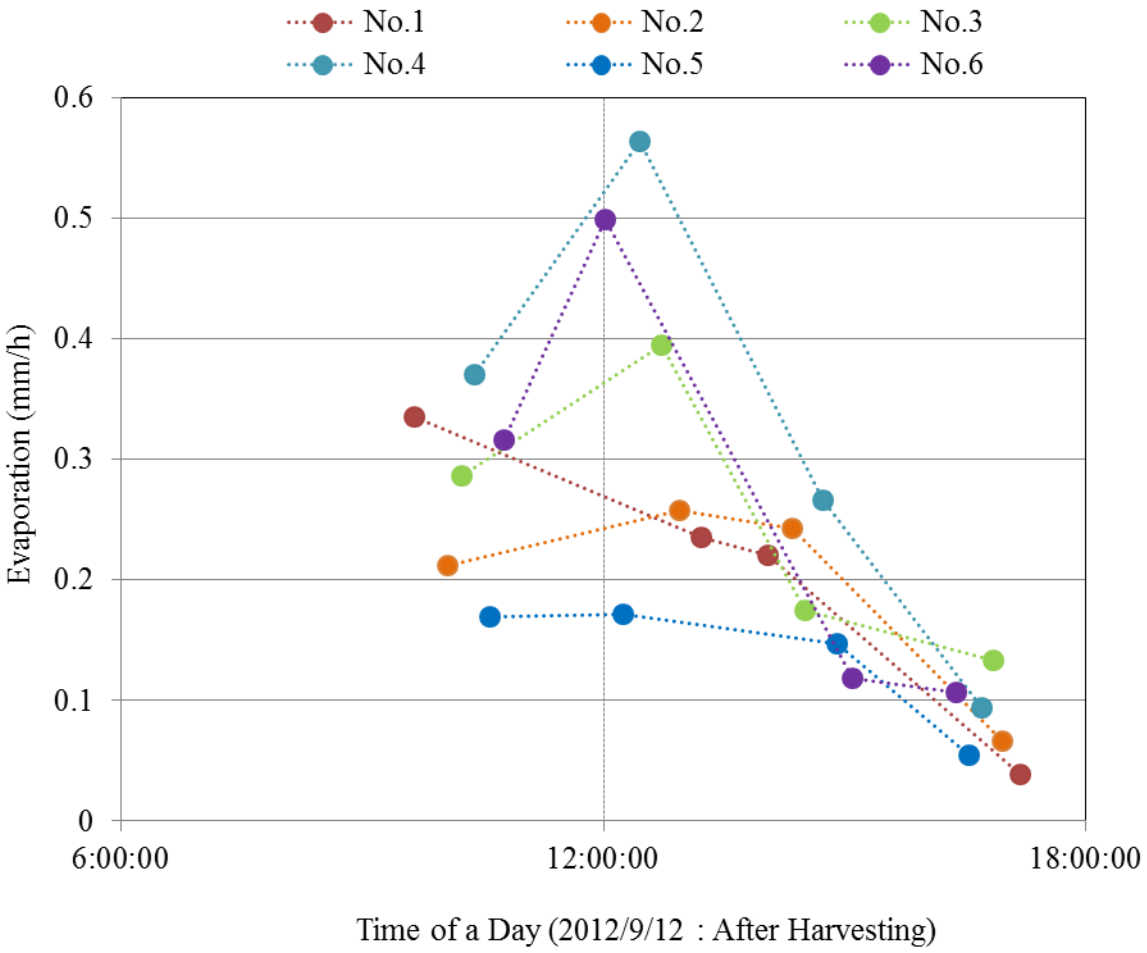

Figure 80 Measured daily variation of evaporation (mm/ h) by chamber method at each measurement points at Al Krakat. (after harvesting)

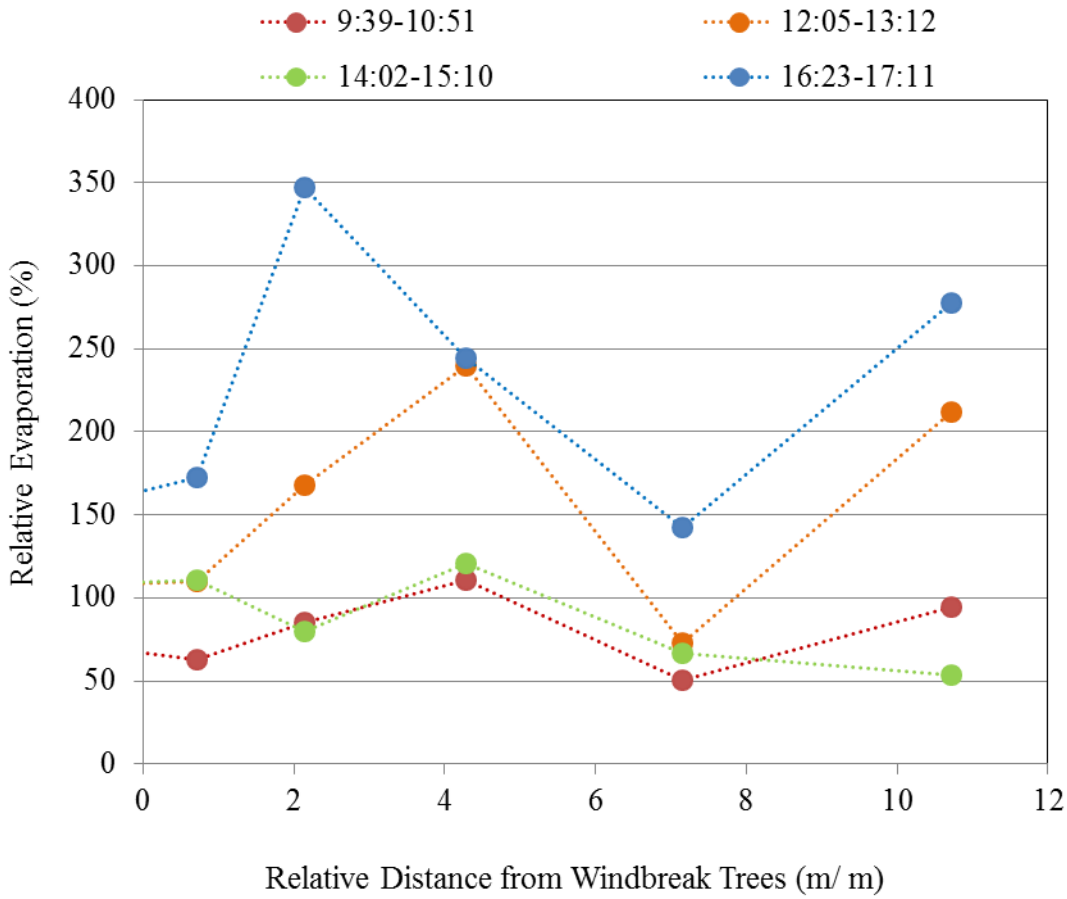

Figure 81 Relative evaporation profiles of four periods in a day of 2012/9/12 at Al Krakat (after harvesting) x-axis: relative distance means the distance from windbreak trees (m) averaged average height of windbreak trees (14 m), y-axis: relative means the values of each variables measured at point 2-6 averaged the values measured at point 1 at Al Krakat

where x_c is synthetic thermal conductivity of three phases of soil (i. e. solid, air and water), x_w, x_s and x_a are thermal conductivity of water, soil which contains air and water and the air, f_w, f_s and f_a are volumetric ratio of water, soil and air in soil, k_s is fraction of thermal inclination between water and soil and k_a is fraction of thermal inclination between in the air and water. These parameters are shown in Table 9. Figure 84 contains all plots of measured data and estimated maximum value of soil thermal conductivity as a blue curve. Plots above the blue curve could be regard as error data, because the blue curve is the maximum limitation (Figure 85).

According to this equation (1.31), some measured plots in 3 fields in the Nile-Delta can be rejected as errors. The scatter diagram of the correlation between soil moisture and soil thermal conductivity after rejecting errors by equation (1.31) is shown in Figure 86. The correlation between soil thermal conductivity and soil water content got much better after removing error plots by Hillel (2001) with $R^2 = 0.42$.

To validate this result, comparisons with some references were made (Figure 87). As Figure 88 shows, the result of this study is similar correlation to previous studies. Especially, the similarities between this study and Simada *et al*. (1992), Kasubuchi (1972) were remarkable.

These values might be influenced by the shadow of windbreak trees, as the shape of shadow changes diurnally. In the measurement at Al Krakat, six sensors were released from the shadow of the windbreak trees one by one, and the interval time was calculated as only 1 to 2 minutes. Thus, in TOPLATS model analysis, the effectiveness of shadow of the windbreak trees against soil water content and soil thermal conductivity was ignored in this study.

3-3. Estimation of evaporation and transpiration in an agricultural land

3-3-1. Daily variation of estimated evaporation and transpiration of an agricultural land without windbreak trees

The annual variations of evaporation and transpiration in an agricultural land at Sakha without windbreak trees are shown in Figure 89, but this result based on an assumption that there were no crops in winter cultivation from October 2010 to March 2011. Daily total evaporation and transpiration were separately estimated by TOPLATS model. Transpiration of crops got gradually larger because of the growth of crops, as shown in Figure 99, as a variation of LAI. Total integrated value of annual evaporation and transpiration are shown in Figure 90.

3-3-2. Validation of estimated evapotranspiration against measured evapotranspiration at Sakha

Validation of estimated soil evaporation was done with measured evaporation by

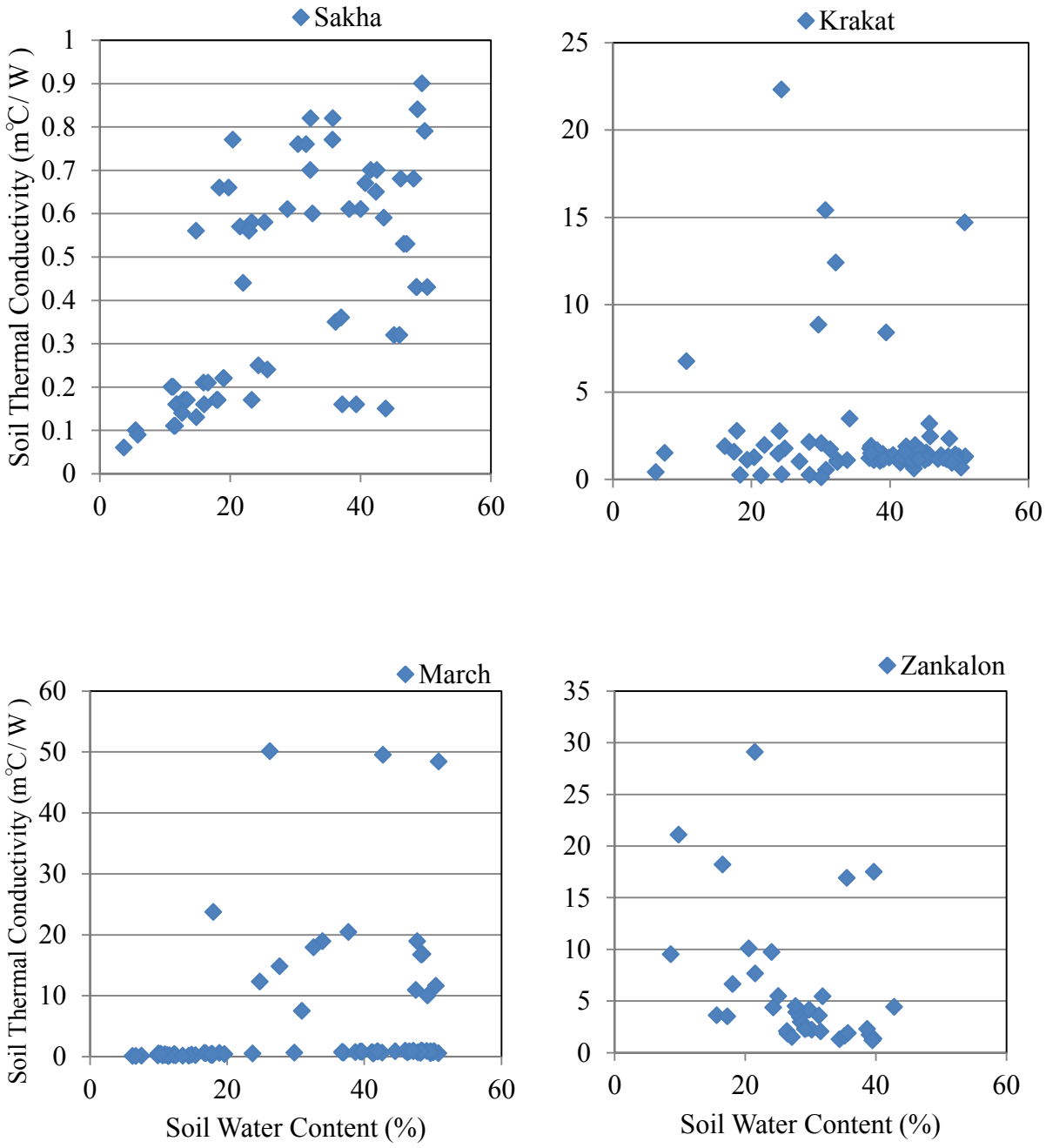

Figure 82　Correlation between soil water content (%) and soil thermal conductivity (m℃/W) for each observation fields.

Table 13　Parameters in Equation (1.30)

x_w	0.57	k_s	0.196
x_s	2.9	k_a	0.044
x_a	0.25	f_s	0.3

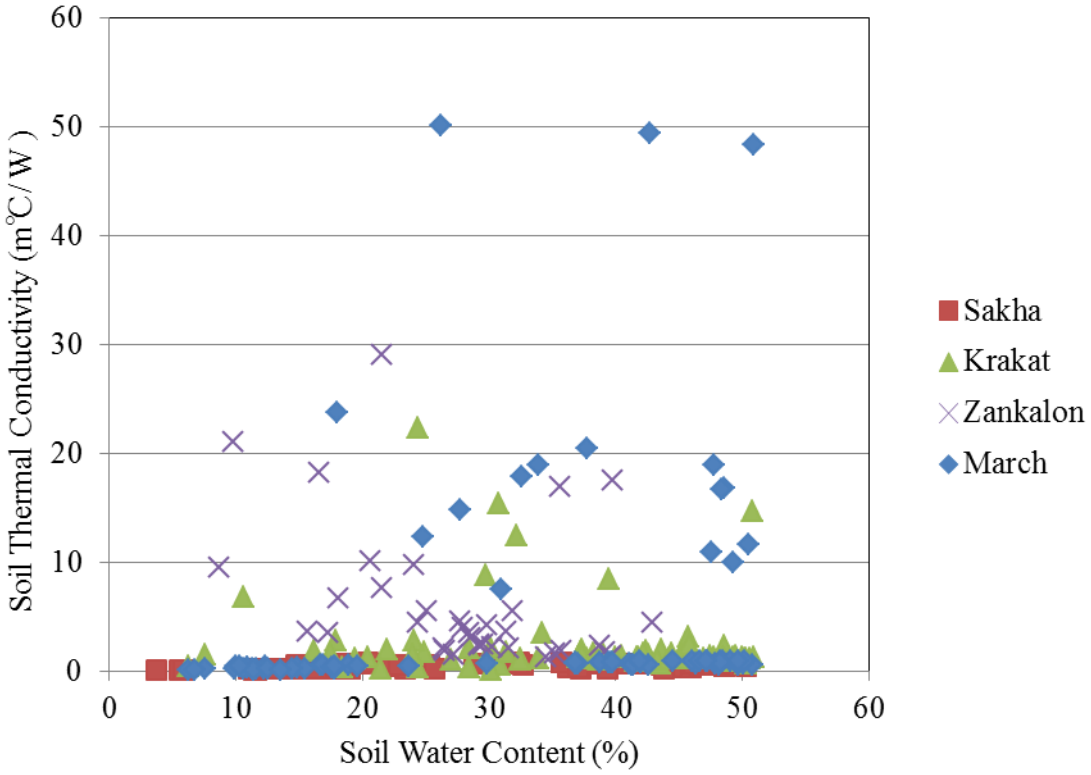

Figure 83 Correlation between soil water content (%) and soil thermal conductivity (m℃/W). (Data of all fields were put together)

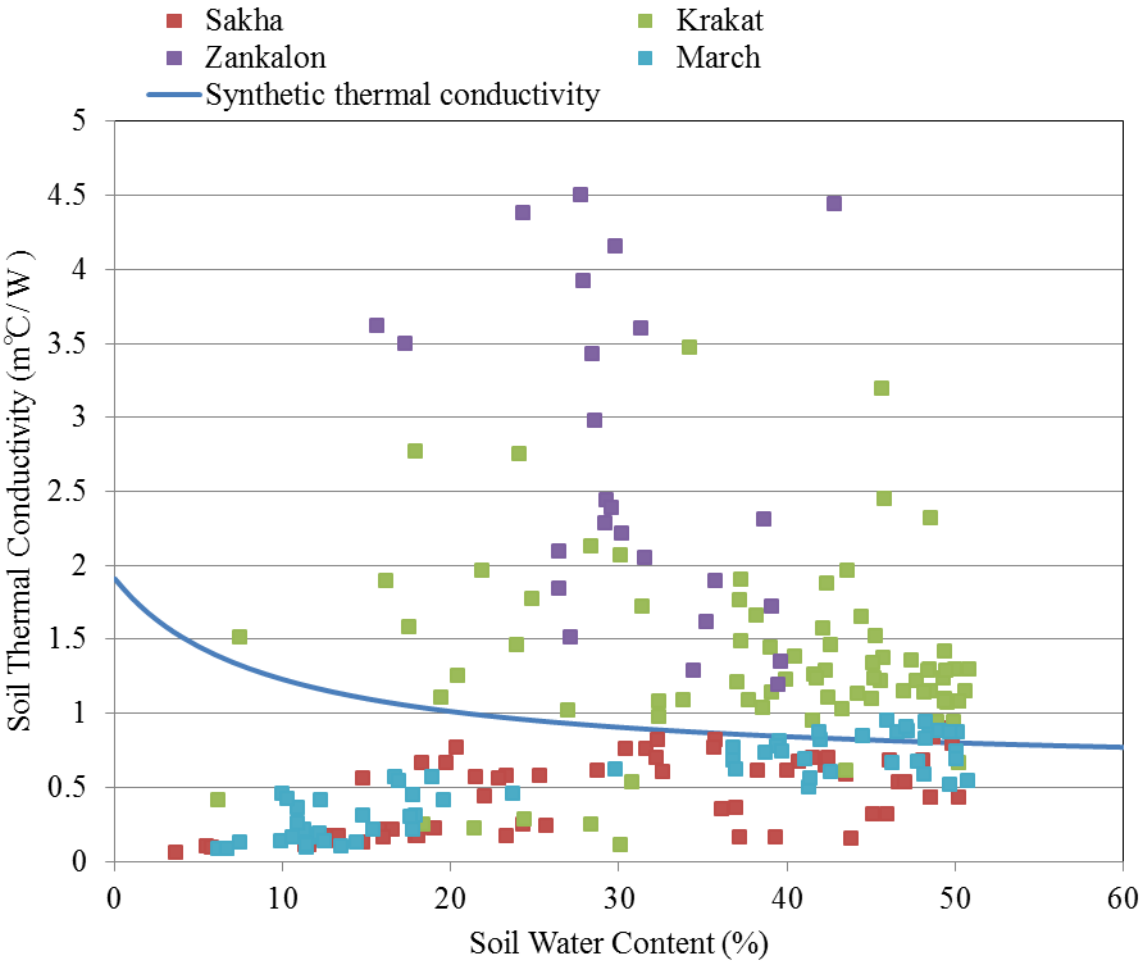

Figure 84 Correlation between soil water content (%) and soil thermal conductivity (m℃/W) and maximum synthetic thermal conductivity in the Nile-Delta. (Synthetic thermal conductivity was calculated by the equation in Hillel, 2001)

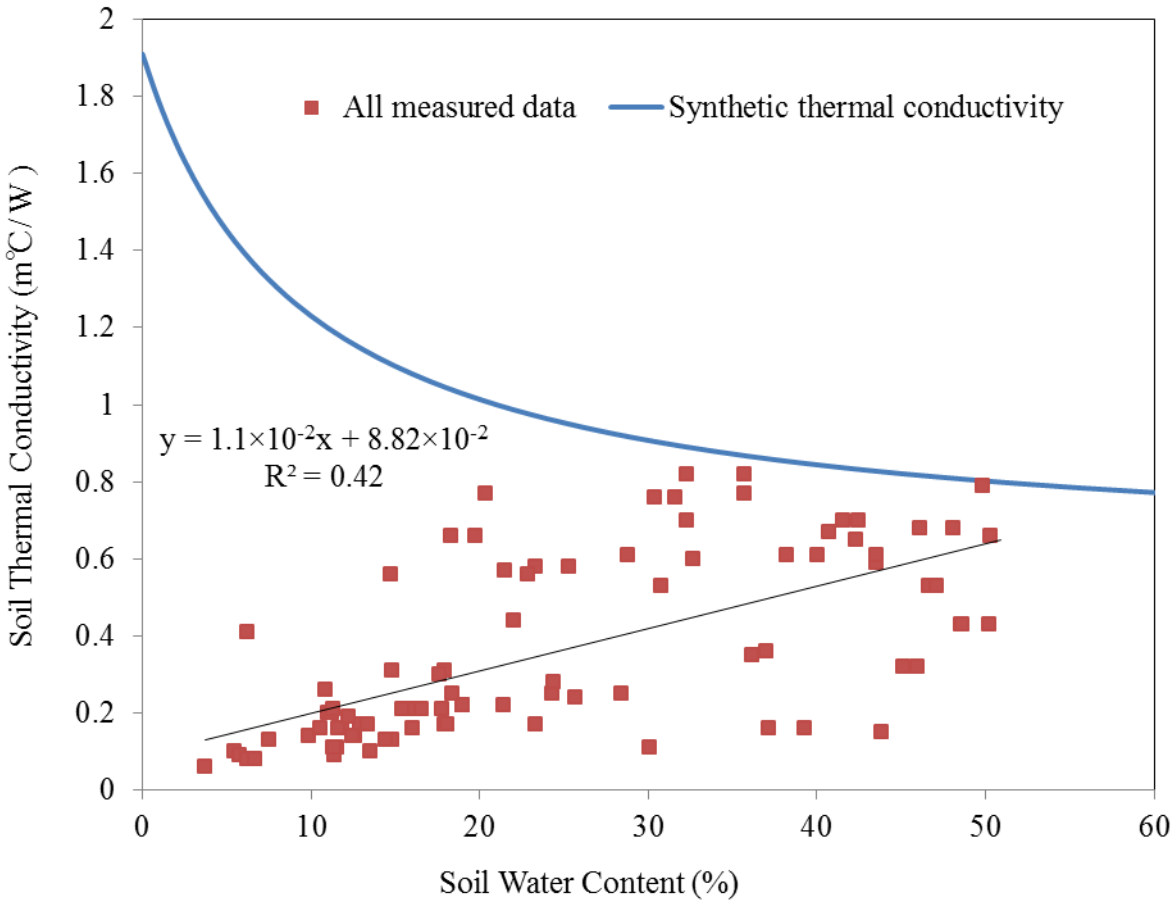

Figure 85 Plots of soil thermal conductivity over synthetic thermal conductivity were removed from Fig. 41, and the linear function and its determination coefficient of available plots of soil water content vs soil thermal conductivity.

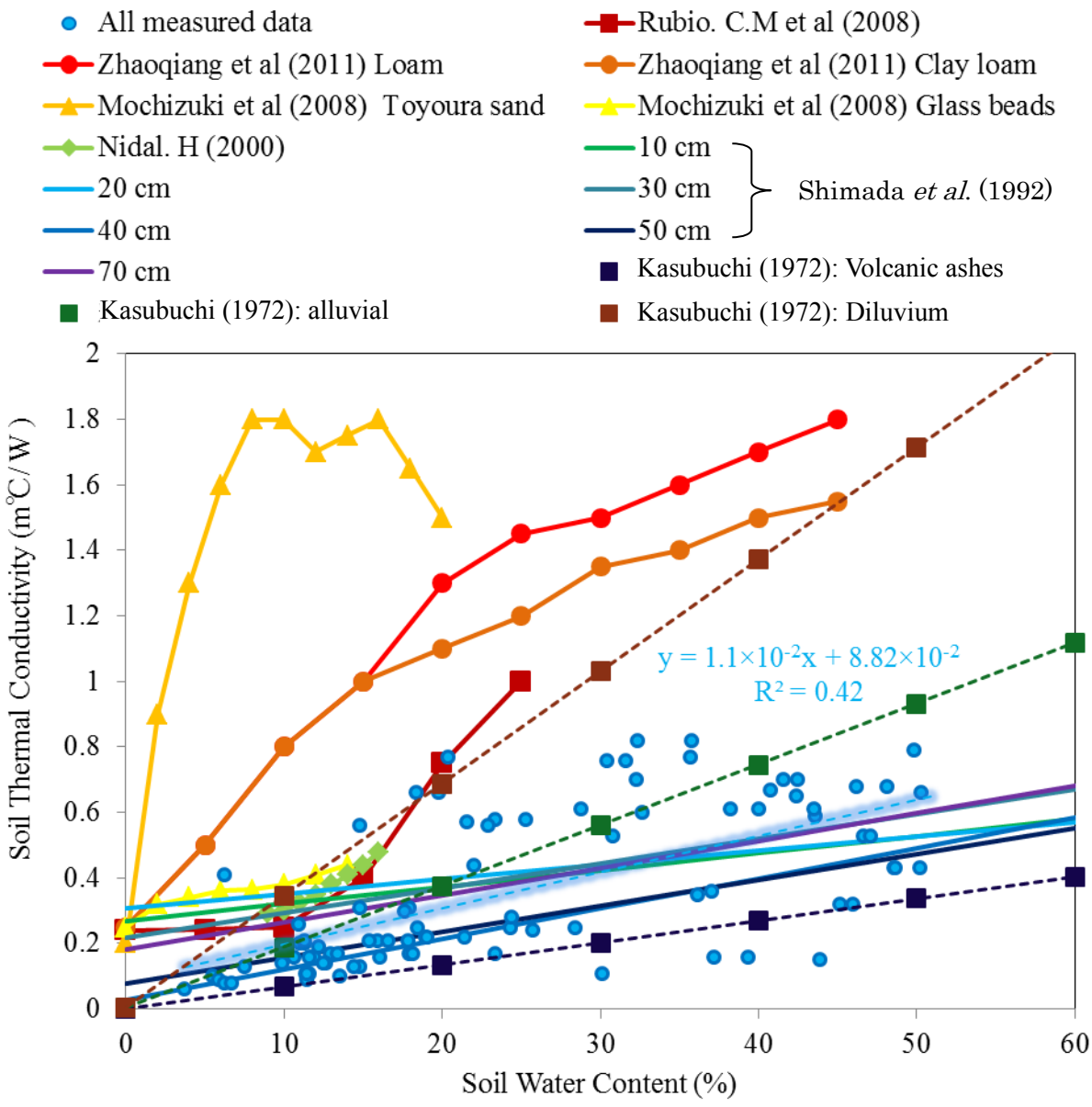

Figure 86 Comparison of the correlation between soil water content and soil thermal conductivity of this study with some previous studies

Chamber method (Matsuno, personal communication). The daily variations of estimated evaporation by TOPLATS model and Chamber method are shown in Figure 91, and the correlation between estimated evaporation by TOPALTS and Chamber method is shown in Figure 92, as a scatter diagram. As they show, estimated evaporation represented actual soil evaporation agree very well at least on this day, July 14th in 2011.

Validation of estimated evapotranspiration was done with measured evapotranspiration by eddy correlation method. The variations of evapotranspiration from April to September in 2011 estimated by TOPLATS and eddy correlation method are shown in Figure 93, and the correlation is shown in Figure 94. As Figure 93 shows, the variation of evapotranspiration estimated by TOPLATS could not represent the variation of evapotranspiration estimated by eddy correlation method very well. However, as Figure 94 shows, the correlation between daily integrated value of evapotranspiration estimated by TOPLATS and eddy correlation method was acceptable. Finally it can be said that the result of estimation of evapotranspiration by TOPLATS could represent the amount of evapotranspiration. However, the estimation of annual variation of evapotranspiration could be modified.

3-3-3. Daily variation of estimated evaporation, transpiration and evapotranspiration of an agricultural land with windbreak trees

By TOPLATS model with estimated input data, the seasonal variation of soil evaporation, crop transpiration and transpiration of windbreak trees themselves in an agricultural land without windbreak trees at Sakha field were estimated as Figure 95, and the result against a field with windbreak trees is shown in Figure 96. This variation reflects the horizontal profile of wind velocity measured at Al Krakat, by assuming there are windbreak trees as described in 2-4-2 section. The variation of evaporation and transpiration were estimated by TOPLATS model, and transpiration of windbreak trees was estimated by Penman-Monteith equation with Jarvis model. To compare the water balance among evaporation, transpiration from an agricultural land and transpiration of windbreak trees, both of them were divided by the area of Sakha field (170×180 m^2). The ratio of integrated values of evaporation and transpiration of windbreak trees are shown in Figure 97 with the amount of soil evaporation from a field without windbreak trees in fallow period. As it shows, the amount of transpiration of windbreak trees occupied only 4.3% of all evapotranspiration in an agricultural land, in spite of reduction of evaporation was 100 mm (52.5%) for two months (Figure 98).

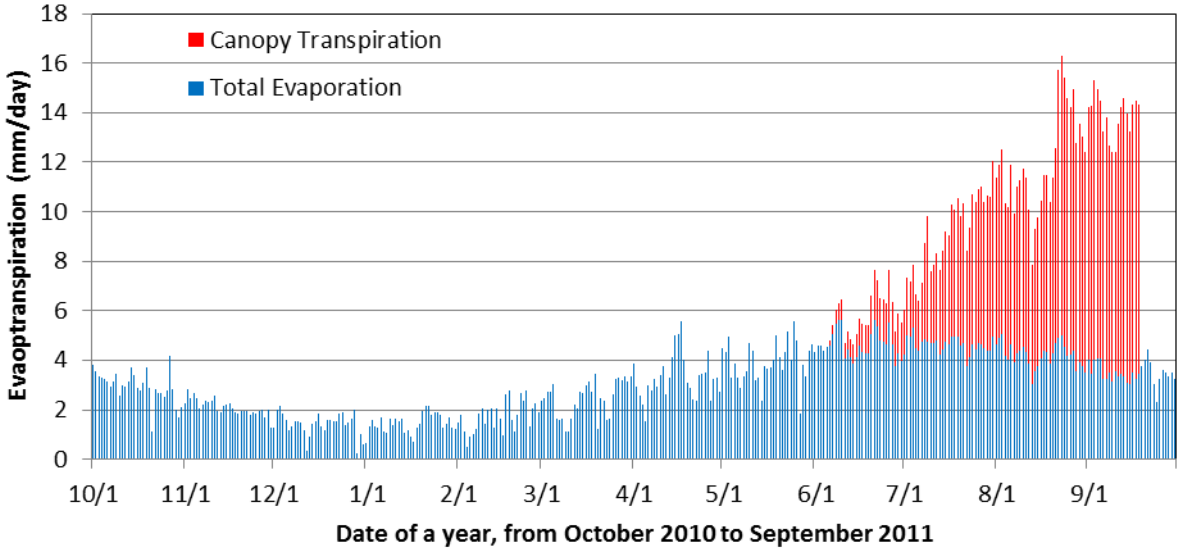

Figure 87 Estimated annual variations of evaporation (mm/day) and transpiration (mm/day) from an agricultural land (Sakha) without windbreak trees by TOPLATS model

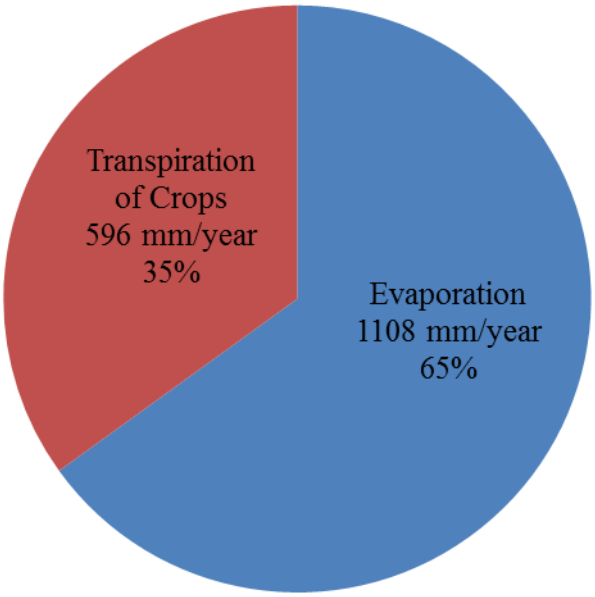

Figure 88 Ratio of integrated values of annual evaporation and transpiration in an agricultural land (Sakha) without windbreak trees

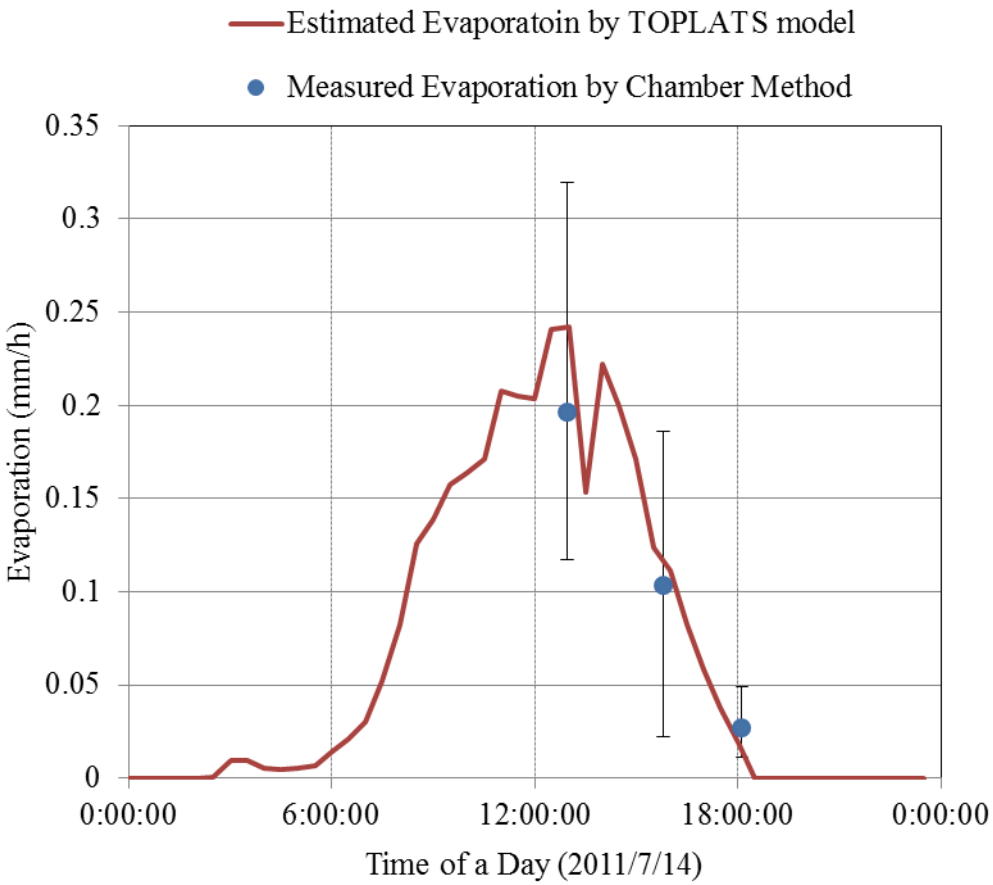

Figure 89 Validation of daily variation of estimated evaporation by TOPLATS model against measured evaporation by chamber method (Matsuno, personal communication): The error bar means maximum and minimum of each measurement.

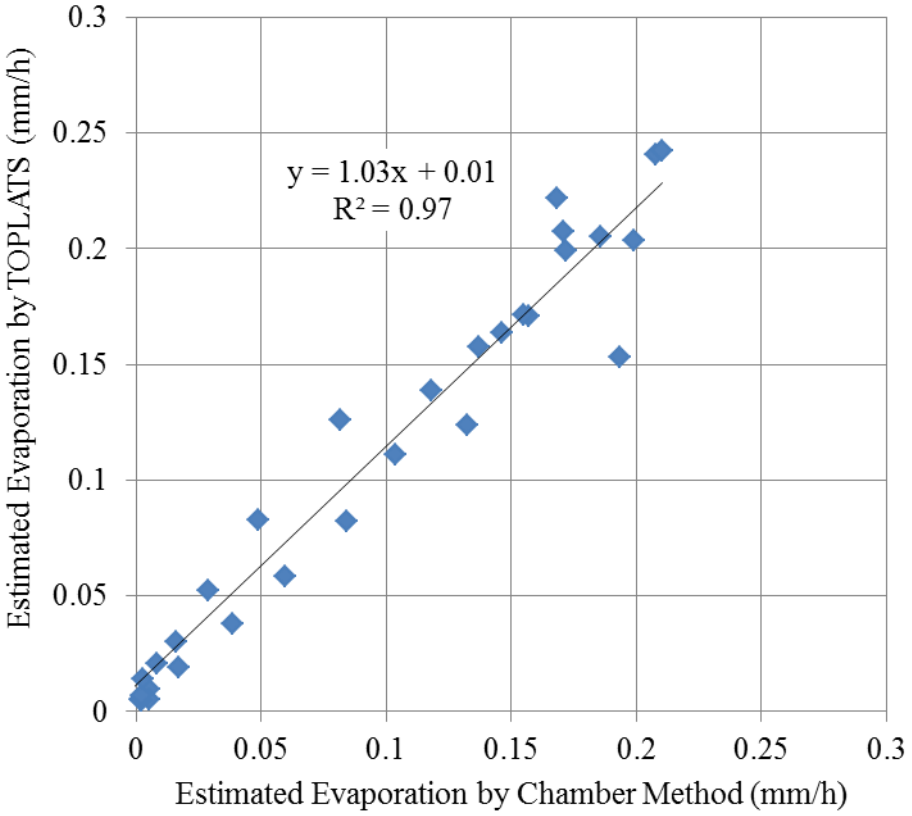

Figure 90　Correlation between estimated evaporation by TOPLATS model and chamber method in 2011/7/14 (Matsuno, personal communication)

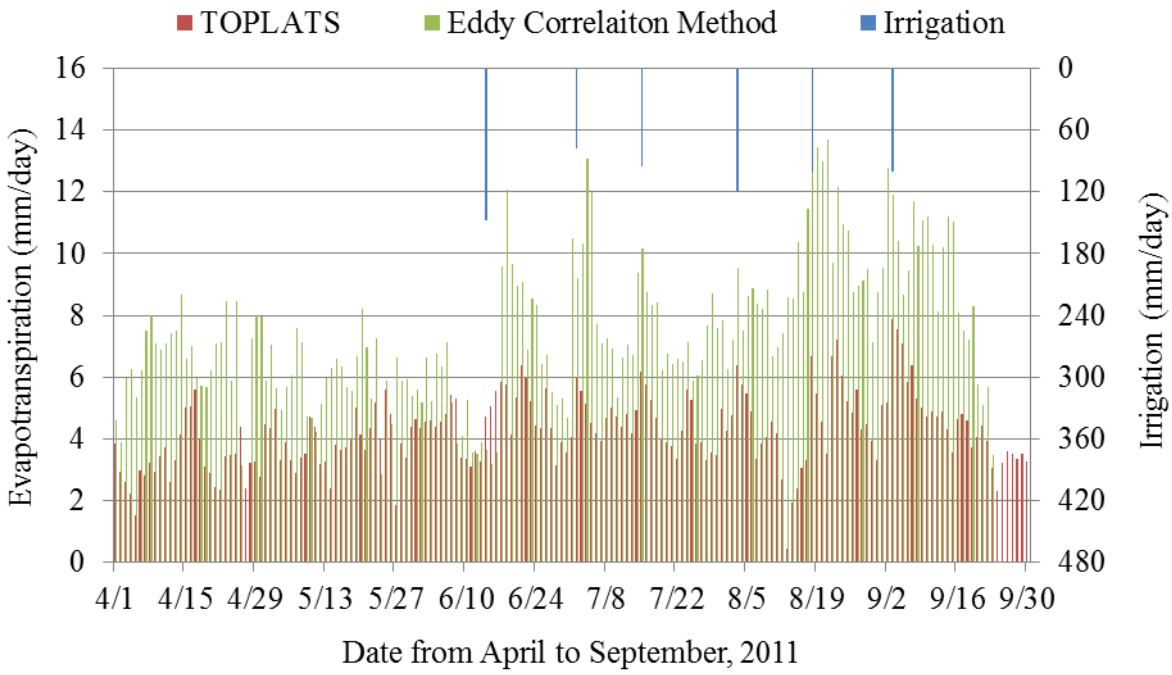

Figure 91 Variations of daily integrated evapotranspiration estimated by TOPLATS model and eddy correlation method (flux data was from AWS at Sakha) of an agricultural land (Sakha) in the fallow and summer growing season in 2011.

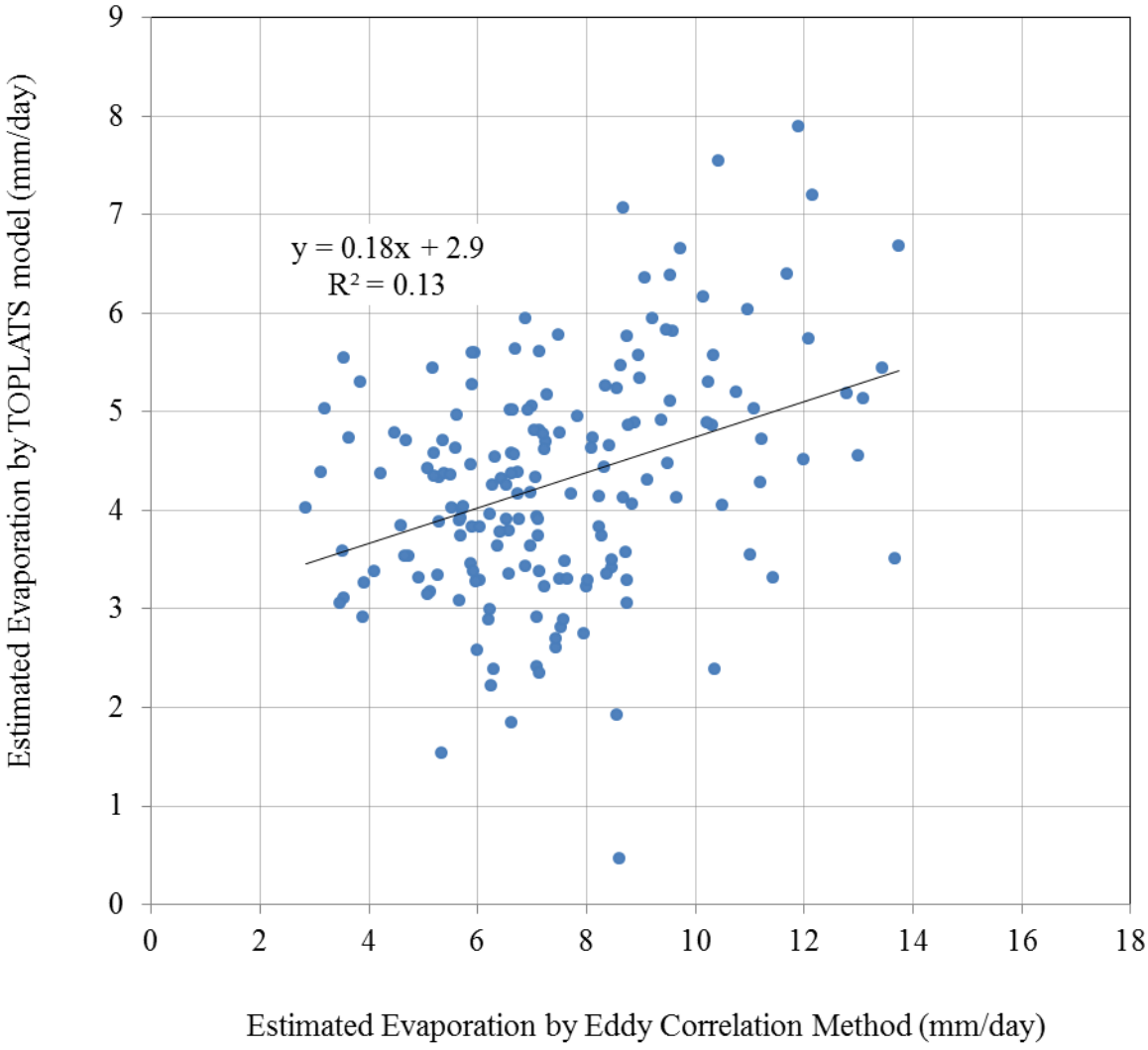

Figure 92 Correlation between estimated evaporation (mm/day) by TOPLATS model and eddy correlation method in the fallow and summer growing season in 2011.

3-4. Validation of the effectiveness of windbreak trees

The variations of soil evaporation, crop transpiration and transpiration of windbreak trees in an agricultural land without windbreak trees are shown in Figure 99, and Figure 100 shows the variations of these three components from a field with windbreak trees, both with the variations of LAI of crops and soil moisture estimated by TOPLATS model. The integrated values of seasonal evaporation, transpiration and transpiration of windbreak trees in an agricultural land with windbreak trees are shown in Figure 101 with the beak-down ratio of the total evapotranspiration. The integrated amount of evaporation and transpiration in an agricultural land without windbreak trees were compared with the integrated amount of evaporation, transpiration and transpiration of windbreak trees in same field with windbreak trees, in Figure 102. According to these results, soil evaporation from the field was reduced by about 68 mm (22.8%) in the summer growing period in 2011 by windbreak trees. At the same time, crop transpiration was also reduced by 66 mm (25.8%) in the summer growing period. However, the amount of reduced crop transpiration was estimated much smaller than the total amount of reduced evaporation from April to September in 2011.

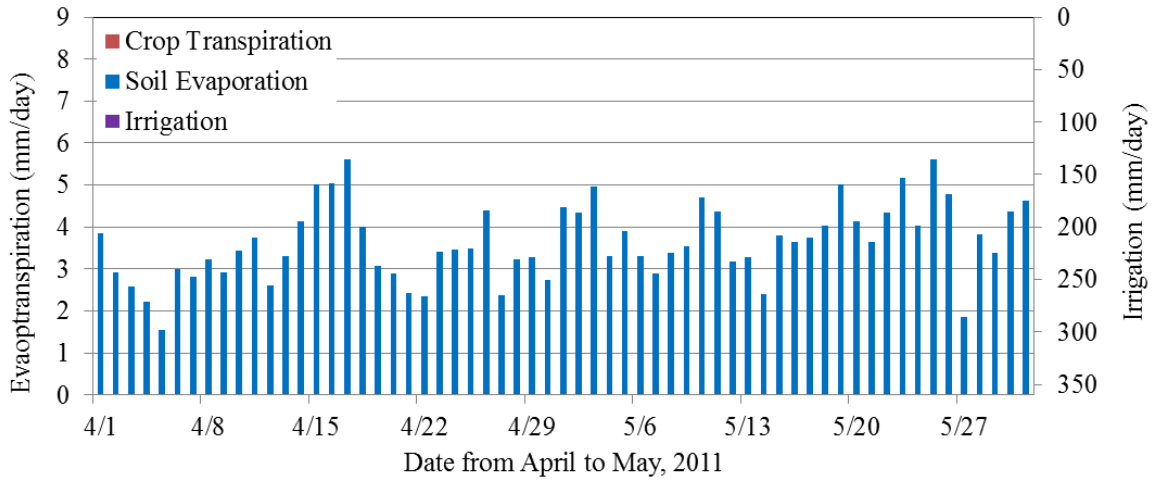

Figure 93 Estimated variation of soil evaporation (mm/day) from an assumed agricultural land (Sakha) to be without windbreak trees, estimated by TOPLATS model in fallow period. Because this field has no-crop in fallow period. Thus crop transpiration and irrigation are not here.

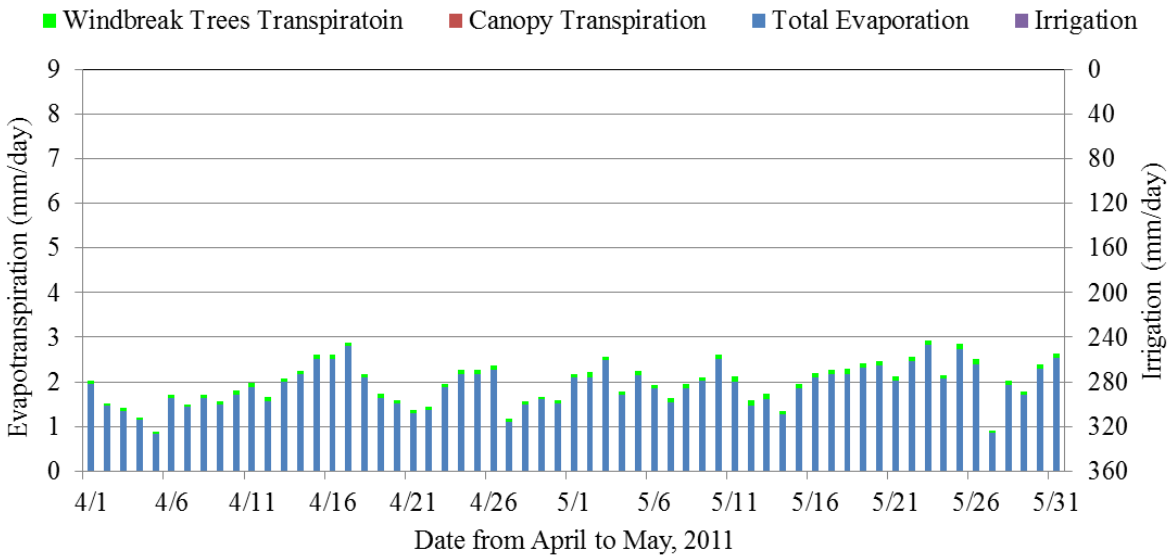

Figure 94 Estimated variations of soil evaporation (mm/day) and transpiration of windbreak trees from an assumed agricultural land (Sakha) to be with windbreak trees, estimated by TOPLATS model, Jarvis model and Penman-Monteith equation in fallow period. Because this field has no-crop in fallow period. Thus crop transpiration and irrigation are not here.

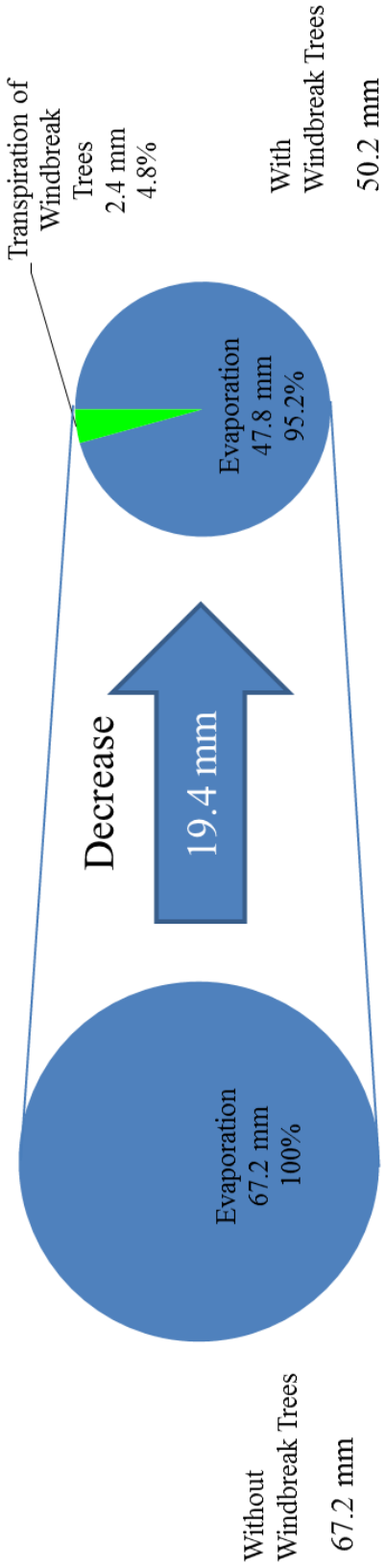

Figure 95 The effectiveness of reduction of windbreak trees against evaporation from the soil in Sakha field regarded as an agricultural land in the fallow period (Apr to May, 2011)

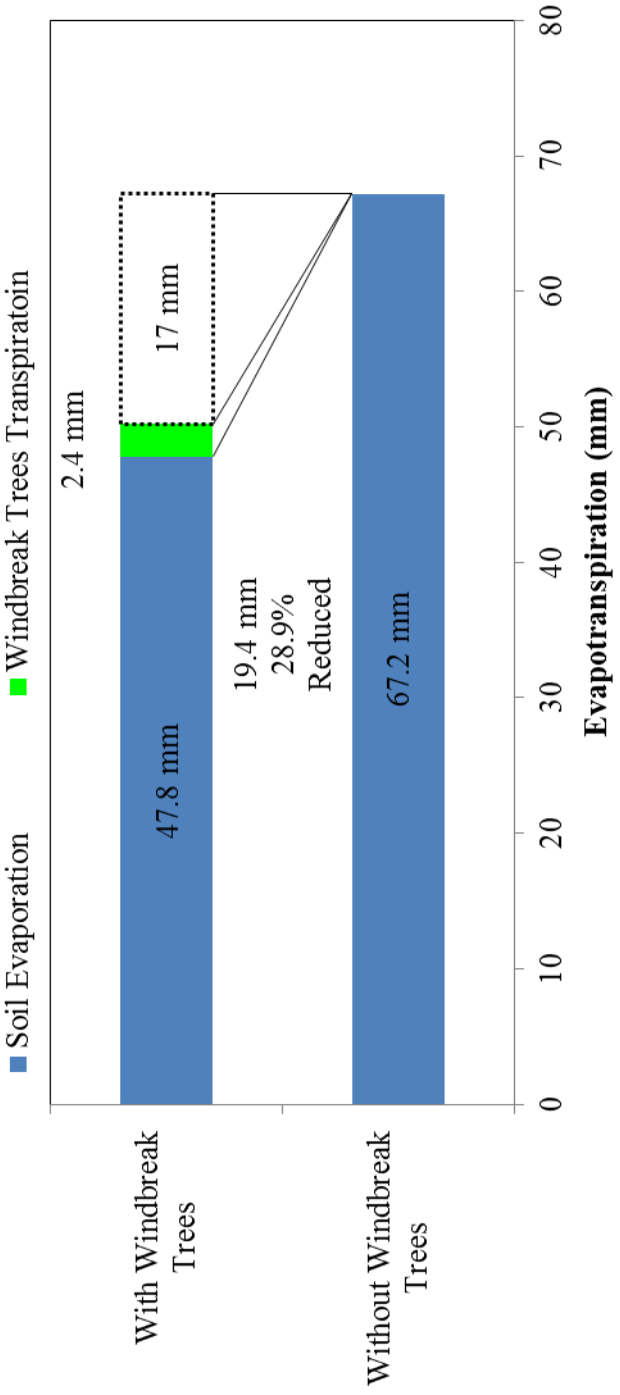

Figure 96 Integrated values of reduced evaporation from the soil and transpiration of windbreak trees in an agricultural land in the no-clop period (Apr to May, 2011)

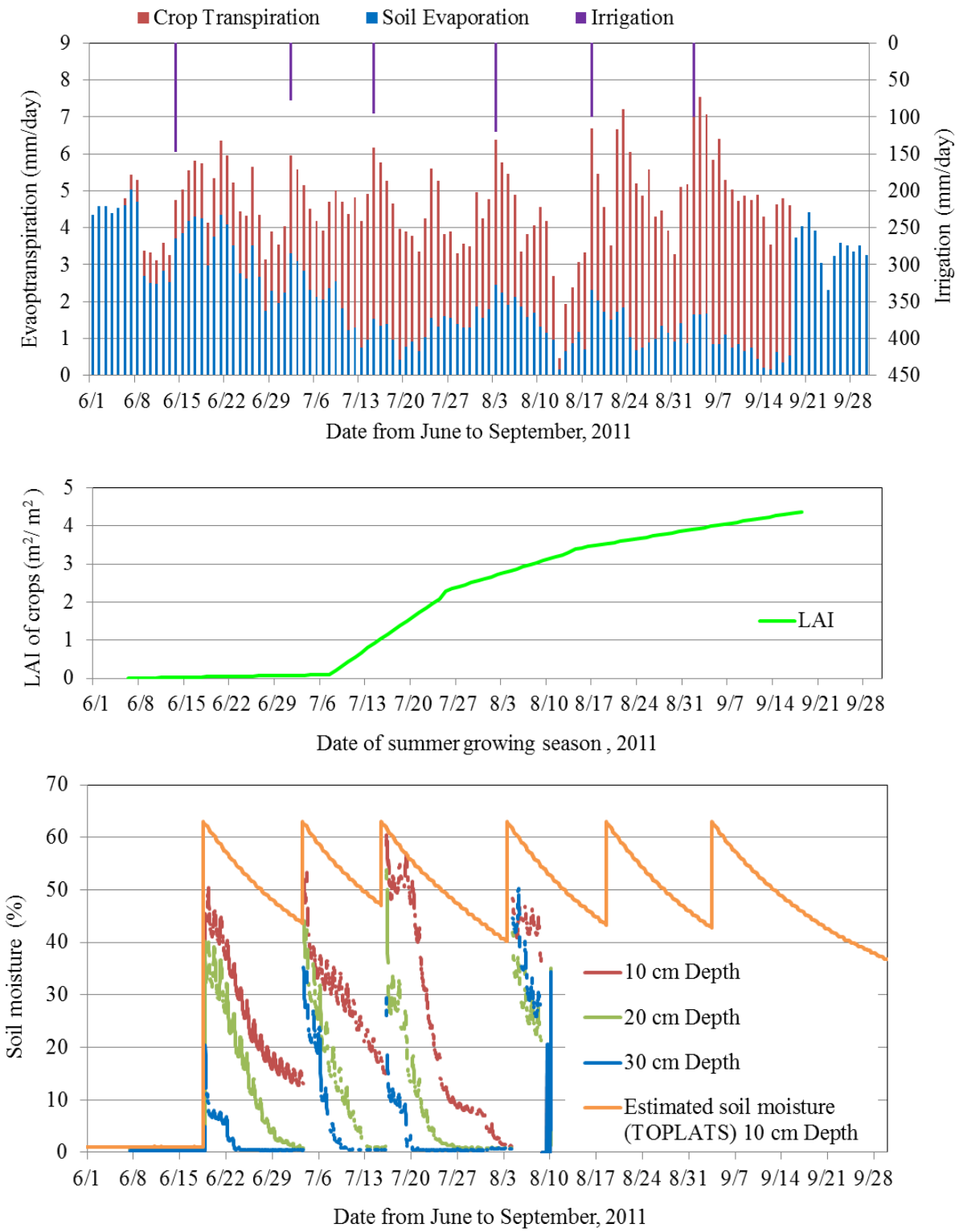

Figure 97 Estimated variations of soil evaporation (mm/day), crop transpiration (mm/day), irrigation (mm/day) in an assumed agricultural land (Sakha) to be without windbreak trees, estimated by TOPLATS model in summer growing period in 2011. Soil moisture and LAI of crops are also shown here in the same period. In the graph of soil moisture, orange line shows estimated soil moisture by TOPLATS model and other lines are measured values for each depth at Sakha.

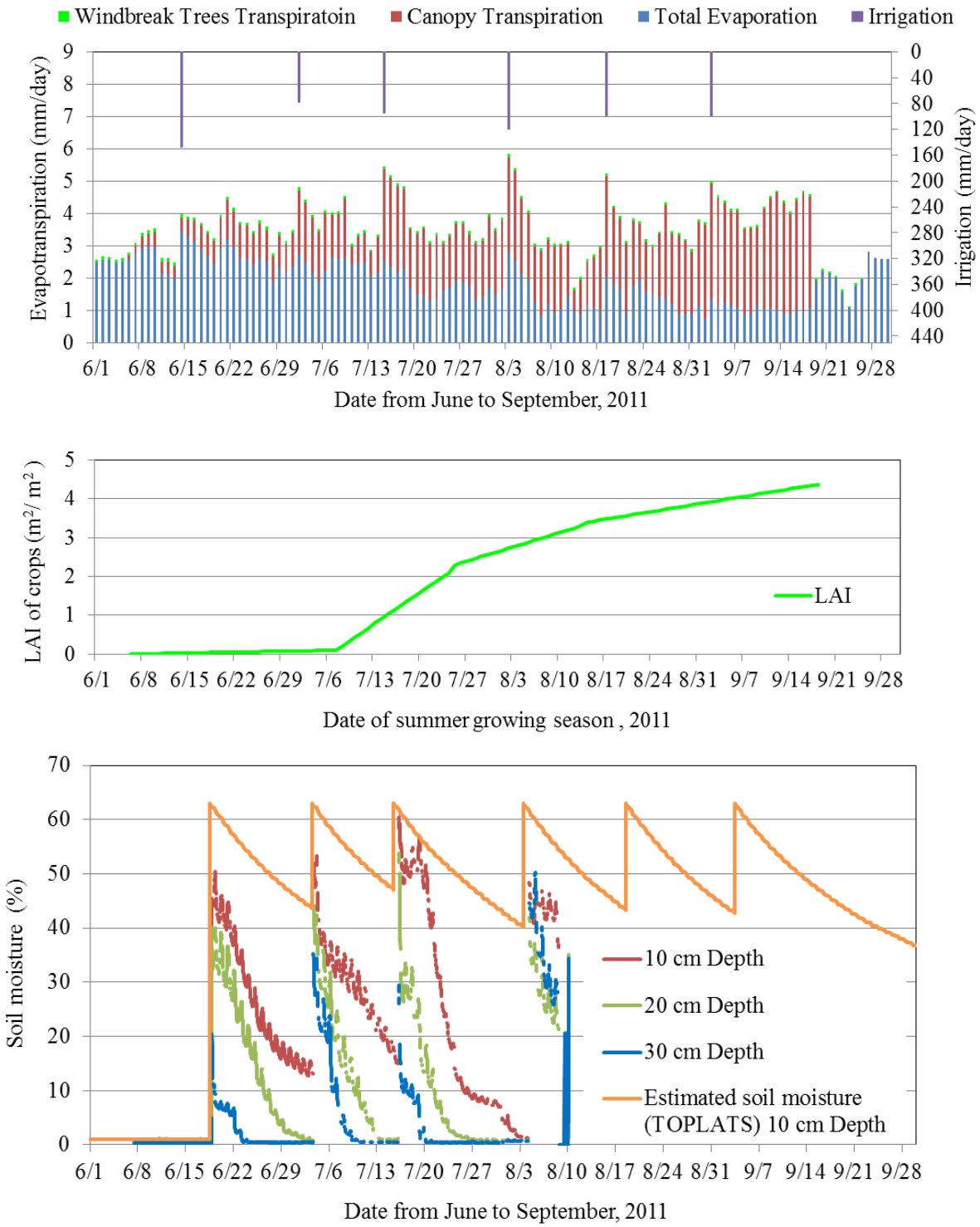

Figure 98 Estimated variations of soil evaporation (mm/day), crop transpiration (mm/day), irrigation (mm/day) and transpiration of windbreak trees (mm/day) from an assumed agricultural land (Sakha) to be with windbreak trees, estimated by TOPLATS model, Jarvis model and Penman-Monteith equation in summer growing period in 2011. Soil moisture and LAI of crops are also shown here in the same period. In the graph of soil moisture, orange line shows estimated soil moisture by TOPLATS model and other lines are measured values for each depth at Sakha.

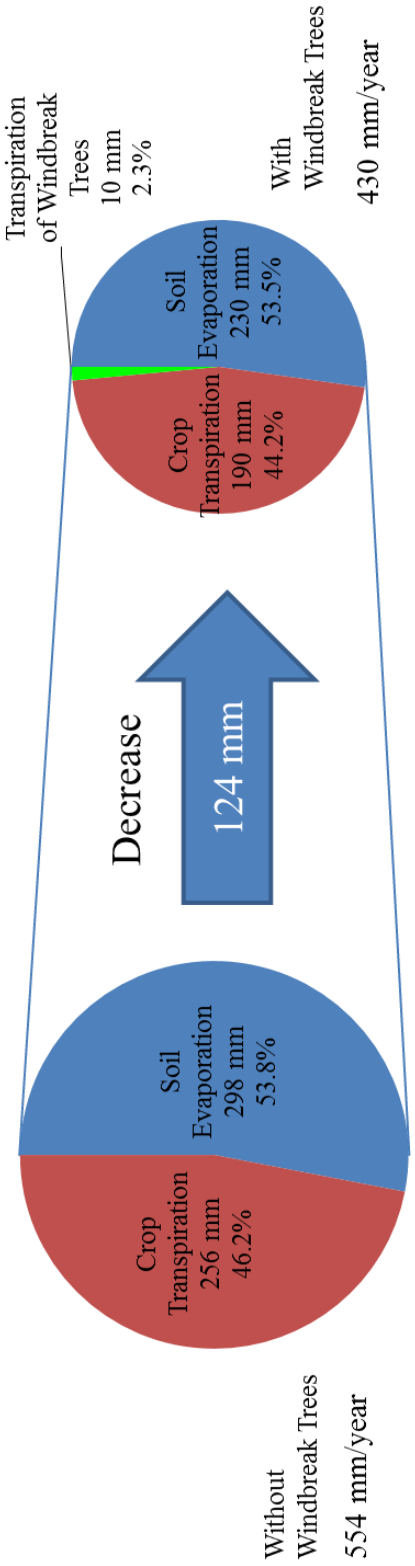

Figure 99 The effectiveness of reduction of windbreak trees against evaporation from the soil and transpiration of crops (Maize) in Sakha field regarded as an agricultural land in the crop growing period (Jun to Sep, 2011)

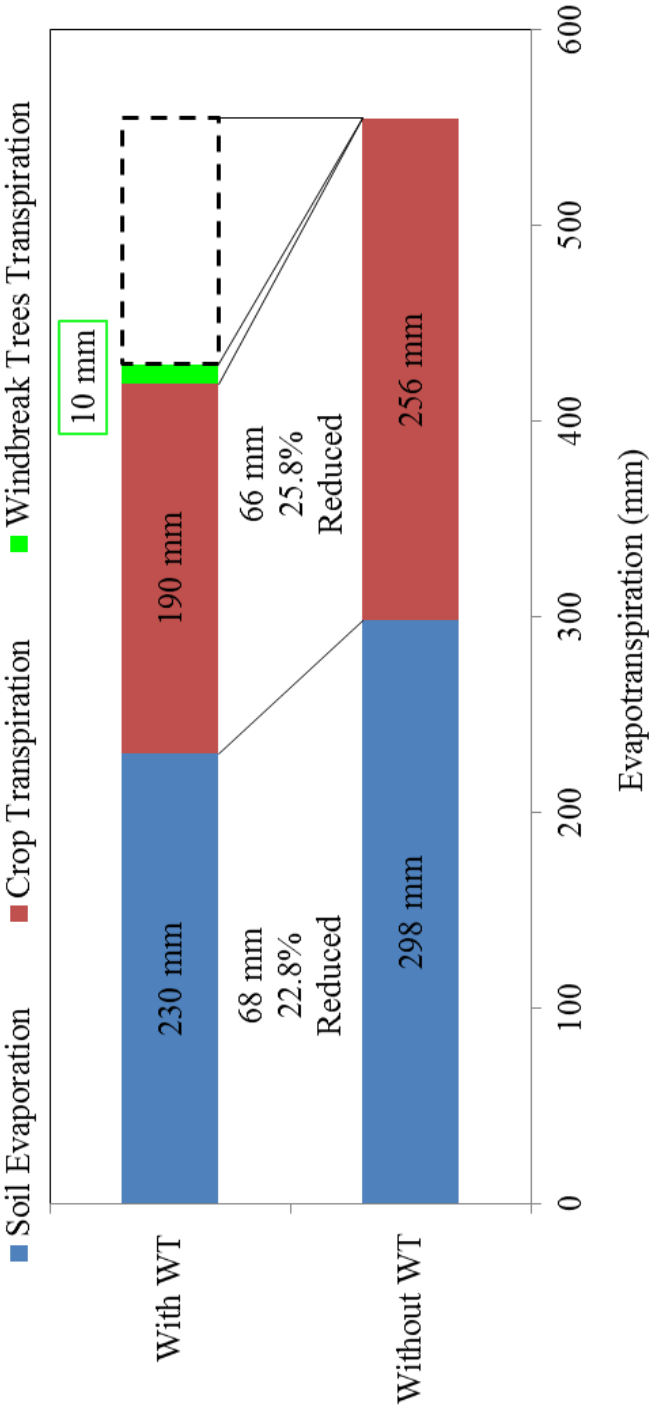

Figure 100 Integrated reduced values of evaporation from the soil and transpiration of crops and integrated transpiration of windbreak trees in an agricultural land in the crop growing period (from June to September, 2011)

4. Discussion

4-1. Estimation of annual transpiration of windbreak trees

The surface conductance was estimated by Jarvis model with the meteorological data and measured LAI at Tomida farm. The functions of the correlations between measured surface conductance and photon flux density and air temperature were very similar to Jarvis (1976). The parameters which were obtained by calibration were a little different from ones in Jarvis (1976). However, the target kind of trees in Jarvis (1976) was *Pine*, and the target kind of tree was *Casuarina* in this study. Therefore this difference of the kind of tree was thought as a cause of the differences of parameters. The correlation between relative surface conductance and CO_2 concentration of this study did not have enough range of seasonal variation of CO_2 concentration to make a function which is mentioned in Jarvis (1976). Therefore, the function of CO_2 concentration of this study referred Jarvis (1976). On the other hand, in the result of the correlation between measured surface conductance and specific humidity and soil moisture deficit, the range of measured data in this study was not enough to get the functions compared with Stewart (1988). Thus, the same parameters were used as in Stewart (1988) in the functions of specific humidity and soil moisture deficit, and the most of plots measured in this study were included in the functions with the same parameters with Stewart (1988). Thus, if there were enough range of data, it would be thought that the accuracy of calibration gets better with other parameters and the correlation between estimated surface conductance and measured conductance and that between estimated transpiration and measured transpiration approaches value of unity. Finally, five environmental factors, such as air temperature, photon flux density, specific humidity deficit, soil moisture deficit and CO_2 concentration could represent the seasonal variation of transpiration of a tree, especially the air temperature, photon flux density and CO_2 concentration. However, looking at the scatter diagram which shows the correlation between measured and estimated transpiration, there seems to be a non-linear correlation between measured and estimated transpiration. The reason of this characteristic can be thought as the difference of the shapes of daily variation between measured and estimated transpiration. Estimated transpiration has more sharp shape than measured transpiration. The reason why the shape of measured transpiration is more gradual than estimated transpiration is thought that “stem water storage”. In the morning of a day, the variation of transpiration have sharp rising, because of stem water storage. Around noon, the water storage has gone into the air from the leaves, and the transpiration rate gets gradual. In the afternoon, transpiration rate gets more rapid decline, because of the work of stomata. Thus, though Jarvis model can represent the work of stomata as in the results of this study, it was mentioned by these results that Jarvis model might not represent the work of “stem water storage” in estimation of transpiration. Finally it can be said, to estimate transpiration of a

tree by Penman-Monteith equation with Jarvis model, the effect of stem water storage should be considered.

However, the result of estimation of transpiration of windbreak trees reflected the seasonal change, and the correlation between estimated and measured transpiration of the tree No.11 was judged reasonable. Furthermore, finally the amount of seasonal transpiration in both no-plant and plant growing periods were much smaller than reduced evaporation, thus the small lack of representativeness does not affect to validate the effectiveness of evaporation reduction of windbreak trees.

4-2. Measurements at Al Krakat and three fields in the Nile-Delta

At Al Krakat, the horizontal profiles of general meteorological data and the data of crops and soil in leeward of windbreak trees were measured, and the results were very various. There were surely correlations between the distance from the windbreak trees and wind velocity, LAI of crops, surface temperature of soil, evaporation from soil surface, soil moisture and soil thermal conductivity. It was clarified that a windbreak trees causes many horizontal profiles of the environmental components, and these profiles might affect the growth of crops. Furthermore, the horizontal profiles of general meteorological data were very similar to references (on the contrast e. g., Hipsey et al., 2004: Wang and Takle. 1997: Cleugh, 1998), except for specific humidity. In this study, specific humidity did not change in horizontal direction. It can be thought that because air temperature did not have horizontal profile which was similar to Hipsey et al. (2004). Furthermore, relative humidity and specific humidity also did not have trends in horizontal direction leeward of windbreak trees. This result is thought that the constant horizontal profiles are features which are seen in arid region. The result of the correlation between soil moisture and soil thermal conductivity which does not include errors rejected by equation (1.24) is very reliable by compared with references (e. g. Kasubuchi, 1972: Shimada et al., 1992).

4-3. Estimation of evaporation and transpiration in an agricultural land

In the case of an agricultural land without windbreak trees, the correlation between estimated evapotrasnpiration by TOPLATS model and estimated evapotrasnpiration by eddy correlation method was high ($R^2 = 0.66$ and the function was $y = 1.03x + 0.01$), and the annual and seasonal variations which were represented by TOPLATS model were very similar to the variations by eddy correlation method. On the other hand, in the case of an agricultural land with windbreak trees, evaporation, transpiration and evapotranspiration were estimated by the same system of the case of an agricultural land without windbreak trees and different parameters and input data of wind velocity.

4-4. Validation of the effectiveness of windbreak trees

As shown in final result in Figures 98 and 102, the amount of evaporation could be reduced by windbreak trees, and in this study, the amount of reduction of soil evaporation was estimated as 100 mm (52.5% of the former soil evaporation), though the windbreak trees added only 22 mm/year (2.3% of the total evapotranspiration) to the water balance of an agricultural land in the fallow period. On the other hand in the summer growing period, windbreak trees might reduce soil evapotranspiration by 124 mm, and evaporation might be reduced by 68 mm (22.8% of former soil evaporation). This result seems that windbreak trees are highly effective to reduce evaporation in an agricultural land. However, windbreak trees reduce some amount of transpiration from crops at a same time. Reduction of transpiration has the possibility to prevent growth of crops. Thus, to validate the windbreak trees if they are effective or not, the influence to the reduction of transpiration of crops must be considered. According to Baker and Musgrave (1964), there is a positive linear correlation between transpiration and photosynthesis of *Maize,* as shown in Figure 103. Thus, it can be said that, if half of the amount of transpiration of Maize was reduced by windbreak trees, the amount of photosynthesis also would be reduced by 50%, and the certain amount of yields of Maize might be reduced at the same time.

According to Jafet *et al*. (2011) which studied the yield of maize in South Africa, there is a positive linear correlation between transpiration and yield of maize, as shown in Figure 104. In addition, according to Patricio *et al*. (2009), it was clarified by overviewing many references that, in Africa region, there also is a positive linear correlation between transpiration and yield of maize, as shown in Figure 105. By combining these references with the results of this study in the crop growing period in the summer in 2011, the possibility of windbreak trees which prevents the growth of maize was validated as follows.

- ✓ The amount of reduced transpiration of crops was estimated by 66 mm for three months (from June to September in 2011).
- ✓ Originally, the amount of transpiration of crops was 256 mm for three months from an agricultural land without windbreak trees.
- ✓ According to the functions estimated from Jafet *et al*. (2011), if the amount of transpiration was reduced by 66 mm from 256 mm, the yield would be reduced by minimum 0.74 tons/ ha from 2.46 tons/ ha, maximum 2.17 tons/ ha from 3.11 tons/ ha for three months in the crop growing period.
- ✓ According to the functions estimated from Patricio *et al*. (2009), if the amount of transpiration was reduced by 66 mm from 256 mm, the yield would be reduced by maximum 0.73 tons/ ha from 1.12 tons/ ha, minimum 0.24 tons/ ha from 0.68 tons/ ha for three months in the crop growing period.

From these analyses, it seems not to be avoided that the yield would be reduced by windbreak trees at the same time of reduction of evaporation from the soil in the crop growing period. Therefore there are two options mentioned by this study to put the effectiveness of windbreak trees to good account as follows. First option is treatment of the porosity of windbreak trees. Actually, the effectiveness of windbreak trees can be regulated by the porosity of windbreak trees, as regulating the horizontal variation of wind velocity leeward of windbreak trees. However, to achieve optimum porosity of windbreak trees for reduction of evaporation and no-negative effect on crop yields, the studies about the interaction between the amount of the effectiveness and the porosity of windbreak trees should be done more and more. Furthermore, such kind of studies must be done against many species of crops to apply for many regions.

Second option is using windbreak nets rather than windbreak trees. It is reported that windbreak net has similar effectiveness to windbreak trees, in such as Ushiyama *et al*. (2009), Heisler *et al*. (1988) and so on. The biggest merit of windbreak nets is removable different from windbreak trees. Because of the merit, farmers can be blessed with windbreak nets only in no-crop period, and in crop growing period, windbreak net would be removed from a land. Furthermore, the first option can be achieved very easily by windbreak nets by just changing nets. However, windbreak nets have also issues. The effectiveness of windbreak is completely influenced by the height of windbreak structures. Therefore, for big scale lands, there is a necessity of construction of big scale nets, such as 10 m, 20 m scale. In cost aspect, there are also issues with windbreak nets. Of course, such kind of big nets seem to cost very expensive. Generally for farmers in the world, it might be difficult to prepare such expensive nets for each season. Furthermore, windbreak nets have many issues, such as difficulty in setting such big nets for people, strength of net which maintains itself for three or four months and impossibility to be sold as some materials despite of usefulness of windbreak trees as construction materials.

In this study, the two options were suggested as above for the improvements of use of windbreak trees. Actually, there are many difficulties of windbreak tree use, however, by considering these options, the best use of windbreak trees can be achieved, I think.

4-5. Application of this study to other cases

This study mainly suggested following three possibilities. First, transpiration of trees can be estimated by Jarvis model and Penman-Monteith equation with general meteorological and radiation data and LAI of the trees, in the arid and hot region. Second, in leeward of windbreak trees, the profiles of meteorological data, characteristics of crops and soil were clarified and these profiles agree with previous studies. Third, windbreak trees have the effectiveness to reduce evaporation in this case. However, to some extent, these expected results could not be applied for everywhere. The reason why suggested

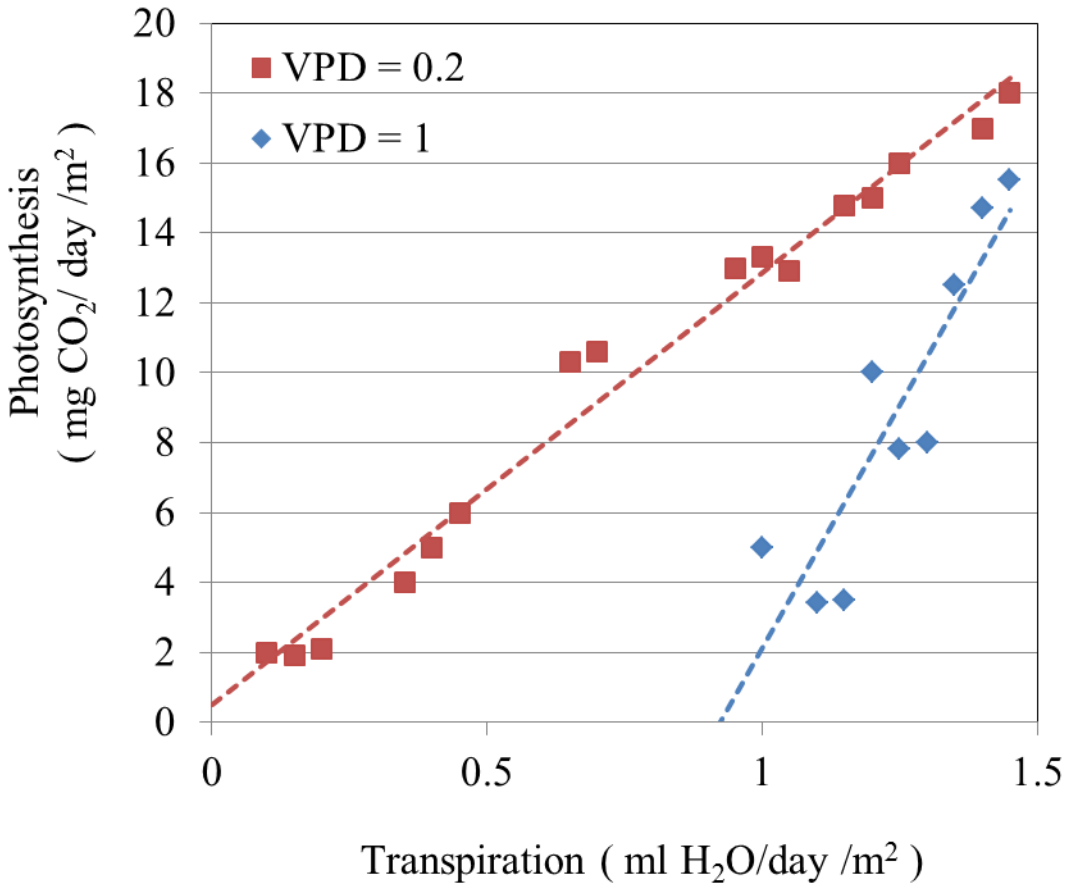

Figure 101 Correlation between transpiration (ml H_2O/ day/ m^2) and photosynthesis (mg CO_2/ day/ m^2) from Baker and Musgrave (1964)

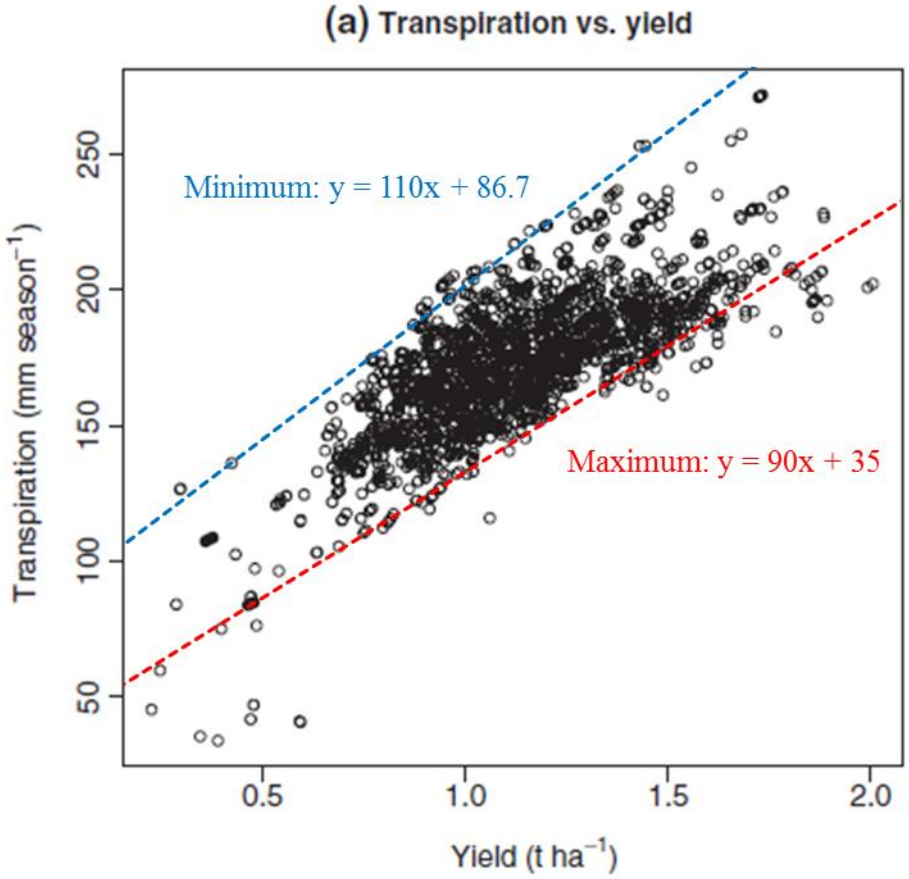

Figure 102 Maximum and minimum functions of correlation between transpiration and yield of maize, estimated from Jafet *et al*. (2011)

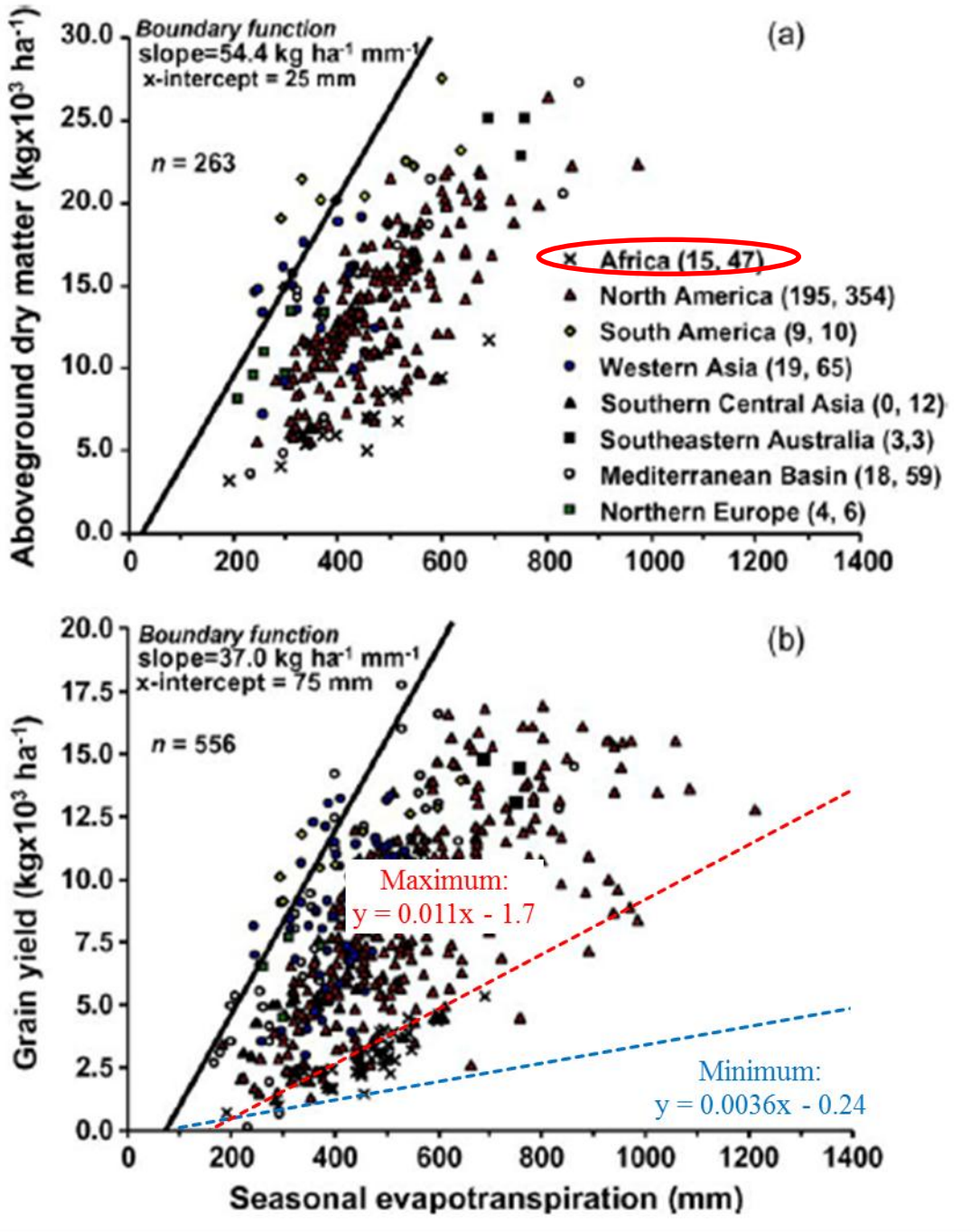

Figure 103 Maximum and minimum functions of correlation between transpiration and yield of maize, estimated from Patricio *et al*. (2009)

like that, is first, the kind of tree is very important. *Casuarina* is a kind of tree which its transpiration is very small compared with other kinds such as *Eucalyptus globules* especially in arid regions. Second, the effect of difference of the porosity of the trees must be considered. In this study, the profiles of environmental components in leeward of windbreak trees of which porosity was measured only one sample. These profiles in leeward of windbreak trees with different porosity from this study might be also different from this study. In application of this effectiveness for other situation, these profiles of environmental components must be measured for each field. Considering these points, the effectiveness can be estimated in the same order, with the data of general meteorological data, kind of crops and soil type and LAI of the trees.

5. Conclusions

The effect of windbreak trees which reduces evaporation in an agricultural land was validated by comparison between evaporation in an agricultural land and transpiration of windbreak trees. Annual transpiration of windbreak trees was estimated by measurement of sap flow and sap wood area at Tomida farm and Penman-Monteith equation and Jarvis model. Measured transpiration of *Casuarina* at Tomida Farm had obvious seasonal change in the summer period, from July to September, in 2011. The measured transpiration was used to estimate surface conductance by Jarvis model. Estimated surface conductance from measured transpiration of *Casuarina* had correlations between five environmental factors, of air temperature, photon flux density, specific humidity deficit, soil moisture deficit and CO_2 concentration), which were similar to the result for *Pine* trees in Stewart (1988). The photon flux density, air temperature and CO_2 concentration were the main factors to determine the seasonal variation of surface conductance, and estimated transpiration by Penman-Monteith equation with substitution of surface conductance estimated by Jarvis model could represent the seasonal variation of transpiration of *Casuarina* in summer period in 2011. Furthermore, annual variation of transpiration of windbreak trees was estimated by the combination of both Penman-Monteith equation and Jarvis model. The estimated transpiration from a tree sample named No.11 had high correlation with measured transpiration of No.11, however, correlation between measured transpiration and estimated transpiration of other tree samples (No.6, 5, 4 and 3) were smaller than that of No.11, represented as determination coefficients.

As results of measurements at Al Krakat, it was observed in leeward of windbreak trees that there is a horizontal variation of wind velocity against relative distance from windbreak trees. In the remarkable horizontal variation of wind velocity, it became smallest around relative distance of 4, and after that it gradually recovered to 100% as the relative distance gets longer. This horizontal variation of wind velocity is very similar to the wind profile from model estimation in Wang and Takle (1997). On the other hand, other environmental factors, such as air temperature, relative humidity and specific humidity did not have such kind of horizontal variation. Furthermore, the profile of wind velocity did not change before and after harvesting. As results of other environmental factors, the correlation between soil moisture and soil thermal conductivity agreed with previous studies, after removing error values which were judged by the equation (1.24). The correlation between soil moisture and soil thermal conductivity in the Nile-Delta was thought as reasonable by comparing with other six references.

The variations of evaporation, transpiration and evapotranspiration from April to September in 2011 were estimated by TOPLATS model for both with and without windbreak trees in an agricultural land. The estimated evapotranspiration by TOPLATS

model had reasonable correlation with the evapotranspiration estimated by eddy correlation method. Additionally, the estimated evaporation by TOPLATS model had high representation compared with the result of Chamber method at Sakha field on July 14th in 2011 from Matsuno (personal communication). According to these validations, the result of estimation of evapotranspiration in Sakha by TOPLATS model can be regarded as reasonable. From TOPLATS model analysis, in the fallow period in 2011, the agricultural land without windbreak trees had 221 mm evaporation for 2 months. On the other hand, the agricultural land with windbreak trees had only 116 mm evaporation and 5.2 mm transpiration of the windbreak trees. By comparing the estimations between a field with and without windbreak trees, in the fallow period, the amount of evapotranspiration of the field and windbreak trees in a field with windbreak trees were much smaller than the field without windbreak trees by 100 mm over 2 months equals to around 50% of the evaporation. In the estimations in the summer crop growing period for 3 months, the amount of evaporation of the soil, transpiration of the crops and transpiration of windbreak trees from the field with windbreak trees were also much smaller than the amount of evapotranspiration from the field without windbreak trees by 575 mm over 3 months equals to around 50% of the evapotranspiration. According to this analysis, windbreak trees reduces total amount of evaporation from the soil by 348 mm over 5 months, on the other hand, the total amount of transpiration of windbreak trees was only 15.2 mm over 5 months, and the amount of transpiration of windbreak trees equals to 4.4% of the amount of reduced evaporation in the land. However, at the same time, transpiration of crops was reduced by 274 mm over 5 months by windbreak trees. Thus windbreak trees reduce evaporation from the soil by 348 mm and transpiration of crops by 274 mm for 5 months. These results indicated that actually windbreak trees have the effectiveness to reduce evaporation in an agricultural land by large amount. However, at the same time, windbreak trees have also the possibility to prevent the growth of crops by reducing transpiration of crops. When windbreak trees are practically used in agricultural fields, the possibility which windbreak trees might prevent growth of crops must be considered with the assumed impact of the effect for each species of crops. According to Baker and Musgrave (1964), in this case of *Maize*, if half of the amount of transpiration of *Maize* were reduced by windbreak trees, the amount of photosynthesis of *Maize* would be reduced by 50%. This reduction of the amount of photosynthesis can be thought that it might have certain negative effects on the growth and yield of *Maize*. However, selection of the porosity of the windbreak trees can make the negative possibility reduced, because the effectiveness can be determined by the porosity of the windbreak trees. Studies on the correlation between the porosity of windbreak trees and the effectiveness against evaporation reduction are still needed.

Acknowledgement

The author wishes to express his sincere gratitude to his academic adviser, Professor Michiaki Sugita for his continuing guidance and encouragement. Special thanks are expended to Professor Satoh, Professor Mruyama, Professor Shimizu, Professor Ishikawa, Professor Fujimaki, Professor Inoue, Professor Rushdi, Dr. Hoshino, Dr. Waleed, Dr. Shin-ichi Iida, Professor Maki Tsujimura and Professor Jun Asanuma for their guidance and helpful comments.

This study was also improved by Japanese supporters, Dr. Matsuno, Mr. Fukuda, Mr. Tsuji, and Egyptian supporters, Dr. Shelif, Mr. Sayed, Mr. Hassan, Mr. Mohamad Samier, Mr. Ahamed, and lots of my friends who supported in the field.

This research was partly supported by the WAT project of SATREPS. Great thanks is also given to coordinators of JICA and JST.

References

Abu-Hamdeh, N. H. (2000): Effect of tillage treatments on soil thermal conductivity for some Jordanian clay loam and loam soils. *Journal of Soil and Tillage Research*, **56**, 145-151

Adamtey, N., Cofie, O., Ofosu-Budu, K, G., Ofosu-Anim, J., Laryea, K, B., Forster, D. (2010): Effect of N-enriched co-compost on transpiration efficiency and water-use efficiency of maize (Zea mays L.) under controlled irrigation. *Journal of Agricultural Water Management*, **97**, 995-1005

Andersson, J, C, M., Zehnder, A, J, b., Johan, R., Yang, H. (2011): Potential impacts of water harvesting and ecological sanitation on crop yield, evaporation and river flow regimes in the Thukela River basin, South Africa. *Journal of Agricultural Water Management*, **98**, 1113-1124

Arai, T., Nishizawa, T. (1974): Sui-mon-gaku-kou-za 10, Sui-on-ron. Kyoritsu Shuppan Co., Ltd., pp. 297

Baker, D, N., Musgrave, R, B. (1964): The effects of low level moisture stresses on the rate of apparent photosynthesis in corn. *Crop Science*, **4**, 249-253

Bolton, D. (1980): The computation of equivalent potential temperature. *Monthly Weather Review*, **108**, 1046-1053

Brutsaert, W. (2005): *Hydrology* : *An Introduction*. Cambridge, pp. 605

Calder, I. R. (1976): The measurement of water losses from a forested area using a "natural" lysimeter. *Journal of Hydrology*, **30**, 311-325

Calder, I. R. (1978): Transpiration observations from a spruce forest and comparisons with predictions from an evaporation model. *Journal of Hydrology*, **38**, 33-47

Choudhury, B, J. (1987): Analysis of an empirical model for soil heat flux under a growing wheat crop for estimating evaporation by an infrared-temperature based energy balance equation. *Journal of Agricultural and Forest Meteorology*, **39**, 283-297

Cleugh, H. A. (1988): Effects of windbreaks on airflow, microclimates and crop yields. Agroforestry Systems, **41**, 55-84

Crow, W, T., Ryu, D., Famiglietti, J, S. (2005): Upscaling of field-scale soil moisture measurements using distributed land surface modeling. *Journal of Advances in Water Resources*, **28**, 1-14

Crow, W. T. and Wood, E. F. (2003): The assimilation of remotely sensed soil brightness temperature imagery into a land surface model using Ensemble Kalman filtering: a case study based on ESTAR measurements during SGP97. *Advances in Water Resources*, **26**, 137-149

Dickinson, R. E. (1984): Modeling evapotranspiration for three-dimensional global climate models. *National Center for Atmospheric Research, Boulder, Colorado*, 58-72

Famiglietti, J. S., Wood, E. F., Sivapalan M., and Thongs D. J. (1992): A catchment scale water balance model for FIFE. *Journal of Geophysical Research*, **97**, 18997-19007

Famigrietti, J. S., Wood, E. F. (1994): Multiscale modeling of spatially variable water and energy balance processes. *Journal of Water Resources Research*, **30** (11), 3061-3078

Fukuda, M., Ishizaki, T. (1980): A simulation model for forest penetration beneath the ground on the basis of equilibrium surface temperature. Journal of The Japanese Society of Snow and Ice. **42** (2), 71-80 (in Japanese)

Fukuda, T. (2010): Estimation of evapotranspiration in agricultural land of the Nile Delta. School of Life and Environmental Sciences, BS thesis, the University of Tsukuba, pp.74

Fukuda, T. (2012): Estimation of evapotranspiration of crop fields in Nile delta: a case study of summer maize. Life and Environmental Sciences, MS thesis, the University of Tsukuba, pp. 107

Granier, A. (1985): Une nouvelle method pour la mesure du flux de seve brute dans le tronc des arbres. *Ann. Science Forest*, **42**, 193-200

Grassini, P., Yang, H., Cassman, K, G. (2009): Limits to maize productivity in Western Corn-Belt: A simulation analysis for fully irrigated and rainfed conditions. *Journal of Agricultural and Forest Meteorology*, **149**, 1254-1265

Haginoya, S. (2002): Observation of heat conductivity using soil temperature sensor with a line heat source. *Journal of Meteorological Society of Japan*, **109**, 21-30 (in Japanese)

Hanawa, K. (2007): The study of influence of land-use on the water cycle in a sub-basin of Kasumigaura using a hydrologic model. School of Life and Environmental Sciences, BS thesis, the University of Tsukuba, pp. 109

Harada, T., Matsuzaka, Y., Yamada, Y., Abe, K. (1966): Preliminary definitions, legend and correlation table for the soil map of the world (world soil resources reports 12): Soil map of the world, FAO/UNESCO project. *Journal of Japanese Society of Soil Science and Plant Nutrition*, **37** (3), 226-242 (in Japanese)

Hata, Akihiko. (2008): Egypt, a desert dominant country and her water resources. *Civil Engineering Consultant*, **238**, 62-65 (in Japanese)

Hattori, S., Tamai, K., Abe, T. (1993): Effects of soil moisture and vapor pressure deficit on evapotranspiration in a hinoki plantation. *Journal of The Japanese Forestry Society*, **75**, 216-224 (in Japanese)

He, B., Oue, H., Oki, T. (2009): Estimation of hourly evapotranspiration in arid regions by a simple parameterization of canopy resistance. *Journal of Agricultural and Forest Meteorology*, **65** (1), 39-46

Heisler, G, M., Dewalle, D, R,. (1988): Effects of windbreak structure on wind flow. *Agriculture, Ecosystems and Environment*, **22**, 41-69

Hipsey, M. R., Sivapalan, M., Clement, T. P. (2004): A numerical and field investigation of surface heat fluxes from small wind-sheltered water bodies in semi-arid Western Australia. *Journal of Environmental Fluid Mechanics*, **4**, 79-106

Iida, S., Kobayashi, Y., Tanaka, T. (2003): Continuous and long-term measurement of sap flux using Granier method. *Journal of Japan Science Hydrology and Water Resources*, **16**, 13-22 (in Japanese)

Iida, S., Nakaya, S., Tanaka, T. (2006): Evaluation of transpiration from a natural deciduous broad-leveled forest located at a headwater catchment based on measurement of sap flux density. *Journal of Japan Society of Hydrology and Water Resources*, **19** (1), 7-16 (in Japanese)

Iida, S., Shimizu, A., Kabeya, N., Nobuhiro, K., Tamai, K., Shimizu, T. (2010): Tree-to-tree variations in stemflow amounts of *Japanese Cedar* in Tsukuba experimental watershed. Kanto-shinrin-kenkyu, **61**, 207-210 (in Japanese)

Iida, S., Tanaka, T. (2010): Effect of the span length og Granier-type thermal dissipation probes on sap flux density measurements. *Analysis of Forest Science*, **67**, 1-10

Jacquemin, B., Noilhan, O. (1990): Sensitivity study and Validation of a land surface parameterization using the HAPEX-MOBILHY data set. *Boundary-Layer Meteorology*, **52**, 93-134

Jarvis, P. G. (1976): The interpretation of the variations in leaf water potential and stomatal conductance found in canopies in the field. *Philosophical Transactions of the Royal Society London B*, **273**, 593-610

Kasubuchi, T. (1972): Effect of water content on thermal conductivity of soils. *Journal of Japanese Society of Soil Science and Plant Nutrition*. **43** (12), 437-441 (in Japanese)

Kasubuchi, T. (1973): Problems of the mechanism of heat conduction in soil. *Journal of National Institute of Agricultural Sciences*, Chemistry Division, **29** (3), 45-51 (in Japanese)

Kitamura, Y., Watanabe, T., Shimbo, Y. (1994): Water resources, irrigation and dranage in Egypt. Technical Report of the National Research Institute of Agricultural Engineering, **189**, 75-99 (in Japanese)

Kondo, J. (2000): *Chihyoumen-ni-Chikai-Taiki-no-Kagaku - Rikai-to-Ouyou* -. University of Tokyo Press, pp. 324

Kotoda, K. (1986): Estimation of River Basin Evapotranspiration. *Environmental Research Center Papers*, *The University of Tsukuba*, **8**, 1-66

Krause-Jensen, D., Sand- Jensen, K. (1998): Light attenuation and photosynthesis of aquatic plant communities. *Journal of Limnology and Oceanography*, **43** (3), 396-407

Lindroth, A. (1985): Canopy conductance of coniferous forests related to climate. *Water Resources Research*, **21** (3), 297-304

Mahmoud, A. Z. (2005): Water for the future – National Water Resources Plan－. Ministry of Water Resources and Irrigation Planning Sector of Egypt, pp. 61

Matsumoto, K., Ohta, T., Nakai, T., Kuwada, T., Daikoku, K., Iida, S., Yabuki, H., Kononov, A. V., Molen, M. K., Kodama, Y., Maximov, T. C., Dolman, A. J., Hattori, S. (2008): Responses of surface conductance to forest environments in the Far East. *Journal of Agricultural and Forest Meteorology*, **148**, 1926-1940

Matsuno, A. (2011): The separation of evaporation and transpiration by using stable isotope and chamber method in different irrigation cultivation land. Life and Environmental Sciences, MS thesis, the University of Tsukuba, pp. 83 + Appendix

McNeil, D, D., Shuttleworth, W, J. (1975): Comparative measurements of the energy fluxes over a Pine forest. *Journal of Boundary-Layer Meteorology*, **9**, 297-313

Mochizuki, H., Mizoguchi, M., Miyazaki, T. (2008): Effects of NaCl concentration on the thermal conductivity of sand and glass beads with moisture contents at levels below field capacity. *Journal of Soil Science and Plant Nutrition*, **54**, 829-838

Monteith, J. L. (1965): Evaporation and environment. *Symposia of the Society for Experimental Biology*, **19**, 206-234

Ono, S., Komatsu, Y., Kimura, S. (1985): Some considerable points on measurement of leaf transpiration by the use of Steady-state Porometer (LI-COR, LI-1600). Report of the Shikoku Branch, *Journal of The Crop Science Society of Japan*, **22**, 1-4 (in Japanese)

Payero, J, O., Melvin, S, R., Irmak, S., Tarkalson, D. (2006): Yield response of corn to deficit irrigation in a semiarid climate. *Journal of Agricultural Water Management*, **84**, 101-112

Prueger, J. H., Kustas, W. P., Hipps, L. E., Hatfield, J. L. (2004): Aerodynamic parameters and sensible heat flux estimates for a semi-arid ecosystem. *Journal of Arid Environments*, **57**, 87-100

Rubio, C. M., Josa, R., Ferrer, F. (2008): Thermal properties as a function of water content in a silty porous media under laboratory conditions. *15th International Congress of ISCO*; *Soil and water conservation climate change and environmental sensitivity*. Budapest, Mayo, 2008

Sato, T., Tanaka, N., Inoue, M., Sawada, H., Watanabe, S., Suzuki, M. (2010): Report on an experiment of dye injection into xylem sap of a Quercus serrate tree in University forest in Aichi. *Journal of the Tokyo University Forests*, **49**, 29-41 (in Japanese)

Shimada, J., Kawamura, R., Taniguchi, M., Tsujimura, M. (1992): Continuous soil moisture content measurement at the experimental field of ERC by using the heat-prove type soil moisture sensor. *Bulletin of the Environmental Research Center, the University of Tsukuba*, **16**, 45-53 (in Japanese)

Shimizu, T. (2011): Evaluation of windbreak trees' transpiration in Nile delta. School of Life and Environmental Sciences, BS thesis, the University of Tsukuba, pp. 143 + Appendix

Sileshi, G, W., Akinnifesi, F, K., Ajayi, O, C., Muys, Bart. (2011): Integration of legume trees in maize-based cropping systems improves rain use efficiency and yield stability under rain-fed agriculture. *Journal of Agricultural Water Management*, **98**, 1364-1372

Stewart, J. B. (1988): Modeling surface conductance of pine forest. *Agricultural and Forest meteorology*, **43**, 19-35

Stewart, J. B., De Bruin, H. A. R. (1984): Preliminary study of dependence of surface conductance of Thetford forest on environmental conditions. *The Forest-Atmosphere interaction*, 177-196

Sugita, M., Kotoda, K. (1985): Effects of soil water deficits on forest evapotranspiration. *Bulletin of the Environmental Research Center, the University of Tsukuba*, **9**, 83-88 (in Japanese)

Sugita, N., Tanaka, T. (2009): *Hydrologic Science*. Kyoritsu Shuppan Co., Ltd., pp.275 (in Japanese)

Takizawa, H., Kubota, J., Tsukamoto, Y. (1996): Distribution of water flow velocity at a stem cross-section. *Journal of The Japanese Forestry Society,* **78** (2), 190-194 (in Japanese)

Tani, N. (1982): *Dojouno-Netsu-You-Ryou. Dojou-Butsurisei-Sokutei-hou-iinkai. Dojou-butsuri-sokutei-hou*. Yokendo, 299-303

Taniguchi, M., Sakura, Y. (1991): A review of studies on soil and groundwater temperature. *Bulletin of the Environmental Research Center, the University of Tsukuba*, **15**, 87-90 (in Japanese)

Tomisaka, K., Maruyama, T. (2007): Measurement of the aerodynamic characteristics of a net. *Journal of Wind Engineering, JAWE*, **32** (3), 103-112 (in Japanese)

Tsuchihira, K. (2011): The estimation of evaporation and transpiration using hydrologic model in crop lands of Nile Delta of Egypt. Life and Environmental Sciences, MS thesis, the University of Tsukuba, pp. 99 + Appendix

Ushiyama, T., Inoue, S., Shibaike, H. (2009): Measurements of wind suppression effects of windbreak net using a wind tunnel for the purpose of applying numerical simulations. *Journal of The Society of Agricultural Meteorology of Japan*, **65** (3), 273-281 (in Japanese)

Wang, H., Takle, E. S. (1997): Momentum budget and shelter mechanism of boundary layer flow near a shelterbelt. *Boundary-Layer Meteorology*, **82**, 417-435

Yamamoto, S. (1983): *Shin-pan-Chika-sui-Tyou-sa-Hou*. Kokin Syoin, Ltd., pp.490

Yang, K., Koike, T. (2004): Comments on "Estimating soil water contents from soil temperature measurements by using an adaptive Kalman Filter". *Journal of Applied Meteorology*, **44**, 546-550

Yoshii, Y. (2008): Grazing effects on carbon dynamics in semi-arid grassland in Mongolia. Life and Environmental Sciences, MS thesis, the University of Tsukuba, pp. 110

Zhaoqiang, J., Tusheng, R., Chunsheng, H. (2011): Soil thermal conductivity as influences by aggregation at intermediate water contents. *Soil Science Society of America Journal*, **75** (1), 26-29